CHARACTERIZING TRANSCRIPTIONAL AND METABOLIC REGULATORY PATHWAYS IN *CHLAMYDIA TRACHOMATIS*

By

Katelyn R. Soules

Submitted to the graduate degree program in Molecular Biosciences and the Graduate Faculty of the University of Kansas in partial fulfillment of the requirements for the degree of Doctor of Philosophy.

_____
Chairperson (P. Scott Hefty, Ph.D.)

_____
(Susan Egan, Ph.D)

_____
(Lynn Hancock, Ph.D.)

_____
(Roberto DeGuzman, Ph.D.)

_____
(Benjamin Sikes, Ph.D.)

Date Defended: 23 April 2020

The Dissertation Committee for Katelyn R. Soules certifies that this is the approved version of the following dissertation:

CHARACTERIZING TRANSCRIPTIONAL AND METABOLIC REGULATORY PATHWAYS
IN *CHLAMYDIA TRACHOMATIS*

_____
Chairperson (P. Scott Hefty, Ph.D.)

Date approved: 24 April 2020

SUMMARY

Chlamydia species all share a unique, phylum-defining biphasic developmental cycle. This developmental cycle is regulated in a strict temporal pattern, although, how this temporal regulation is controlled is poorly understood. Sigma factors are thought to play a pivotal role in the global regulation of the genes throughout the different stages of the developmental cycle. My research looks into two protein pathways that are regulating sigma factors in order to regulate the temporal transcriptional and metabolic activity of the human pathogen *Chlamydia trachomatis.*

First, the Rsb partner-switching phosphoregulatory pathway will be investigated. This pathway consists of a transmembrane phosphatase protein, RsbU, that can dephosphorylate a cytosolic $RsbV_1$, and a protein kinase, RsbW, that rephosphorylates RsbV1. RsbW inhibits another target protein when it is not employing its kinase activity. The identity of that target protein is one of the unknown details of this pathway in *Chlamydia.* Additionally, the signaling ligand for the RsbU protein has not been determined. My research addresses both of these questions concerning the Rsb pathway in *Chlamydia*, connecting the pathway to the central metabolism of this bacteria and the activation its main sigma factor.

Secondly, determination of the chlamydial regulon will be discussed. The two-component regulatory pathway that activates σ^{54}-dependent transcription was manipulated in order to constitutively activate σ^{54} during a chlamydial infection. A subset of differentially regulated genes was determined to constitute the σ^{54} regulon, with additional studies to support its validity. Interestingly, the genes that appear to be regulated by σ^{54} are all normally up-regulated during the later stages of the

developmental cycle and include a relatively large number of genes that encode for proteins enriched in the infectious Elementary Body form of the bacteria, including membrane and T3SS-associated proteins. These data support that σ^{54} plays a role in the preparation and arming of the chlamydial cells for release from their current host cell and infect a new cell.

Together these two pathways play important roles in the regulation of the chlamydial developmental cycle and the transition between the two phases that *Chlamydia* take. We hypothesize that the Rsb pathway is involved in the initial conversion event to the metabolically-active form, as well as at the end of the developmental cycle when the *Chlamydia* is overall slowing transcription. Additionally, σ^{54} is active as the *Chlamydia* cells prepare to transition into the infectious form and propagate infection. This research presented here fills in large gaps in our understanding of the basic biology of *Chlamydia.*

ACKNOWLEDGEMENTS

I would like to acknowledge my mentor Dr. Scott Hefty for his involvement in my graduate career. My time in Dr. Hefty's lab has made me a better and more independent scientist. I would also like to thank all the members of the Hefty lab, past and present, for their hard work, for my research would not have been possible without their efforts. Aidan Dmitriev, especially, deserves to be acknowledged for his hard work on the RsbU project and for all that he taught me. Ben May was the best undergraduate researcher I could have asked for and helped me out immensely.

I would like to thank my all my graduate student friends, especially Kelly Harrison and Megan McKinney. Kelly is one of the reasons that I decided to go to graduate school in the first place. She taught me so much and is the type of scientist that I hope to be. Megan was with me in the trenches for the majority of my graduate career. She has been my ride or die, my best friend through this whole process, and I could not have done it without her.

I would also like to thank all faculty that have been the members of my committee, both past and present. Your support and advice have been extremely helpful, and you are the reason that I strive for excellence. Dr. Benedict in particular was a huge inspiration for me. He was the kind of scientist and person that I strive to be.

I have to acknowledge Drs. Bill and Wendy Picking for their influence in my scientific career. They employed me as a laboratory technician right after I graduated with my Bachelor's degree, and it was during that short time in their lab that I found my

true passion for research. Without that opportunity and their encouragement, my life would likely have taken a different trajectory.

Of course, I have to thank my parents. It is with their support that I was able to get to this level of education without any debt. Being able to live with minimal expenses because of their help allowed me to have less stress and focus on what really mattered. They have always pushed me to do my best in school, and have always believed in whatever path I wanted to pursue.

I have to also thank Ryan Leibach. He was such a huge support during the first few years of my graduate career. I could never repay him for the stability that he provided me during such a critical time. Although we are no longer together, I still owe him a lot, and must express my gratitude for everything that he gave me.

TABLE OF CONTENTS

Collaborator Contributions:

Dr. Scott Lovell (Del Shankel Structural Biology Center, University of Kansas) produced Figures 3.5, 3.6, 3.7, and 3.9. The structure of RsbU was solved by Dr. Kevin P. Battaile (IMCA-CAT, Hauptman-Woodward Medical Research Institute) with the assistance of Aidan Dmitriev (Molecular Biosciences, University of Kansas). Genome sequencing of the RsbU* null-mutant strain and generation of Table 3.6 was performed by Zoë E. Dimond (Molecular Biosciences, University of Kansas). All IFA imaging was performed by Scott D. LaBrie (Molecular Biosciences, University of Kansas). BACTH analysis, Figure 4.1, and Tables 4.1 and 4.2 were done by Megan McKinney (Molecular Biosciences, University of Kansas). Recombinant CtcC protein variant purification and ATP hydrolysis assays were performed with great help from Ben H. May (Molecular Biosciences).

Information included in the "*Chlamydia* Gene Regulation" subsection of "Chapter I: General Information" is partially from writing that I contributed as a co-author to the book chapter Rosario, C. J., Soules, K. R., Hefty, P. S., & Tan, M. (2020). *Chlamydia* Gene Regulation In M. Tan, J. H. Hegemann, & C. Sutterlin (Eds.), *Chlamydia Biology: From Genome to Disease* (pp. 219-240). Norfolk, UK: Caister Acedemic Press. "Chapter II: Structural and ligand binding analyses of the periplasmic sensor domain of RsbU in *Chlamydia trachomatis* supports role in TCA cycle regulation" is a published manuscript in Molecular Microbiology (Soules, K. R., et al. (2019). "Structural and ligand binding analyses of the periplasmic sensor domain of RsbU in Chlamydia trachomatis supports role in TCA cycle regulation." Mol Microbiol.) "Chapter IV: Conversion to

infectious elementary bodies is regulated by Sigma 54 in *Chlamydia trachomatis*" is a manuscript in preparation being submitted for publication. The subsection "Bacterial two-hybrid system screen supports σ^{66} as binding partner for RsbW" in "Chapter III: RsbW is an anti-sigma factor that inhibits the activity of the major sigma factor in *Chlamydia"* was contributed by Megan McKinney as part of her work for her Master's thesis "Utilizing a Two-Hybrid System to Determine Possible Roles and Functions of Hypothetical Proteins in *Chlamydia trachomatis"* (2019).

Chapter I: General Information

Public health impact of *Chlamydia*

Chlamydia is an Gram-negative, obligate intracellular bacteria with a unique, phylum-defining developmental cycle that is intrinsically linked to its ability to cause disease (Elwell, Mirrashidi et al. 2016). Members of the phylum *Chlamydia*e infect a wide variety of organism from mammals, to fish, to amoeba (Cheong, Lee et al. 2019). *Chlamydia abortus* infects primarily ruminants and livestock including sheep, cattle, and horses, causing reproductive failure and spontaneous abortions, costing upwards of $20 million of economic loss annually (Longbottom and Coulter 2003). *Chlamydia suis* is a pig pathogen that has already shown instances of tetracycline resistance, increasing the potential for antibiotic resistance to jump into human strains of *Chlamydia* (De Puysseleyr, De Puysseleyr et al. 2014, LaBrie, Dimond et al. 2019). There are three species of *Chlamydia* that infect humans: *Chlamydia trachomatis, Chlamydia pneumoniae,* and *Chlamydia pscittaci.*

C. pneumoniae and *C. pscittaci* both cause respiratory infections (Knittler and Sachse 2015, Porritt and Crother 2016). Most individuals are exposed to *C. pneumoniae* in their lifetime, with about 80% of the population having antibodies towards it by age 70. *C. pneumoniae* has also been linked to the atherosclerosis and arthritis (Porritt and Crother 2016). Conversely, *C. pscittaci* infections are rare in humans, typically causing disease in birds, but zoonotic transmission can be fatal (Knittler and Sachse 2015).

Chlamydia trachomatis is the most prevalent sexually transmitted disease (CDC 2018). Serovars D through K cause the genital infections, while serovars L1, L2, and L3 are associated with lymphogranuloma venereum (LGV) (Quinn, Goodell et al. 1981). In 2018, nearly 1.8 million cases of *Chlamydia* infections were reported to the CDC in the United States alone (CDC 2018); however, because *Chlamydia* infections are often asymptomatic, this is likely a large underestimation. Unnoticed or untreated infections can lead to prolonged infections or reinfections which can cause a buildup of scar tissue and sustained inflammation and can lead to permanent tissue damage (Cates and Wasserheit 1991, Haggerty, Gottlieb et al. 2010). In women, damage from *Chlamydia* infections can lead to pelvic inflammatory disease and ectopic pregnancy (Haggerty, Gottlieb et al. 2010). In men, *Chlamydia* infections can lead to a painful swelling of the epididymis, known as epididymitis (Berger, Alexander et al. 1978). In both men and women, infertility can be a consequence of chronic *Chlamydia* infections.

C. trachomatis is also the leading cause of preventable blindness worldwide (Hu, Harding-Esch et al. 2010). Serovars A, B, and C cause the ocular disease trachoma, which can lead to scarring of the cornea. Ocular infections are largely present in developing countries, especially in parts of southern Asia and sub-Saharan Africa (Burton and Mabey 2009). In 2002, the WHO estimated that nearly 1.3 million people were blind due to trachoma, with an additional 40 million having active trachoma (Resnikoff, Pascolini et al. 2004, Mariotti, Pascolini et al. 2009).

Chlamydia infections can be treated with antibiotics, typically a single dose of azithromycin or a 7-day course of doxycycline (Lau and Qureshi 2002). While treatment with antibiotics is effective >90% of the time, treatment failure can lead to persistent infections that can lead to pathology. Although the *Chlamydia* bacteria itself causes death to infected epithelial cells, tissue damage is thought to largely be due to the host inflammatory response to the infection (Darville and Hiltke 2010).

Basic biology of the chlamydial developmental cycle

Among all species of *Chlamydia,* there is a shared, unique developmental cycle (Figure 1.1). This cycle is biphasic, meaning that there are two forms that the *Chlamydia* cells take: a highly condensed, infectious form, called an Elementary Body (EB); and a metabolically active, non-infectious form, called a Reticulate Body (RB). In an EB, the DNA is highly condensed, wrapped around histone-like proteins (HctA and HctB), and their cellular envelope has a high degree of disulfide cross-linking making these cells stable and resistant to the osmotic pressure in the outside environment (Newhall and Jones 1983, Allan, Hatch et al. 1985, Hackstadt, Todd et al. 1985, Barry, Hayes et al. 1992, Barry, Brickman et al. 1993, Brickman, Barry et al. 1993, Hatch 1996). The outer membrane of EBs is composed mostly of cysteine-rich proteins, like OmcA and OmcB, that can be oxidized to form cross-links and increase the rigidity of the cellular envelope (Hatch, Allan et al. 1984, Hackstadt, Todd et al. 1985, Hatch 1996). However, because of this rigidity of the membrane and the supercoiled

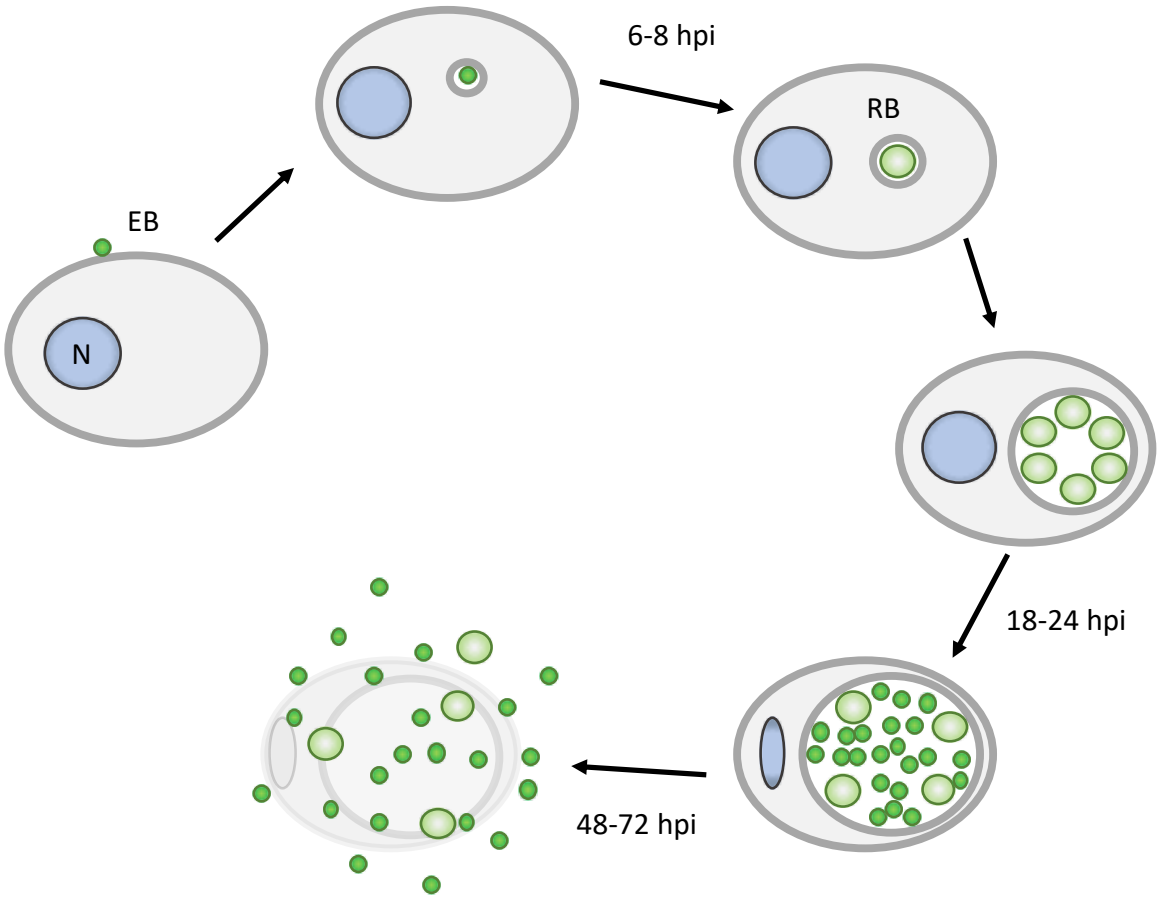
6-8 hpi
RB
EB
N
18-24 hpi
48-72 hpi

Figure 1.1 *Chlamydia* developmental cycle. The biphasic developmental cycle starts when Elementary bodies (EB) attach to the outside of a host cell. Following endocytosis, the chlamydial cell modifies the host cell vacuole into what is termed the chlamydial inclusion, and then converts into the replicative Reticulate Body (RB). After several round of replication, the RBs convert back into EBs before lysing the host cell and infecting neighboring cells. The times listed for each transition period in the developmental cycle are the hours post-infection (hpi) from the initial attachment to the host cell for *Chlamydia trachomatis.*

nature of the DNA, these cells are thought to be virtually metabolically inactive and do not grow or divide (Moulder 1991, Barry, Brickman et al. 1993). RBs, on the other hand, uncoil the DNA from the histone-like proteins, allowing more access for transcriptional machinery, and have a more reduced cellular envelope, allowing for cellular division to occur, but leaving them vulnerable to lysis outside the host cell.

The chlamydial developmental cycle begins with the EB attaching to the outside of the host cell and is subsequently endocytosed. Using type 3 secretion system (T3SS) effector proteins, the EB is able to modify the host cell vacuole into what is then termed a chlamydial inclusion. These early effectors remodel the inclusion membrane and facilitate nutrient acquisition from the host cell to the chlamydial inclusion, as well as allowing the *Chlamydia* to avoid being lysed by the host cell's defenses (Moore and Ouellette 2014). After 6 to 8 hours post-infection (hpi) for *C. trachomatis*, the EB will transition to the RB form. The RBs will then divide asynchronously. At 18 to 24 hpi, some RBs will convert again into the EB form. Lee *et al.* (2018) showed evidence that suggest that the RB-to-EB transition happens after an RB has undergone several rounds of replication, reducing in size with each division, until it reaches a size small enough to differentiate into the EB form (Lee, Enciso et al. 2018).

Progression of the chlamydial developmental cycle is regulated by temporal differential expression of genes, meaning that specific subsets of genes are turned on at specific times during the bacteria's infection of a host cell. These subsets of genes have been classified into groups based on the time when they

are normally upregulated during the developmental cycle. Some evidence has shown that EBs become transcriptionally active within an hour of entering the host cell (Belland, Zhong et al. 2003, Humphrys, Creasy et al. 2013). The 29 genes that are expressed within one hour of entry into the host cell have been called immediate early genes (Belland, Zhong et al. 2003, Nicholson, Olinger et al. 2003). By 3 hpi, an additional 200 genes are expressed, making up the early genes. Early genes are thought to be important for establishing the chlamydial inclusion and encode for machinery for basic processes such as transcription, translation, and DNA replication (Belland, Zhong et al. 2003). The largest temporally divided subset of genes is the midcycle genes. About 650 genes are upregulated during the midcycle period of the developmental cycle, starting at about 8 hpi (Belland, Zhong et al. 2003, Elwell, Mirrashidi et al. 2016). Midcycle genes are also often referred to as constitutively active genes and include many housekeeping genes involved in growth and replication, metabolic processes, and general inclusion and cellular maintenance (Belland, Zhong et al. 2003, Nicholson, Olinger et al. 2003). Nicholson *et al.* (2003) includes a subset of genes that they termed midlate genes which are upregulated at 18 hpi when the RB production has reached maximal levels. Nicholson *et al.* (2003) proposes that this midlate cluster of genes is crucial for the early stages of RB-to-EB conversion (Nicholson, Olinger et al. 2003). Finally, late stage genes are upregulated after 24 hpi. The late stage genes include genes important for DNA condensation, such as *hctA* and *hctB* that encoding for histone-like proteins, and

those genes important for EB function and structure, such as *omcA* and *omcB* which encode for an outer membrane protein enriched in EBs.

Chlamydia gene regulation

The chlamydial developmental cycle proceeds in a specific sequence of events with a predictable pattern of gene expression (Abdelrahman and Belland 2005). The temporal expression pattern of genes throughout the developmental cycle is regulated by stage-specific factors, including DNA super-coiling, transcriptional activators and repressors, response regulators, small regulatory RNA, and alternative sigma factors (Elwell, Mirrashidi et al. 2016, Rosario, Soules et al. 2020).

In EBs, the chlamydial DNA is condensed into a nucleoid and wrapped around two nucleoid-associated, histone-like proteins, HctA and HctB, universally repressing transcription (Barry, Hayes et al. 1992, Barry, Brickman et al. 1993, Brickman, Barry et al. 1993). The topology of the DNA is thought to largely account for EBs being essentially metabolically inert. During midcycle time points, the DNA becomes relaxed and allows for the transcriptional machinery to access the DNA (Orillard and Tan 2016).

Chlamydia are predicted to have around 12 to 15 transcription factors, the majority of which have orthologues in other bacteria (Domman and Horn 2015). This is a relatively small number of transcription factors compared to other bacteria, but because of the obligate intracellular niche, *Chlamydia* have a reduced genome size, and thus has a less variable interactions with

environmental stresses (Madan Babu, Teichmann et al. 2006, Galan-Vasquez, Luna et al. 2011, Yamamoto, Watanabe et al. 2014). Table 1.1 summarizes the known transcription factors in *Chlamydia;* however, because of the high proportion of hypothetical proteins (about 30% of the genome are *Chlamydia*-specific proteins of unknown function), there is the possibility for other currently uncharacterized transcription factors to be present (Stephens, Kalman et al. 1998).

Most of the transcription factors in *Chlamydia* are transcriptional repressors, down-regulating transcription by binding to an operator sequence on the DNA near a gene promoter to interfere with the RNA polymerase's ability to initiate transcription of the gene. Genes that are classified as early genes have not been found to have any transcriptional repressors, and while these genes are initially transcribed soon after host cell entry, their expression continues throughout replication until the RB-to-EB conversion near the cell lysis phase of the developmental cycle (Belland, Zhong et al. 2003, Nicholson, Olinger et al. 2003). The transcriptional regulators encoded by the chlamydia genome appear to be regulating when the remainder of the genome is being expressed throughout the cycle; allowing for expression of genes at specific times to allow the cycle to progress. EUO, for example, is a master regulator of late stage genes (Rosario and Tan 2012, Rosario, Hanson et al. 2014). Expression of EUO itself is during the early stages of the developmental cycle, so this protein is able to repress transcription of late stage genes from start of the host cell infection (Zhang, Douglas et al. 1998, Zhang, Howe et al. 2000).

Table 1.1 Transcription factors in Chlamydia

Transcription Factor	Function	References
EUO	Master repressor of late genes	(Zhang, Douglas et al. 1998, Zhang, Howe et al. 2000, Rosario and Tan 2012, Rosario, Hanson et al. 2014)
TrpR	Repressor of tryptophan biosynthesis operon	(Carlson, Hughes et al. 2004, Akers and Tan 2006)
ArgR	Repressor of arginine transport genes	(Schaumburg and Tan 2006)
YtgR	Repressor of iron transport genes	(Akers, HoDac et al. 2011)
NrdR	Repressor of nucleotide triphosphate (NTP) transport genes	(Case, Akers et al. 2011, Hanson and Tan 2015)
HrcA	Stress response expression of heat shock proteins; co-repressor with GroEL	(Hanson and Tan 2015, (Wilson and Tan 2002, Wilson and Tan 2004)
GrgA	Activator of sig-66 and -28 dependent transcription	(Bao, Nickels et al. 2012, Desai, Wurihan et al. 2018)
ChxR	Activator of virulence genes	(Koo, Walthers et al. 2006, Yang, Kari et al. 2017)
CtcC	Sig-54 activator	(Koo and Stephens 2003)
DksA	No functional studies	(Domman and Horn 2015)
PhoU	No functional studies	(Domman and Horn 2015)
YebC	No functional studies	(Domman and Horn 2015)
YbjN	No functional studies	(Domman and Horn 2015)
CdsZ	Potential repressor of sig-54	(Barta, Battaile et al. 2015)
RsbW	Potential repressor of sig-66	(Thompson, Griffiths et al. 2015)
Scc4	Potential regulator of sig-66	(Rao, Deighan et al. 2009)
Pgp4	Potential activator	(Song, Carlson et al. 2013, Zhong 2017)
Pgp5	Potential repressor	(Liu, Chen et al. 2014)

While the vast majority of the gene regulation mechanisms in *Chlamydia* are involved in the temporal regulation of the developmental cycle, there are a few transcription factors that control nutrient biosynthesis and transport. ChxR is an ortholog to response regulators that response to changes in osmolarity, and is thought to affect virulence genes in a *Chlamydia* infection (Koo, Walthers et al. 2006). Additionally, HcrA is a transcription factor that controls the expression of the main heat shock proteins (DnaK, GroEL, and GroES) in *Chlamydia* (Wilson and Tan 2002, Wilson and Tan 2004, Chen, Wilson et al. 2011).

Another method of transcriptional regulation is small RNA (sRNA). These are short (typically 50 to 200 nucleotides), non-coding RNAs that post-transcriptionally regulate gene expression (Storz 2002). sRNA are divided into two classes: *cis*-encoded and *trans*-encoded (Gottesman and Storz 2011). A *cis*-encoded sRNA is transcribed form the complementary strand of its target gene and regulate the stability of the target mRNA. Trans-encoded sRNAs can either block or promote translation of the target mRNA by altering the structure of the ribosomal binding site (Gottesman and Storz 2011). Albrecht and colleagues used deep-sequencing to identify 43 potential sRNA in *C. trachomatis* and 75 in *C. pneumoniae* (Albrecht, Sharma et al. 2010, Albrecht, Sharma et al. 2011). One interesting example of sRNA regulation is the in the case of *hctA* which encodes a protein necessary in the late stages of the developmental cycle, but its expression is repressed by a sRNA for the majority of the time (Grieshaber, Grieshaber et al. 2006, Tattersall, Rao et al. 2012).

Arguably the most important universal regulatory element used by *Chlamydia* is the sigma factor. Sigma factors are the subunit of the RNA polymerase (RNAP) that allow the enzyme promoter-specific transcription initiation (Murakami and Darst 2003). *Chlamydia* only encode three sigma factors: σ^{66}, σ^{28}, and σ^{54} (Stephens, Kalman et al. 1998). σ^{66} is a σ^{70} homolog and is responsible for transcribing the majority of the chlamydial genome (Koehler, Burgess et al. 1990). σ^{28} is an alternate sigma factor, also in the σ^{70} protein family, that facilitates transcription for only a few late stage genes, including *hctB* (Yu and Tan 2003, Yu, Kibler et al. 2006*)*. While σ^{66} and σ^{28} are relatively well studied, the third sigma factor in *Chlamydia*, σ^{54}, has yet to be fully investigated.

Sigma factors' activity can additionally be influenced by other regulatory factors. Scc4 (CT633) inhibits σ^{66} by interacting with the sigma factor itself, as well as the β-subunit of the RNAP (Rao, Deighan et al. 2009). RsbW is also a potential regulator of σ^{66} and will be discussed more in depth below (Thompson, Griffiths et al. 2015). CdsZ (CT398) has been proposed to be a regulator of σ^{54} with Barta *et al*. (2015) showing an interaction between the two proteins by both bacterial two-hybrid and *in vitro* affinity pull-down studies (Barta, Battaile et al. 2015). σ^{54} proteins in all bacteria require activation by an ATPase protein in order to initiate transcription, and the chlamydial σ^{54} is no exception (Koo and Stephens 2003, Wigneshweraraj, Bose et al. 2008). These additional regulatory components modifying sigma factor activity create the opportunity for additional layers of regulation in response to environmental conditions, but unfortunately,

there are still large gaps in our understanding of how these fit into the global gene regulation control the chlamydial developmental cycle.

Sigma-54 and its regulatory system

The σ^{54} class of sigma factors consists of a single protein with no alternate forms thus far identified (Hong, Doucleff et al. 2009). Typically, only one gene encoding the σ^{54} protein is present in bacteria; however, some bacterial genomes including *Bradyrhisobioum japonicum, Rhodobacter sphaeroides,* and *Rhisobium etli*, do contain two. This gene duplication possibly allows of differential regulation of the genes, or the potential for divergent evolution to create alternate versions of the σ^{54} protein throughout time (Collado-Vides, Magasanik et al. 1991, Michiels, Moris et al. 1998).

σ^{54} associated with the same RNAP core enzyme as σ^{70}-class factors, although it has no sequence homology to σ^{70} (Merrick 1993, Hong, Doucleff et al. 2009). σ^{54} recognizes a promoter sequence that is centered at the -12 and -24 position upstream of its target genes, and this consensus sequence is highly conserved across bacteria phyla, as compared to the -10/-35 position and highly variable sequence recognition for σ^{70} homologs (Morett and Buck 1989, Barrios, Valderrama et al. 1999).

Additionally, σ^{54} has a unique mechanism of transcription initiation (Merrick 1993). Unlike σ^{70}-type factors, σ^{54} imposes kinetic and thermodynamic constraints on the open complex formation of the RNAP (Wigneshweraraj, Bose et al. 2008). This means that the RNAP holoenzyme is initially in a conformation

that is incapable of spontaneous isomerization. Transition from the closed- to open-complex by σ^{54}-RNAP requires an ATP-hydrolyzing activator (Schumacher, Joly et al. 2006, Snider, Thibault et al. 2008). This activator protein is part of an upstream signaling cascade (i.e. a two-component regulatory system) that responds to a particular regulatory cue.

The conical two-component regulatory system for σ^{54} consists of the ATPase activator protein NtrC and the sensor kinase protein NtrB. The NtrC protein is composed of three domains: a DNA-enhancer binding domain, an ATPase domain, and a receiver domain that gets phosphorylated by NtrB (Schumacher, Joly et al. 2006). In response to a signal, NtrB will become autophosphorylated and subsequently phosphorylate NtrC at a conserved aspartate residue. This permits the NtrC protein to oligomerize, typically into a hexamer, allowing for binding to the enhancer DNA sequence, and relieves inhibition of the ATPase domain allowing for the activation of σ^{54} (Schumacher, Joly et al. 2006).

Despite the canonical sequence of events for σ^{54} activation including enhancer binding by the NtrC activator protein, there are examples where the DNA-binding domain of these proteins is absent. *Helicobacter pylori* is an example of a bacterial species whose σ^{54} activator protein has lost its DNA-binding domain (Brahmachary, Dashti et al. 2004). The loss of this domain in *H. pylori* appears to be recent in evolutionary time based on the evidence that the homologous protein in the closely related species *Helicobacter hepaticus* and *Campylobacter jejuni* still retains their DNA-binding domains (Brahmachary,

Dashti et al. 2004). Previous studies have shown that the DNA-binding domain is not necessary for activation of the σ54-RNAP holoenzyme; and interesting, loss of the regulatory domain leads to a constitutively active ATPase function of the activator protein (Huala, Stigter et al. 1992, Xu, Gu et al. 2004, Samuels, Frye et al. 2013).

Chlamydia has homologs to the two-component regulatory system sensor kinase and ATP-hydrolyzing activator protein, known as CtcB and CtcC, respectively (Koo and Stephens 2003). Like in *H. pylori,* the CtcC protein has lost its DNA-enhancer binding domain. Figure 1.2 depicts this regulatory pathway in *Chlamydia.* The regulon for σ^{54} in *Chlamydia* has yet to be fully investigated.

σ^{54} was originally identified as a regulatory factor for the expression of glutamine synthetase in enteric bacteria and was later found to be required for the expression of genes for protein involved in the assimilation of nitrogen, earning it the name σ^{N} (Garcia, Bancroft et al. 1977, Magasanik 1982, Dixon 1984, Gussin, Ronson et al. 1986). It has since became clear that σ^{54} is responsible for the transcription of genes whose products have different physiological functions in a variety of organisms (Kustu, Santero et al. 1989) Francke *et al*. (2011) performed a comparative analyses of the σ^{54} regulons across different bacteria, and concluded that the common theme among σ^{54}-regulated genes was those that contribute to changes in the membrane components of the cell and metabolic changes in response to the external environment (Francke, Groot Kormelink et al. 2011).

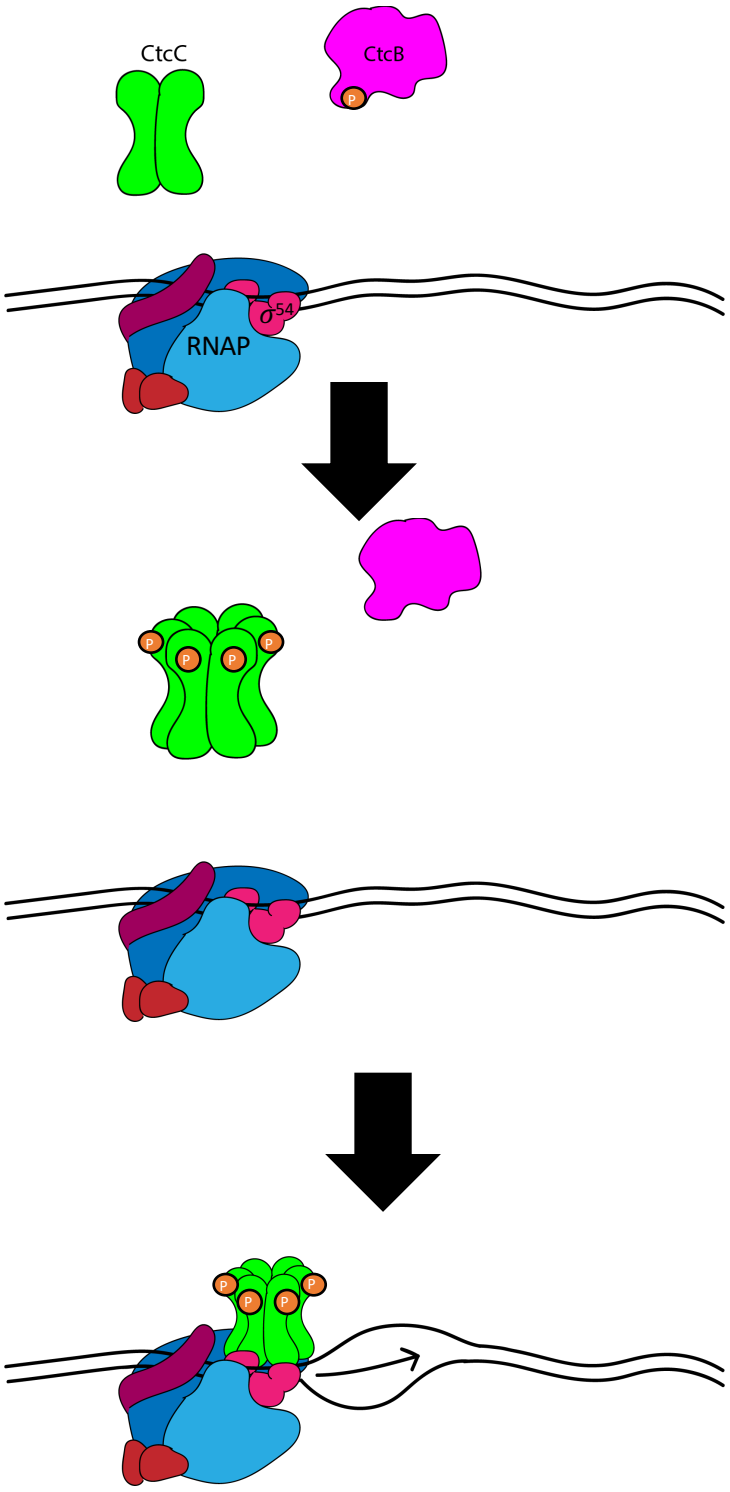
CtcC
CtcB
P
RNAP
σ54
P
P
P
P
P
P
P
P

Figure 1.2 Two-component regulatory system for the activation of σ^{54} in *Chlamydia.* CtcB is the sensor kinase protein that upon receiving a stimulus in the chlamydial cytosol becomes autophosphoylated. CtcB will then phosphorylate CtcC which typically exists as a dimer but will then oligomerize into a hexamer. The CtcC hexamer can then activate transcription by assisting the σ^{54}-RNAP holoenzyme to transition from the closed-complex to the open-complex on the DNA.

The Rsb regulatory system

Another regulatory system that has been shown to control sigma factor function is the Rsb system of proteins. Originally characterized as the Regulator of Sigma B in *Bacillus subtillus,* the Rsb phosphoregulatory system is composed of several proteins that act as antagonists to each other (Haldenwang and Losick 1980, Benson and Haldenwang 1993, Voelker, Dufour et al. 1995, Voelker, Voelker et al. 1995, Wise and Price 1995). In *B. subtillus,* the Rsb pathway responds to both environmental and energy stress, with up to eight proteins involved in the regulation, some of which the function has yet to be fully investigated (Kang, Brody et al. 1996). σ^B in *Bacillus* is responsible for transcription of a large subset of genes that have been linked to general stress responses, including environmental stressors such as heat, hyperosmosis, oxidative stress, and ethanol (Boylan, Redfield et al. 1993, Boylan, Redfield et al. 1993). σ^B in *Bacillus* has shown to be activated in the stationary phase of normal growth, but is not important for sporulation (Haldenwang and Losick 1979). The Rsb system is found mainly in Firmicutes as a regulator of general stress response. However, homologous protein pathways have been associated with regulating a variety of processes in other bacteria phyla including biofilm formation, type 3 secretion, and swarming motility (Kozak, Mattoo et al. 2005, Morris and Visick 2013). *Chlamydia* also has an Rsb system, although the regulatory role has yet to be fully evaluated.

In the chlamydial Rsb system, RsbU is a transmembrane protein with a periplasmic sensor domain and a cytosolic phosphatase domain (Thompson,

Griffiths et al. 2015). The sensor domain of RsbU detects a stimulus in the periplasm that has yet to be identified. The phosphatase domain of RsbU will dephosphorylate the cytoplasmic protein $RsbV_1$, which can then be subsequently re-phosphorylated by the protein kinase RsbW. RsbW is typically characterized as an anti-sigma factor; binding to and inhibiting a specific sigma factor and preventing it from binding to the RNAP core enzyme (Hecker, Pane-Farre et al. 2007). However, RsbW can change partners and instead bind to $RsbV_1$, freeing up the sigma factor to bind to the RNAP core. The Rsb system in *Chlamydia* is summarized in Figure 1.3.

While the chlamydial Rsb lacking some of the components that are present in *B. subtillis,* there are a couple proteins that appear to be associated with this system in *Chlamydia* that are absent from other systems and do not have assigned functions at this point. CT589 appears to be a paralog of RsbU, but CT589 lacks two important amino acid residues necessary to do phosphatase activity, and the periplasmic domains of these proteins do not share sequence similarity (Hua, Hefty et al. 2006). Furthermore, there are two RsbV proteins present in *Chlamydia*. RsbW has been shown to bind and phosphorylate both $RsbV_1$ and $RsbV_2$, although it has a greater affinity for $RsbV_1$ (Thompson, Griffiths et al. 2015). This association between the chlamydial RsbV's and RsbW is unusual because it requires ATP, which is not a feature of the RsbW-RsbV interaction in *Bacillus* (Thompson, Griffiths et al. 2015). Additionally, RsbU has been shown to dephosphorylate only $RsbV_1$, and not $RsbV_2$ (Thompson, Griffiths et al. 2015).

Figure 1.3 Modified from Soules *et al.* (2019) Rsb phosphoregulatory pathway in *Chlamydia*. RsbU is a transmembrane protein with a periplasmic sensor domain and a cytosolic phosphatase domain. Upon stimulation of the sensor domain, RsbU will dephosphorylate another cytosolic protein, $RsbV_1$. $RsbV_1$ can be phosphorylated by RsbW, but in order to do so, RsbW must release its target protein (black box) for which it typically binds to and inhibits the function. A second RsbV protein is also present in *Chlamydia,* although its function in the Rsb pathway is less apparent. Additionally, CT589 shares sequence homology to the cytoplasmic portion of the RsbU protein, although it lacks the residues necessary for phosphatase activity, and its periplasmic domain is dissimilar to that of the chlamydial RsbU protein.

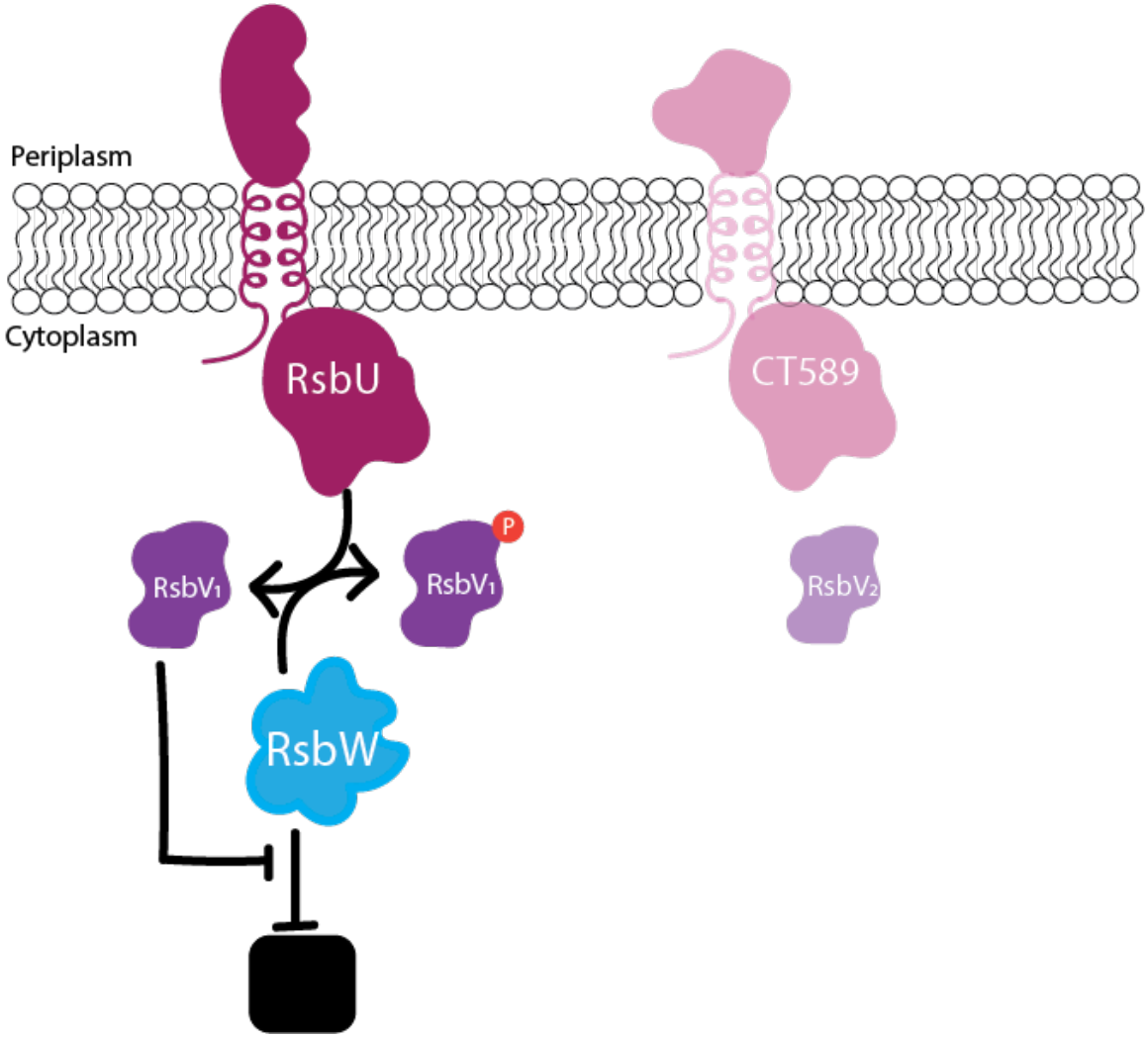
Periplasm
Cytoplasm
RsbU
CT589
RsbV1
RsbV1
P
RsbV2
RsbW

There is controversy about the target for RsbW in *Chlamydia*. Douglas and Hatch showed that RsbW bound to σ^{28} in a pull-down assay (Douglas and Hatch 2006). However no interactions were detected between any of the three chlamydial sigma factors and RsbW by a yeast two-hybrid study performed later that same year (Hua, Hefty et al. 2006). Most recently, Thompson and colleagues showed that RsbW interacted with σ^{66} by surface plasmon resonance, and also reported changes in transcription of σ^{66}-target genes in mutant strains overexpressing or lacking RsbW or $RsbV_1$ (Thompson, Griffiths et al. 2015).

The remainder of this dissertation will be focused on the protein pathways that appear to be regulating metabolic and transcriptional activities in *C. trachomatis.* We will begin by discussing the role of the Rsb system in *Chlamydia* by investigating the ligand for the RsbU protein and how that pathway is important for growth and metabolism during the developmental cycle. Additionally, we will show further support for the Rsb system's regulation of the main sigma factor in *Chlamydia,* σ^{66}. Then we will discuss the discovery of the role and regulon of σ^{54} by manipulating its activator protein CtcC. The data from these experiments support the role of σ^{54} being involved in the preparation and arming of the chlamydial cells for conversion form the replicative RB form to the infectious EB form and subsequent propagation of infection to new host cells. Lastly, we will tie these protein pathways into the larger picture of the chlamydial regulation of metabolism, transcription, and the developmental cycle as a whole.

Chapter II: Structural and ligand binding analyses of the periplasmic sensor domain of RsbU in *Chlamydia trachomatis* supports role in TCA cycle regulation

Abstract

Chlamydia trachomatis are obligate intracellular bacteria that undergo dynamic morphologic and physiologic conversions upon gaining access to a eukaryotic cell. These conversions likely require the detection of key environmental conditions and regulation of metabolic activity. *Chlamydia* encodes homologs to proteins in the Rsb phosphoregulatory partner-switch pathway, best described in *Bacillus subtilis.* ORF CT588 has strong sequence similarity to RsbU cytoplasmic phosphatase domain but also contains a unique periplasmic sensor domain that is expected to control phosphatase activity. A 1.7 Å crystal structure of the periplasmic domain of the RsbU protein from *C. trachomatis* (PDB 6MAB) displays close structural similarity to DctB from *Vibrio* and *Sinorhizobium*. DctB has been shown both structurally and functionally to specifically bind to the TCA cycle intermediate succinate. Surface plasmon resonance and differential scanning fluorimetry of TCA intermediates and potential metabolites from a virtual screen of RsbU revealed that alpha-ketoglutarate, malate, and oxaloacetate bound to the RsbU periplasmic domain. Substitutions in the putative binding site resulted in reduced binding capabilities. A RsbU-null mutant showed severe growth defects which could be restored through genetic complementation. Chemical inhibition of ATP

synthesis by oxidative phosphorylation phenocopied the growth defect observed in the RsbU null strain. Altogether, these data support a model with the Rsb system responding differentially to TCA cycle intermediates to regulate metabolism and key differentiation processes.

Introduction

Bacteria possess the ability to sense changes in environmental conditions and adjust biologic activities through diverse regulatory components and mechanisms (Zhulin, Nikolskaya et al. 2003). Often times these reactions are in responses to general environmental stresses as is the case with the Regulator of Sigma B or Rsb system. This phosphoregulatory partner switching system is found mainly in Firmicutes and is most thoroughly described in *Bacillus subtilis* (Hecker, Pane-Farre et al. 2007). A central regulatory component in this system is a phosphatase termed RsbU. Under stressful conditions, such as nutrient depletion, RsbU dephosphorylates a serine on an intermediate protein partner, RsbV. This allows another protein partner and kinase, RsbW, to 'switch' from association with sigma B to rephosphorylate RsbV. Ultimately, this enables the alternative sigma factor to freely diffuse and form an RNA holoenzyme polymerase, which activates the transcription of over a hundred genes that assist with the response to environmental stress (Benson and Haldenwang 1993, Voelker, Dufour et al. 1995, Voelker, Voelker et al. 1995, Wise and Price 1995, Kang, Brody et al. 1996, Yang, Kang et al. 1996, Hughes and Mathee 1998, Kang, Vijay et al. 1998). While the Rsb system is typically associated with general stress responses in Firmicutes, it has also been associated with regulating diverse processes in other bacteria phyla including biofilm formation, type III secretion, and swarming motility (Kozak, Mattoo et al. 2005, Morris and Visick 2013).

Chlamydia undergo dynamic morphologic and physiologic conversions upon gaining access to a eukaryotic cell. These conversions occur as *Chlamydia*

grows and propagates through a phylum-defining biphasic developmental cycle. The initial phase of the chlamydial developmental cycle is conversion from an infectious, non-replicative and metabolically inert form known as an elementary body (EB) to a non-infectious, metabolically active and replicative form, known as a reticulate body (RB). This conversion occurs upon gaining access to the cell and establishing the intracellular vacuole termed the inclusion (Elwell, Mirrashidi et al. 2016). Many ATP requiring processes occur during the EB to RB conversion including protein secretion and de novo transcription and translational activity. RBs also need to acquire most macromolecules from the host cell, including glucose-6-phosphate, nucleotides, amino acids, lipids, and other metabolic precursors for growth and multiple rounds of replication (Mehlitz, Eylert et al. 2017). The second phase is the asynchronous RB to EB conversion which occurs later in the developmental cycle through unknown signals and poorly understood mechanisms. This conversion also requires coordinated events that includes membrane remodeling and infectious capability preparation while metabolic processes, including transcription and translation, are silenced (Hatch, Allan et al. 1984, Hackstadt, Todd et al. 1985). *Chlamydia* also organize the escape from the infected host cell through either cell lysis or extruding vacuoles which enables the infection of new cells and possible a new host.

Chlamydia appear to acquire ATP from the host cell using ATP translocases and can also generate ATP through unique substrate-level and oxidative phosphorylation processes. Interestingly, these processes appear to be functional at different developmental stages. ATP stored in EBs may allow for initial protein

secretion and transcription and translation processes to occur until RB conversion. After the initial entry into the host cell, ATP translocases are utilized to obtain ATP from the host cell (Liang, Rosas-Lemus et al. 2018). During RB replication and midcycle growth stage, Liang *et al.* (2018) demonstrated that *Chlamydia* can also generate ATP using a sodium-ion gradient to drive the ATP-synthase (Liang, Rosas-Lemus et al. 2018). Critical for this process is the TCA cycle (Liang, Rosas-Lemus et al. 2018). *Chlamydia* spp. lack three canonical TCA enzymes: citrate synthase (*gltA)*, aconitase (*acn*), and isocitrate dehydrogenase (*icd*) (Stephens, Kalman et al. 1998, Iliffe-Lee and McClarty 1999). Due to the absence of these enzymes, *Chlamydia* possess a truncated TCA cycle that starts with alpha-ketoglutarate and ends with oxaloacetate that can then be shuttled to other metabolic pathways (Mehlitz, Eylert et al. 2017). This truncated TCA cycle does enable the chlamydial RBs to generate NADH, which drives the sodium-dependent NADH dehydrogenase and, subsequently, ATP generation (Liang, Rosas-Lemus et al. 2018). However, because of the incomplete TCA cycle, *Chlamydia* must scavenge dicarboxylate intermediates, such as glutamate and alpha-ketoglutarate, from the host cell (Stephens, Kalman et al. 1998, Iliffe-Lee and McClarty 1999, Iliffe-Lee and McClarty 2000). Consequently, there are substantial interactions between the parasitic chlamydial cells and the infected host cell. The intimate association between the host and chlamydial metabolisms suggests that signaling pathways in *Chlamydia* responding to the host's metabolic milieu play critical roles in development and pathogenesis. Despite the likely importance of these signals, much of the basic biology of these pathways remains poorly understood, including

Figure 2.1 The Rsb phospho-switching pathway in *Chlamydia* as current research describes. RsbW binds and inhibits the activity of a target protein (black box). However, when $RsbV_1$ is dephosphorylated, RsbW will release its target protein to act as a kinase to phosphorylate $RsbV_1$ (Hua, 2006; Thompson, 2015). RsbU acts as an antagonist of RsbW by dephosphorylating $RsbV_1$ in response to binding a ligand in the periplasm (Thompson, 2015). Ultimately, the binding of the ligand to the RsbU protein leads to the release of the target protein.

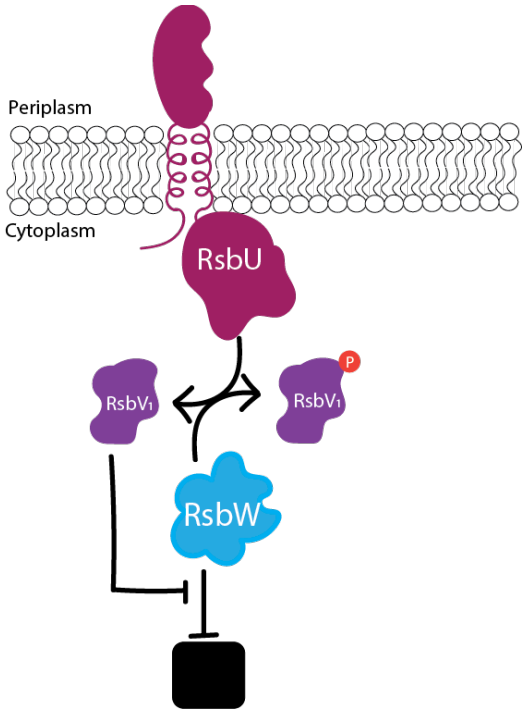
Periplasm
Cytoplasm
RsbU
RsbV1
RsbV1
P
RsbW

the signal for the EB-to-RB conversion, mechanisms for sensing environmental stimuli, and the differential regulation of ATP acquisition.

A partner-switching pathway with similarities to the Rsb regulatory pathway could be a primary mechanism for *Chlamydia* to sense environmental conditions and regulate metabolic activity (Stephens, Kalman et al. 1998). The chlamydial genome encodes genes for the production of RsbU (CT588), $RsbV_1$ (CT424), $RsbV_2$ (CT765), and RsbW (CT549) proteins (Figure 2.1) (Stephens, Kalman et al. 1998). However, there are distinct differences from the canonical Rsb system in *B. subtilis*. For one, chlamydial RsbU is a transmembrane protein situated in the inner membrane with a periplasmic sensor domain attached to a cytoplasmic phosphatase domain (Figure 2.2) (Douglas and Hatch 2000, Hua, Hefty et al. 2006, Thompson, Griffiths et al. 2015). In contrast, RsbU in *B. subtilis* are strictly cytoplasmic and do not contain a sensor domain, only possessing a phosphatase domain. It is expected that the chlamydial RsbU sensor domain is critical for controlling the phosphatase activity and downstream regulatory processes. Chlamydial RsbU has been shown to de-phosphorylate $RsbV_1$ but not $RsbV_2$ (Thompson, Griffiths et al. 2015). Importantly, multiple studies on the biologic and functional outcomes of the terminal component and kinase, RsbW, support binding and inhibiting the primary sigma factor, σ^{66} (Douglas and Hatch 2000, Hua, Hefty et al. 2006, Thompson, Griffiths et al. 2015). The expected result of this activity would be a global shutdown of most transcription in *Chlamydia*.

To discover the potential binding ligands and response regulatory role of the Rsb system in *Chlamydia,* a crystal structure of the RsbU periplasmic domain

was determined. This structure was used to identify structurally similar proteins for putative function predictions as well as direct virtual and experimental ligand-binding analyses. Growth phenotypes of RsbU null mutant strains and in the presence of chemical inhibitors of key ATP generating functions were evaluated. Together, these observations support that RsbU is binding to TCA cycle intermediates and may play a role in global gene regulation in *Chlamydia*.

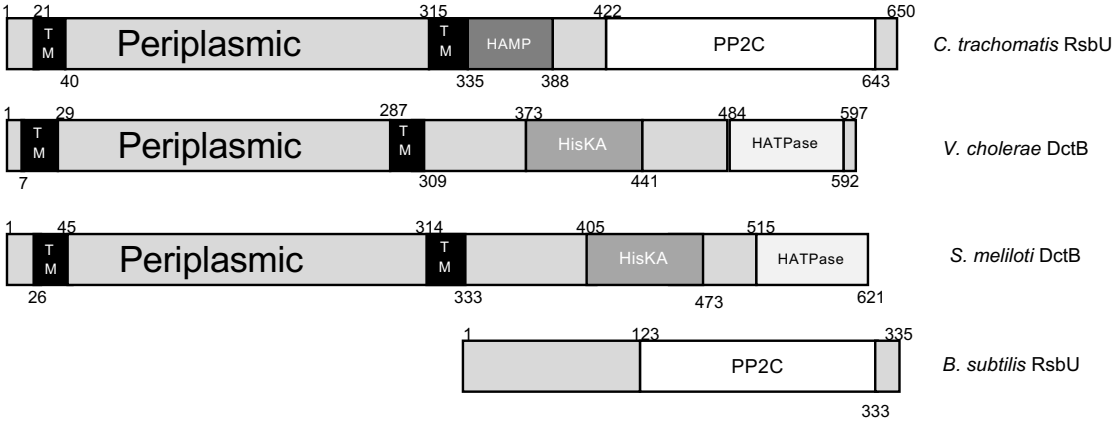
1
21
315
422
650
TM
Periplasmic
TM
HAMP
PP2C
40
335
388
643
C. trachomatis RsbU
1
29
287
373
484
597
TM
Periplasmic
TM
HisKA
HATPase
7
309
441
592
V. cholerae DctB
1
45
314
405
515
TM
Periplasmic
TM
HisKA
HATPase
26
333
473
621
S. meliloti DctB
1
123
335
PP2C
333
B. subtilis RsbU

Figure 2.2 Domain organization of RsbU from *C. trachomatis* and homologs from other bacteria. RsbU from *C. trachomatis* bears sequence similarity to RsbU from *B. subtilis* in the cytoplasmic domain, both containing PP2C domains. RsbU in *B. subtilis,* however, does not contain any transmembrane helices, nor a periplasmic portion. Structural comparison of the periplasmic portion of RsbU reveals similarity to the periplasmic domain of DctB proteins in *V. cholerae* and *S. meliloti*. Amino acids are numbered at the beginning and end of domains. TM denotes transmembrane helices.

Materials and Methods

Overexpression and purification of recombinant $RsbU_{45-313}$. A fragment of *ctl0851* encoding residues 45 through 313 of the open reading frames was amplified via polymerase chain reaction (PCR) from *C. trachomatis* L2 434/Bu (AM884176) genomic DNA. *ctl0851* is homologous and 99% identical to CT588 (RsbU) from *C. trachomatis* D/UW-3. This fragment was inserted into the pTBSG vector in frame and immediately downstream of a sequence encoding an N-terminal hexahistidine tag and TEV protease recognition site. After confirming sequence accuracy, this vector was transformed into BL21 (DE3) *E. coli* competent cells, which were then grown at 37°C (200 rpm) in Terrific Broth supplemented with 100 μg/mL Carbenicillin to an OD_{600} of 0.8. Overnight protein expression (15°C, 200 rpm) was induced at this optical density with the addition of IPTG (isopropyl 1-thio-β-D-galactopyranoside) to a final concentration of 1mM. Following *E. coli* collection by centrifugation (10,000g; 15 minutes), cells were resuspended in lysis buffer [20 mM Tris pH 8.0, 500 mM NaCl, 10 mM imidazole, 1 mM phenylmethane sulfonyl fluoride (PMSF), and 1000U benzonase endonuclease (EMD Millipore) per liter of Terrific broth culture] and lysed by sonication. After centrifugation (23,000g; 30 minutes), the supernatant was clarified through a 0.45 μm filter and purified on a gravity flow column containing 3 mL of HisPur Cobalt Resin (ThermoFisher) per liter of Terrific Broth culture. Following washes with 5 column volumes (CVs) of lysis buffer and then 3 CVs of wash buffer (20 mM Tris pH 8.0, 500 mM NaCl, and 50 mM imidazole), immobilized His_6-$RsbU_{45-313}$ was eluted with

3 CVs of elution buffer (20 mM Tris pH 8.0, 500 mM NaCl, and 500 mM imidazole). The eluate was buffer exchanged into Buffer A (20 mM Tris pH 8.0, 500 mM NaCl, and 10 mM imidazole) on a HiPrep 26/10 Desalting column (GE Healthcare) and then incubated overnight at 4°C with 5 mM dithiothreitol (DTT) and recombinant polyhistidine-tagged TEV protease for His_6-tag removal. Recombinant TEV protease and cleaved His_6-tag were then removed from this mixture via flow over a 5 mL HisTrap HP column (GE Healthcare). Following buffer exchange into Buffer X (10 mM Tris pH 7.5, 50 mM NaCl, and 1mM DTT) as described above, the sample was concentrated to a volume of 1.5 mL with an Amicon-15, Ultracel-10 centrifugal filter (EMD Millipore). Final purification was achieved via size exclusion chromatography using a flow rate of 0.2 mL/minute on a HiPrep 16/60 Sephacryl S-200 HR column (GE Healthcare). Collected fractions containing $RsbU_{45-313}$ were concentrated to 15.9 mg/mL (by Bradford assay) via ultracentrifugation and stored at 4°C until further use.

Crystallization and data collection. All crystallization screening was conducted in Compact 300 (Rigaku Reagents) sitting drop vapor diffusion plates at 18°C using equal volumes of protein solution and crystallization solution equilibrated against 75 μL of the latter. Prismatic crystals grew within one day and continued to grow for approximately one week from Wizard 1-2 screen (Rigaku Reagents) condition E10 (1M ammonium phosphate dibasic, 100 mM Tris pH 8.5) and the Crystal Screen HT (Hampton Research) condition D5 [20% (w/v) PEG 4000, 10% (v/v) 2-propanol, 100 mM Hepes pH7.5]. A heavy atom derivative was prepared by

soaking a crystal obtained from Wizard 1-2 condition E10 for 22 hours in crystallant containing 5 mM K_2PtCl_4. Native and heavy atom-soaked crystals were transferred to a fresh drop containing 80% crystallant and 20% ethylene glycol before flash freezing in liquid nitrogen. Data were collected at the Advanced Photon Source IMCA-CAT beamline 17-ID using a Dectris Pilatus 6M pixel array detector.

Structure solution and refinement. Intensities were integrated using XDS via Autoproc, and the Laue class analysis and data scaling were performed with Aimless (Kabsch 1983, Evans 2011, Vonrhein, Flensburg et al. 2011). The highest probability Laue class was *4/m*, for either space group *I4* or $I4_1$. The Matthew's coefficient (Vm) and solvent content were estimated to be Vm = 2.3/47% solvent for 1 molecule in the asymmetric unit (Matthews 1968). Data for phasing were collected using the platinum-soaked crystals, at the absorption edge λ = 1.0716 Å (11.570 keV) as determined from an X-ray fluorescence scan. Integrated defraction data from two crystals were scaled together with Aimless in order to increase the multiplicity. Structure solution was conducted using the SAD method with Autosolve via the Phenix interface, which yielded a figure of merit of 0.23 and a Bayes-CC of 0.299 (Adams, Afonine et al. 2010). The Autobuild step of Autosolve produced a model containing 188 of the possible 272 residues which converged at R= 0.35, R_{free} = 0.44 following refinement. Crystals of native RsbU obtained from the Crystal Screen HT condition D5 yielded the highest resolution diffraction (1.7 Å) and were used from this point forward. The resulting model from Autosolve was used for molecular replacement with Phaser against a native RsbU

data set and the top solution was obtained in the space group *I4* (TFZ = 45.8, LLG = 1,836) (McCoy, Grosse-Kunstleve et al. 2007). The model was further improved by automated model building using Arp/wARP and subsequent rounds of structure refinement and manual model building were carried out using Phenix and Coot (Langer, Cohen et al. 2008, Emsley, Lohkamp et al. 2010). Residues P162, L163 and R313 were not modeled due to inadequate electron density. TLS refinement was incorporated in later rounds to model anisotropic atomic displacement parameters (Winn, Isupov et al. 2001, Painter and Merritt 2006). Structure validation was conducted with Molprobity, and relevant crystallographic data are provided in Table 2.1 (Chen, Arendall et al. 2010). Coordinates and structure factors for RsbU were deposited to the Worldwide Protein Databank (wwPDB) with the accession code 6MAB.

Structural alignments and superimposition. Structures of DctB were obtained from the PDB. Apo DctB (3E4Q), Malonate-bound DctB (3E4P), and apo RsbU were aligned to beta sheet residues (120-198) of succinate-bound DctB (3E4O) using the Combinatorial Extension alignment method (O'Hearn, Kusalik et al. 2003). Alignments were performed using the NCBI Blast webserver (Coordinators 2017). Global alignments were performed using the Needleman-Wunch method, and local alignments were performed using BLAST. Proteins with the same fold were identified by performing a TM-alignment (Zhang and Skolnick 2005) of RsbU against the non-redundant structures from the PDB (Yang, Yan et al. 2015).

Table 2.1 X-ray diffraction data and structure refinement

	RsbU (K2PtCl4)	RsbU (Native)
Data Collection		
Cell dimensions		
a, b, c (Å)	96.71, 96.71, 96.49	96.71, 96.71, 96.39
a, β, γ (°)	90.00, 90.00, 90.00	90.00, 90.00, 90.00
Space group	I4	I4
Resolution (Å)a	48.36 - 2.30 (8.91 - 2.30)	48.36 - 1.70 (1.73 - 1.70)
Wavelength (Å)	1.0716	1
Temperature (K)	100	100
Observed reflections	352,983 (33,886)	225,529 (11,050)
Unique reflections	13,526 (1,297)	33,233 (1,758)
<I/σ(I)>a	18.5 (1.7)	17.9 (1.7)
Completeness (%)[a]	100.0 (100.0)	100.0 (100.0)
Multiplicity	26.1 (26.1)	6.8 (6.3)
R_{merge} (%)[a,b]	11.5 (119.6)	6.1 (111.0)
R_{meas} (%)[a,c]	11.7 (122.0)	6.6 (121.1)
R_{pim} (%)[a,c]	2.3 (23.9)	2.5 (47.8)
Refinement		
Resolution (Å)		36.07 - 1.70
Reflections (working/test)		33,231 (3,266)
R_{factor}/R_{free} (%)[d]		16.36/19.73
No. of atoms (protein/ligand/water)		2,101/1/203
Model Quality		
R.m.s. deviations		
Bond length (Å)		0.008
Bond angles ()		0.914
Average B factor (Å)		
All Atoms		23.11
Coordinate error, maximum likelihood (Å)		0.19
Ramachandran Plot		
Most favored (%)		98.11
Additionally allowed (%)		1.89

a. Values in parentheses are for the highest resolution shell.
b. $R_{merge} = S_{hkl} S_i |I_i(hkl) - \langle I(hkl)\rangle| / S_{hkl} S_i I_i(hkl)$, where $I_i(hkl)$ is the intensity measured for the *i*th reflection and $\langle I(hkl)\rangle$ is the average intensity of all reflections with indices hkl.
c. R_{meas} = redundancy-independent (multiplicity-weighted) R_{merge} (Evans, 2011; Diedrichs, 1997).
R_{pim} = precision-indicating (multiplicity-weighted) R_{merge} (Evans, 2006; Weiss, 2001).
d. $R_{factor} = S_{hkl} ||F_{obs}(hkl)| - |F_{calc}(hkl)|| / S_{hkl} |F_{obs}(hkl)|$; Rfree is calculated in an identical manner using 5% of randomly selected reflections that were not included in the refinement

Proteins that had a TM-Score of at least 0.5, when normalized against RsbU, were considered to have the same fold (Zhang and Skolnick 2004, Xu and Zhang 2010).

Virtual screen of human metabolite and chlamydial metabolite libraries. The human metabolites set of compounds was downloaded from the Human Metabolite Database and compounds with molecular weight greater than 300 were discarded (Wishart, Tzur et al. 2007, Wishart, Knox et al. 2009, Wishart, Feunang et al. 2018). The *Chlamydia* metabolites set of compounds was downloaded from the *Chlamydia trachomatis* database in BioCyc (Caspi, Billington et al. 2016). Up to 250 conformers were generated using Omega (version 2.5.1.4) by OpenEye (Santa Fe, NM) (Hawkins, Skillman et al. 2010). The receptor was prepared using APOPDB2RECEPTOR and compounds were docked into using FRED (version 3.2.0.2) at the "Standard" docking resolution (Santa Fe, NM), (McGann 2011). Docked models were refined using SZYBKI (version 1.9.0.3) (Sant Fe, NM). Compounds with docking scores above -6 (chosen based on the docking score of succinate), positive interaction energies, and minimized ligand poses that moved more than 1.5 Å were discarded. The remaining compounds were enriched with malate, malonate, alpha-ketoglutarate, succinate, α-D-glucose, fumarate, glutamate, pyruvate, 3-phosphoglyceric acid, oxaloacetate, and aldohexose stereoisomers. Compounds were prepared using LigPrep by Schrodinger using the default settings (New York, NY) to identify the physiologically relevant protonation states. The receptor was prepared using the protein preparation wizard in Schrodinger, which optimizes the hydrogen bonding and protonation state,

followed by a constrained minimization. These compounds were then docked into the receptor using Glide (release 2017-3) by Schrodinger. Up to 5 docked poses were generated per compound, using extra precision (XP) settings (Friesner, Banks et al. 2004, Halgren, Murphy et al. 2004, Friesner, Murphy et al. 2006). Docked poses were then refined and free energies of binding were predicted using Prime MM-GBSA, allowing flexibility in residues within 8Å of the ligand (Jacobson, Friesner et al. 2002, Jacobson, Pincus et al. 2004). Compounds were selected based on the docking score, MM-GBSA predicted energy, predicted ligand efficiency, and visual inspection of the models.

The docking models of oxaloacetate, alpha-ketoglutarate, and malate to RsbU were generated by docking using Glide XP followed by Prime MM-GBSA refinement, allowing flexibility in residues within 8Å of the ligand.

Surface plasmon resonance. SPR runs were performed on a Biacore T200 (GE Healthcare Life Sciences) with cell culture grade Phosphate Buffered Saline (Corning). Purified $RsbU_{45\text{-}313}$ protein in PBS was immobilized onto a Series S NTA or CM5 sensor chip (GE Healthcare Life Sciences). All ligands were dissolved in PBS and PBS only was used as a negative control. A flow cell with no protein bound was used as a reference cell for all runs. Ligands were injected over the chip for 30 seconds, with a 60 second dissociation period. Binding affinity was manually estimated using the steady state affinity equation:

$$R_{eq} = \frac{C R_{max}}{K_D + C}$$

where R_{eq} is the measured resonance units at steady state binding levels, C is the concentration of the ligand, and R_{max} is the maximum binding capacity determined for each respective ligand assuming a 1:1 ratio of binding to protein.
Data was analyzed using Biacore T200 Software (version 3.0).

Differential scanning fluorimetry (DSF). $RsbU_{45-313}$ was purified as described above and buffer exchanged into PBS (Corning). DSF were performed with SyproOrange (Invitrogen) in 384-well plate (Roche) format (Niesen, Berglund et al. 2007). The following potential ligands were tested: succinate, malonate, glutamate, alpha-ketoglutarate, fumarate, oxaloacetate, malate, 2-phosphoglycerate, glucose, pyruvate, phosphoenolpyruvate, and ATP (Sigma-Aldrich). All ligands were dissolved in PBS. Compounds were added to each well, followed by DSF buffer HEPES-NaOH pH7.5 (100mM), and a 10X SyproOrange dye. Reliable baselines for Tm shifts were established using 10X SyproOrange and 10 μM $RsbU_{45-313}$. The mixture was heated from 20 to 85 °C. Melting curves were analyzed on Roche Tm Analysis Software.

Isothermal titration calorimetry (ITC). $RsbU_{45-313}$ (30 μM) was purified as described above and buffer exchanged into PBS (Corning). Alpha-ketoglutarate, malate, oxaloacetate, malonate, and succinate (Sigma-Aldrich) were dissolved in the same PBS used for the buffer exchange of the $RsbU_{45-313}$ protein at a concentration of 30 mM. ITC was performed on a MicroCal PEAQ-ITC (Malvern Panalytical and analyzed using MicroCal ITC Analysis Software (version 1.21).

Growth Curves. An EMS mutant strain of *Chlamydia trachomatis* L2 was obtained from the Valdivia lab at the Duke University Medical Center (Nguyen and Valdivia 2012, Kokes, Dunn et al. 2015). A confluent monolayer of L929 mouse fibroblast cells was infected with an MOI of 0.5 mutant or wild-type chlamydial cells with centrifugation and using Hanks' Balanced Salt Solution with calcium and magnesium (Corning). After centrifugation, the HBSS was removed from the cells and replaced with RPMI (Corning) supplemented with 5% FBS (Millipore), 10 μg/mL gentamycin, and 1 μg/mL cycloheximide. For the growth curves with the addition of chemical inhibitors, the BKA and HQNO were added into the RPMI at the time of infection. HQNO was added at a final concentration of 1μM. BKA was added at a final concentration of 0.25 μM. The infected cells were incubated at 37°C, 5% CO_2 until harvested. Total DNA was harvested from infected cells at 0, 12, 24, 36, 48, and 72 hours post infection. DNA was harvested by adding 200 μl of 5mM DTT, 200 μL of Buffer AL from a Blood and Tissue Kit (Qiagen), and 20 μl of Proteinase K (Qaigen) to each well and incubated at room temperature for 10 minutes. Wells were then scrapped and washed twice with the lysate before being collected. Following harvest, the lysate was heated at 56°C for 10 minutes and then frozen until all time point samples were collected. The remainder of the DNA isolation was performed using the Blood and Tissue Kit (Qiagen).

After DNA isolation was complete, the number of host genome copies and *Chlamydia* genome copies was determined by Droplet Digital PCR (ddPCR) (Hindson, Ness et al. 2011). *Chlamydia* genome copies were assessed by the

amplification of *secY,* and host cell genome copies were assessed by amplification of *rpp30*. Quantification of copy numbers was determined using Quantasoft software version 1.7 (Bio-Rad).

Progeny assay. L929 cells were infected with wild-type or RsbU* mutant strains of *C. trachomatis* L2 with BKA (0.25 μM) and HQNO (1μM) added at the time of infection when indicated. At 36 hpi, cells were either fixed and stained using MicroTrack *C. trachomatis* culture confirmation test (Syva Co., Palo Alto, CA), or lysed with water and passaged onto a new monolayer of host cells. An additional 36 hours after passaging, the infections were fixed and stained. Fold changes were calculated by counting the IFUs of the infections after the first 36 hours and comparing to the IFU counts after the infections were passaged.

Immunofluorescence microscopy. L929 cells were grown to confluency in an 8-well ibiTreat μ-Slide (Ibidi, Martinsried, Germany) and were infected with respective wild-type *C. trachomatis* L2*,* RsbU* mutant, RsbU+ complemented strain, or *ct575*::Tn *bla* strain. Chemical inhibitors (HQNO and BKA) were added to the indicated conditions immediately after infection. At 24 and 72 hpi, infected cells were fixed with 100% methanol for 10 minutes at room temperature. Cells were washed once with HBSS and again with PBS then stained using 180μl of the MicroTrack *C. trachomatis* culture confirmation test (Syva Co., Palo Alto, CA) diluted 1:40 in PBS 1 hour and 50 minutes at room temperature. 20μl of 1μM 4', 6-diamidino-2-phenylindole (DAPI) diluted 1:100 in PBS was then added to wells and

allowed to stain for 10 minutes, room temperature in the dark. Stain was then removed, and the cells washed with PBS. A final overlay of Vectashield antifade mounting medium (Burlingame, CA) was added and slides were immediately imaged. Cells were visualized on an Olympus IX81/3I spinning disk confocal inverted microscope at 150X magnification and captured on an Andor Zyla 4.2 sCMOS camera (Belfast, Northern Ireland). Microscope and camera were operated using SlideBook 6 software (Intelligent Imaging Innovations, Denver, USA). Exposure time remained consistent for all fields captured, with exposure for DAPI at 2 seconds, OmpA 3 seconds, and cytoplasm 3 seconds. Seven Z-stack images at 0.3μm apart were taken per field imaged. Images were processed in SlideBook 6 and a No Neighbors Deconvolution with a subtraction constant of 0.4 was applied to all images. Images represent a maximum projection over the Z axis of all 7 acquired stacks for each field shown.

Whole genome sequencing. Chlamydial DNA was extracted from RsbU* EBs. Briefly, 200uL of renografin-purified EBs were pelleted, resuspended in RQ1 DNase buffer, water and RQ1 Dnase, incubated and stopped as per manufacturer's instructions (Promega, Madison, WI). 2uL DTT was added to the EBs and DNA was extracted using the Qiagen Blood and Tissue DNA Extraction Kit (Qiagen, catalog number 69506) with following steps that optimize for DNA sequencing. Libraries were generated using the NEBNext Ultra II DNA library Prep kit (New England Biolabs, catalog number E7645S). DNA was sequenced by the Illumina Nextseq MO-SR150bp. Over 91 million reads were generated with a mean

quality score of 32.78. Approximately 3% of reads were mapped to the Chlamydia trachomatis L2/434 (NC_010287) parent genome through reference-guided assembly using the Geneious assembler with up to 5 iterations. Total average coverage for the RsbU* genome was 400x. Through direct comparison with the reference genome, 33 SNPs were evaluated, including the RsbU* truncation which was confirmed to be a monoclonal polymorphism as 98.6% of reads at that site confirmed the SNP. For the 32 other SNPs discovered in the RsbU* genome, potential effects on secondary structure were analyzed using Geneious secondary structure predictions based on the EMBOSS 6.5.7 tool garnier or signal cleavage site prediction with sigcleav.

Generation of RsbU complemented mutant (RsbU+) by lateral gene transfer. A confluent layer of Vero monkey kidney cells in a T-75 cell culture flask was infected with 100µl of RsbU* lysate in 1X SPG buffer. Briefly, the monolayer was washed once with HBSS, and 10ml of HBSS was added to the culture flask along with RsbU* lysate. Cells were spun at 550XG for 30 minutes at room temperature. Infection material was aspirated from the flask and 15ml of RPMI containing 1µg/ml cycloheximide was added to the flask. Infected cells were incubated at 37°C for 85 hours post-infection. RsbU* infected cells were then co-infected, as described above, with a *C. trachomatis* mutant containing a transposon insertion in *ct575* (*ct575*::Tn *bla*). Co-infected cells were incubated another 48 hours at 37°C. Cells were then lysed by water lysis and transferred to Vero cell monolayers in a 24-well plate with each well containing variable concentrations of rifampicin and ampicillin

to facilitate successful lateral gene transfer of the *bla* resistance marker of the *ct575*::Tn into the RsbU* mutant clone. After 24hpi, WT-like *Chlamydia* growth was identified by phase contrast microscopy in a well containing 0.01µg/ml rifampicin and 5 ug/ml ampicillin. After 32hpi, cells in the well containing growth were lysed by water and the lysate then underwent two rounds of limiting dilution in a 96-well plate to isolate a clonal population of RsbU complemented mutant recombinants. Mutants with dual antibiotic resistance to rifampicin and ampicillin were evaluated by PCR amplification and sequencing for the genotype of the *rsbU* and *ct163* genes, followed by the other SNPs present in the EMS mutant genome to determine where the area of homologous recombination occurred.

Transcriptional analysis. A confluent monolayer of L929 cells were infected with either WT L2 *C. trachomatis* or the RsbU* mutant strain at an MOI of 1. At 24 hpi, the infections were harvested for RNA using TRIzol (Invitrogen). RNA was purified by phenol/chloroform extraction followed by DNase treatment with TURBO DNase (Invitrogen). A final purification step was performed using the RNeasy Mini Kit (Qiagen) before converting the RNA to cDNA using the High-Capacity cDNA Reverse Transcription Kit (Thermo Fisher). DNA contamination was assessed using a no reverse transcriptase control reaction. After gDNA depletion has been confirmed for all RNA samples, transcript counts are quantified using ddPCR (Bio-Rad). gDNA taken from the infections was used to normalize the transcript counts.

Results

CT588 has a unique domain organization with conserved cytoplasmic RsbU phosphatase domain and an uncharacterized domain predicted to localize to the periplasm. CT588 is a 650-residue protein with a carboxyl-terminal domain (269-645) that has high sequence similarity to the RsbU superfamily phosphatases (Figure 2.2). This cytoplasmic domain contains HAMP (residues 338-385) and PP2C serine phosphatase (residues 422-625) subdomains with Smart E-values of 4.35×10^{-5} and 3.09×10^{-72}, respectively (Schultz, Milpetz et al. 1998). The HAMP and PP2C domains together comprise a conserved RsbU family domain (residues 269-645, E-value 5.23×10^{-99}) (Schultz, Milpetz et al. 1998) in support of original protein annotation. HAMP domains function as linker regions in order to modulate the transduction between sensor and effector domains (Hulko, Berndt et al. 2006). This transduction can occur with cytosolic as well as membrane associated proteins (Elliott, Zhulin et al. 2009). PP2C domains are metal-dependent protein phosphatases (PPMs), which catalyze the dephosphorylation of either a serine or threonine residue (Shi 2009).

BLAST search using the N-terminus of CT588 (1-315) revealed sequence similarity to proteins only encoded by *Chlamydia*; however, the predicted function of these orthologs were unknown. In contrast to other RsbU family members, CT588 has two transmembrane helices that flank residues 40 through 315, which implies that this domain is localized to the periplasm. Based on sequence similarities, it is expected that a periplasmic signal is transduced by the HAMP domain to regulate the PP2C phosphatase activity of CT588. However, while this

A

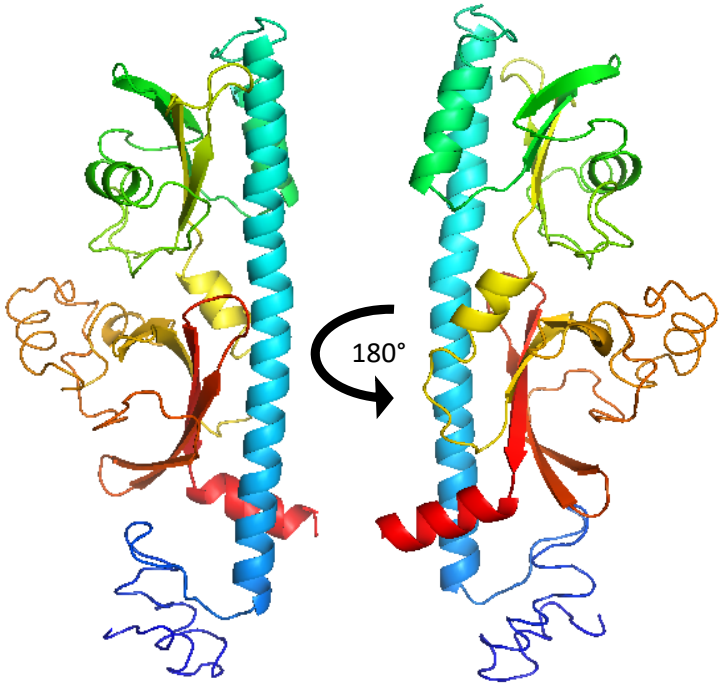

B

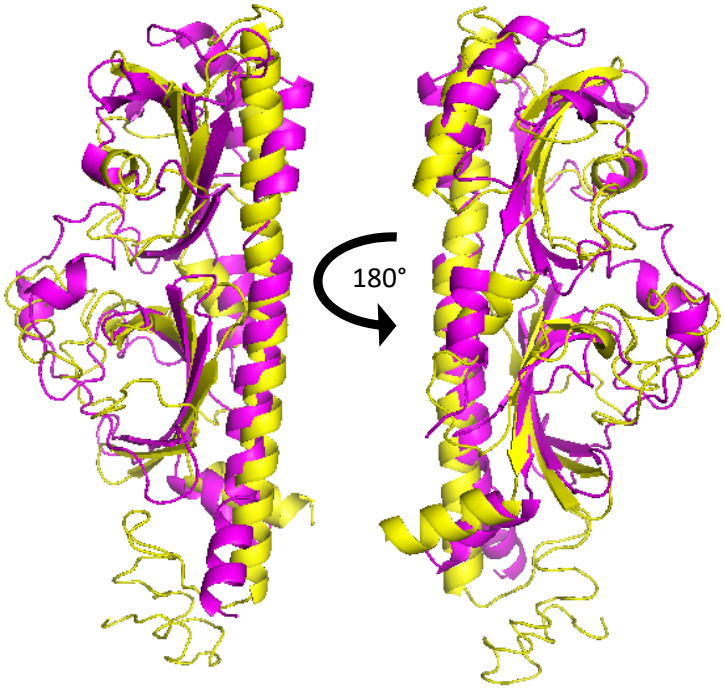

Figure 2.3 I-TASSER model of $RsbU_{1-315}$ shares structural similarity to periplasmic domain $RsbU_{45-313}$ crystal structure. A) I-TASSER protein structure model with residues 1 through 315 of *C. trachomatis* RsbU. **B)** Structure overlay of $RsbU_{45-313}$ crystal structure (magenta) and I-TASSER model (yellow). Structure comparison has Z-score of 14.4 and a RMSD of 4.0 Å.

domain organization of CT588 appears to be unique among bacteria, this protein is widely conserved among *Chlamydiaceae* family.

I-TASSER was used to model protein structures for the N-terminus RsbU (Yang, Yan et al. 2015). Four structural models with relatively poor C-scores (range from -3.19 to -3.84) were generated reflecting the absence of sequence similarity to PDB templates. These models predict two protein domains that are tethered to a single alpha helix, which extends the length of these domains (Figure 2.3). Using these models, DALI searches of the Protein Data Base (PDB) were performed to identify potential structural homologs and associated functional information. This search revealed that the top matches (Z-score > 15; range 16-21) were all periplasmic-localized chemoreceptors with PAS-like domains attached to kinase or methyl-accepting chemotaxis-like domains by linker regions such as HAMP or HisKA domains from diverse bacteria (Table 2.2). Many of these I-TASSER model structural homologs also had identified ligands that include L-Arginine, C4 dicarboxylates, and asparagine.

A 1.7 Å crystal structure of the RsbU periplasmic domain reveals similarity to periplasmic domains of dicarboxylate binding sensor proteins. A crystal structure of the CT588 (RsbU) periplasmic domain was solved in order to better understand its function. A construct comprised of residues 45-313 ($RsbU_{45-313}$) was recombinantly expressed and purified via affinity and size exclusion chromatography (Figure 2.4) and then used to screen for crystallization conditions which led to a 1.7 Å resolution crystal structure.

Table 2.2 Non-redundant structural matches for $RsbU_{45-313}$ from *C. trachomatis*.

Hit Rank	Protein Name	Z-score	RMSD (Å)	% ID to $RsbU^{45-313}$	% ID to binding pocket (residues 111-189)	Best Match PDB code
1	DctB:succinate *V. cholerae*	17.8	3.2	13	6	3by9
2	DctB:malonate/succinate *S. meliloti*	16.5	3.7	12	0	3e4p
3	PctA:L-Met *P. aeruginosa*	15.1	3.71	12	0	5ltx
4	vpHK1S-Z8:acetate *V. parahaemolyticus*	14.5	3.8	9	0	2pj7
5	PctB:L-Gln *P. aeruginosa*	14.3	3.5	11	0	5lto
6	Tlp3:isoleucine *C. jejuni*	13.8	4	15	16	4xmq
7	Mlp37:alanine *V. cholera*	13.8	4.4	11	0	5avf
8	PctC:GABA *P. aeruginosa*	13.8	3.5	12	0	5ltv
9	Histidine kinase *R. palustris*	13.5	4.1	9	8	3lif
10	McpN *V. cholerae*	13.5	4.1	11	0	3c8c
11	KinD:pyruvate *B. subtilis*	13.2	3.8	12	0	4jgo
12	Dret_0059:cysteine *D. retbaense*	13	4.9	11	0	5ere
13	Tlp1 *C. jejuni*	12.8	4.4	13	0	4wy9
14	AHK4:isoentyladenine *A. thaliana*	11.5	4	11	5	3t4t

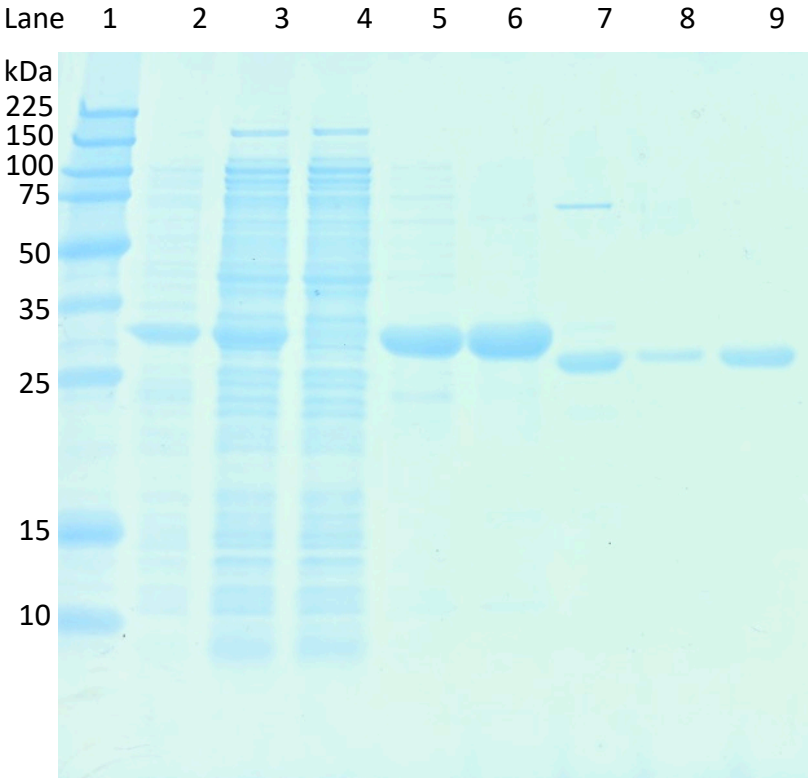
Lane 1 2 3 4 5 6 7 8 9
kDa
225
150
100
75
50
35
25
15
10

Figure 2.4 SDS-PAGE gel showing purification of $RsbU_{45-313}$. Lane 1, protein marker; lane 2, lysate supernatant; lane 3, lysate pellet; lane 4, IMAC flow-through; lane 5, IMAC elution; lane 6, post-buffer exchange; lane 7, post-TEV protease treatment; Lane 8, post-reverse nickel column; lane 9, SEC column peak fraction.

$RsbU_{45\text{-}313}$ adopts a mixed α/β fold with two similar PAS subdomains, each containing antiparallel β-strands flanked by pairs of α-helices (Figure 2.5). The proximal domain contains five long and two short (two residues) β-strands and the distal domain is composed of five long and one short strand. The secondary structure elements for RsbU were calculated using DSSP (Kabsch 1983). Interestingly, the proximal and distal subdomains exhibit a high degree of structural similarity, reflected by a root mean square deviation (RMSD) value of 1.37 Å for 47 aligned C^{α} atoms (Z=7.73) (Bryant and Altschul 1995, Nguyen, Tan et al. 2011). Additionally, the total accessible surface area of the subdomains, calculated using Areaimol via CCP4 (Winn, Ballard et al. 2011), are similar with 5,021.6 Å for the distal (K114-D192) and 5,880.8 Å for the proximal subdomain (K210-E302). Another interesting feature in the RsbU structure is that helix α1 is kinked near I54/T55 (Figure 2.5A, right panel). The angle between the two portions of this helix defined by Q45-S53 (α1) and S56-T72 (α1') was found to be 36.7° as calculated using least-squares fitting of Cα atoms with Pymol.

A DALI search comparing the $RsbU_{45\text{-}313}$ crystal structure to all Protein Database (PDB) entries identified 14 non-redundant matches based on global structural similarity (Z-score >3.0; Table 2.2). The top two hits (Z-scores >15.5) were of the sensor domain from the histidine kinase DctB in *Vibrio cholerae* and *Sinorhizobium meliloti* (3BY9 and 3E4O, respectively), which binds to C_4 di-carboxylates (e.g. succinate). Looking broadly at the domain organization of RsbU

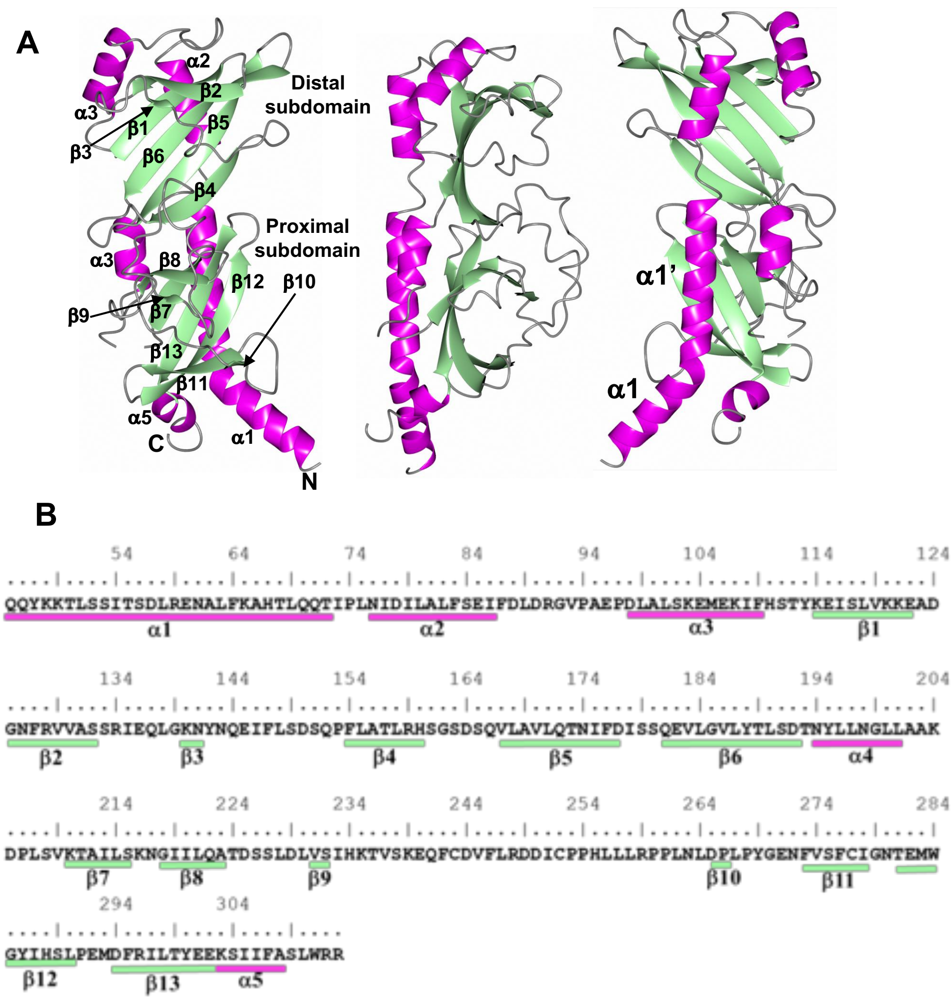
A
α3
α2
β2
Distal
subdomain
β1
β3
β5
β6
β4
Proximal
subdomain
α3
β8
β12
β10
β9
β7
β13
β11
α5
C
α1
N
α1'
α1
B
54 64 74 84 94 104 114 124
QQYKKTLSSITSDLRENALFKAHTLQQTIPLNIDILALFSEIFDLDRGVPAEPDLALSKEMEKIFHSTYKEISLVKKEAD
α1 α2 α3 β1
134 144 154 164 174 184 194 204
GNFRVVASSRIEQLGKNYNQEIFLSDSQPFLATLRHSGSDSQVLAVLQTNIFDISSQEVLGVLYTLSDTNYLLNGLLAAK
β2 β3 β4 β5 β6 α4
214 224 234 244 254 264 274 284
DPLSVKTAILSKNGIILQATDSSLDLVSIHKTVSKEQFCDVFLRDDICPPHLLLRPPLNLDPLPYGENFVSFCIGNTEMW
β7 β8 β9 β10 β11
294 304
GYIHSLPEMDFRILTYEEKSIIFASLWRR
β12 β13 α5

Figure 2.5 Structure of RsbU periplasmic domain (residues 43-313). **A**) Tertiary structure showing helices (magenta) and b-sheets (green). The middle and right panels are views rotated 90^{o} and 180^{o} about the vertical direction. The two regions of the kinked helix are denoted as a1 and a1'. **B**) Secondary structure annotation relative to the RsbU sequence.

from *C. trachomatis* compared to DctB in *V. cholerae* and *S. meliloti,* these proteins do appear similar in respect to the length of the periplasmic domain and the presence of two flanking transmembrane domains (Figure 2.2). DctB is the membrane-bound sensor histidine kinase of a two-component system in Rhizobia, *Vibrio*, *Escherichia,* and other bacteria that sense extracellular C_4-dicarboxylates and reactively regulate their TCA cycle, one of the central metabolic processes (Janausch, Zientz et al. 2002). C_4-dicarboxylates are four-carbon small molecules, such as the TCA cycle intermediates malate and oxaloacetate. Once DctB senses its ligand, it phosphorylates and thereby activates the system's response regulator DctD. Activated DctD then activates the expression of the σ^{54}-dependent promoter of a C_4-dicarboxylate:cation symporter, DctA (Zhou, Nan et al. 2008, Nan, Liu et al. 2010, Liu, Yang et al. 2014). Protein homologs of DctB, each of which are membrane bound kinases with periplasmic sensor domains, regulate a variety of responses beyond the TCA cycle as well (Cheung and Hendrickson 2008, Chang, Tesar et al. 2010, Liu, Machuca et al. 2015).

Nine of the other matches from the DALI search were structures also co-crystalized with ligands. These ligands range from amino acids and other carboxylates to nucleic acids. The remaining three protein matches have no ligands solved in their binding site. These 14 structural matches all are predicted to be membrane-bound proteins with PAS-like domains attached to kinase or methyl-accepting chemotaxis-like domains by linker regions such as HAMP or HisKA domains (Schultz, Milpetz et al. 1998). They regulate a variety of downstream processes such as chemotaxis, sporulation, and differential

metabolite utilization (Cheung and Hendrickson 2008, Zhang and Hendrickson 2010, Wu, Gu et al. 2013, Liu, Machuca et al. 2015, Nishiyama, Takahashi et al. 2016).

Residues in the DctB binding pocket are not conserved in the putative binding pocket of $RsbU_{45-313}$. As noted above, RsbU shares the highest degree of structural similarity with DctB. Superposition of DctB from *V. cholera* (3BY9) and *S. meliloti* (3E4O) with RsbU using Gesamt (Krissinel 2012) yielded RMSD deviations of 2.58 Å and 3.38 Å between Cα atoms for 205 and 196 residues aligned, respectively (Figure 2.6A and B). The RMSD deviation between Cα atoms for RsbU and apo DctB (3E4Q) is 3.45 Å (196 residues). Given the structural similarity with DctB, we set out to determine if a similar ligand binding site was present in RsbU. DctB crystal structures from *V. cholerae* and *S. meliloti* have both been obtained with succinate bound in the ligand-binding pocket (Cheung and Hendrickson 2008, Zhou, Nan et al. 2008). Additionally, a structure of *S. meliloti* DctB has also been obtained as a complex with malonate. Although the structural similarity between $RsbU_{45-313}$ and DctB from *V. cholerae* is greater, the availability of both apo and ligand-bound structures for DctB from *S. meliloti* allowed for a more in-depth comparison with $RsbU_{45-313}$ using these structures. Zhou *et al.* (Zhou, Nan et al. 2008) describe DctB as having an opened apo/C_3-dicarboxylate (malonate) bound structure form, and a closed form when bound to a C_4-dicarboxylate. The superposition of $RsbU_{45-313}$ and apo and succinate-bound DctB is depicted in Figure 2.6C which highlights the ligand binding region.

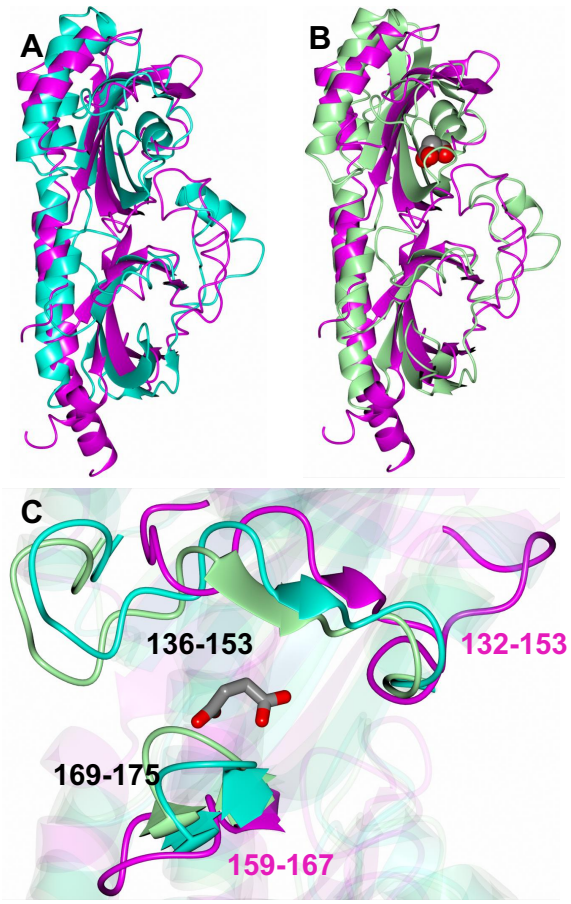
A
B
C
136-153
132-153
169-175
159-167

Figure 2.6 Superposition of RsbU (magenta) with A) **Apo (3E4Q, cyan) and B) succinate-bound (3E4O, green) DctB structure.** The succinate molecule is rendered as spheres to highlight the ligand binding region. **C**) Zoomed in view of the ligand binding pocket with succinate rendered as cylinders. There are evident differences between RsbU and DctB, which is more enclosed. However, structural comparison between the apo and succinate-bound forms of DctB from *S. meliloti* reveal that the linker between strands 3 and 4 (residues 169-175) shift a distance of 2.2 Å in towards the binding pocket when succinate is bound, thereby facilitating pocket enclosure (Zhou *et al*).

Specifically, when DctB binds to a C_4-dicarboxylate, residues 136-153 and 169-175 close around the ligand. For DctB the binding of succinate leads to a 2.2Å movement in residues 169-175 towards the ligand (Zhou, Nan et al. 2008). However, for RsbU these loop regions, which correspond to 132-153 and 159-167, are in a more open position suggesting that a conformational change may occur upon ligand binding.

Despite the structural similarity, there is less than 20% sequence identity between RsbU and DctB sensor domains, particularly around the binding site as a BLAST search yielded no significant conservation of this region. Additionally, the ligand binding pocket of DctB contains a large patch of positively charged residues whereas RsbU has both positive and negatively charged regions (Figure 2.7). Relative to the superimposed structures, S161 and S163 of RsbU are similarly located relative to T171 and S173 of DctB. Additionally, Y142 of RsbU is positioned in a similar location relative to Y149 of DctB. The position of several charged residues within the binding site differ between DctB and RsbU, as highlighted in Figure 2.7. In RsbU there are no positively-charged residues in the corresponding location of R152 which interacts with succinate (Figure 2.7C). Instead there is a negatively-charged residue, E145, located in a similar region. Additionally, K197 of DctB, which is located on the middle β-strand of the binding site β-sheet, forms a salt bridge with the dicarboxylate ligand. While there is not a positively-charged residue in the corresponding location on the same β-strand, K114 of RsbU is located on a neighboring β-strand (Figure 2.7D). Overall, RsbU contains eight charged residues at or around the putative ligand binding site. These include

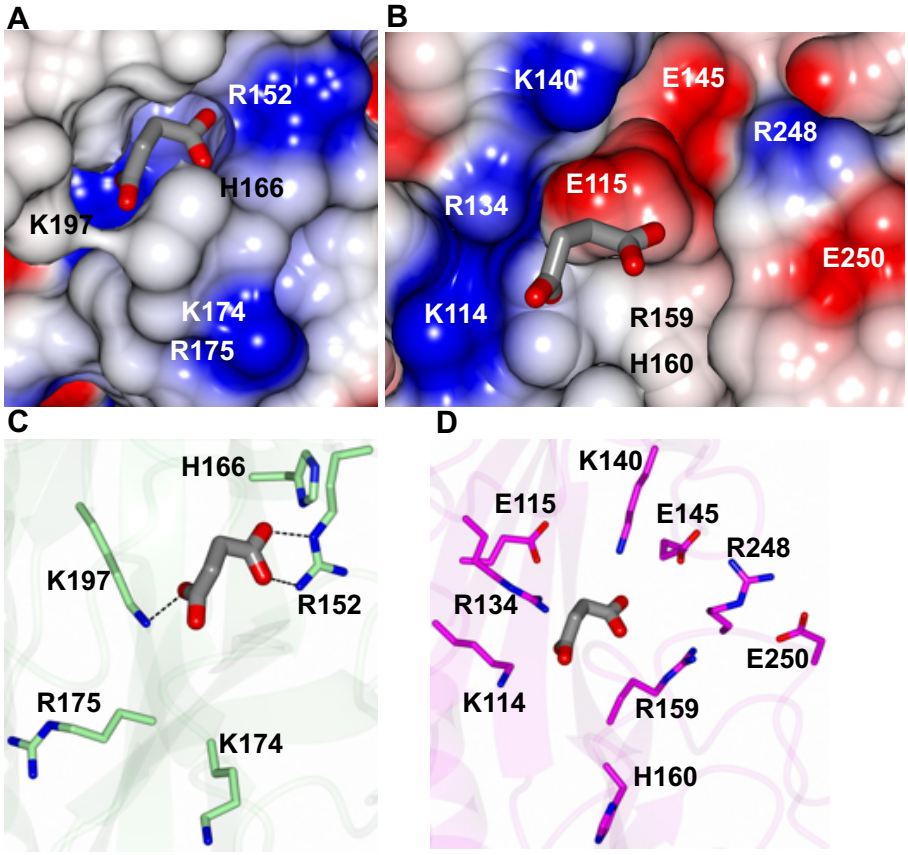
A
R152
H166
K197
K174
R175
B
K140
E145
R248
E115
R134
E250
K114
R159
H160
C
H166
K197
R152
R175
K174
D
K140
E115
E145
R248
R134
E250
K114
R159
H160

Figure 2.7 Residues in the ligand binding pocket of DctB (3E4O) and putative site of RsbU. The succinate molecule is rendered as gray cylinders. A) Electrostatic surface for DctB and B) RsbU. C) Charged residues for DctB showing hydrogen bond interactions with succinate (dashed lines). D) Charged residues in the putative ligand binding pocket of RsbU.

negatively-charged E145, E115, E250 and positively-charged residues K114, R134, K140, and R248 lining the perimeter of the pocket.

I-TASSER *ab initio* model of CT588 closely matches crystal structure. A pairwise structure comparison of the I-TASSER model and the $RsbU_{1-315}$ structure reveals a robust Z-score of 14.4 and RMSD of 4.0 Å (Figure 2.3). These data support that, despite extremely low sequence similarity between $RsbU_{1-315}$ and other proteins (maximum sequence similarity below 2% of the templates), I-TASSER was effective in accurately modeling this protein. This *ab initio* protein modeling is particularly challenging, especially for proteins over 200 amino acids (Zhang, Yang et al. 2016). Additionally, comparison between DALI searches of I-TASSER and crystal structure highlights that more than half of the top 15 proteins with structural similarity are shared, including DctB (Table 2.2).

Virtual screen of human metabolite and chlamydial metabolite libraries yielded a small list of potential ligands for further testing. While the structure of RsbU is most similar to DctB, it shares the same fold as several other proteins that bind ligands other than dicarboxylates, such as amino acids, nitrogenous bases, and pyruvate (Table 2.3). Preliminary docking studies indicated that the C_4-dicarboxylate succinate could interact with the positively charged sidechains of K140 and R134, however, these residues are located on the outer edge of the binding pocket, distal to where a tight-binding ligand would be expected to bind. In order to rationally select additional compounds for testing, a virtual screen was

Table 2.3 Potential ligands tested for $RsbU_{45-313}$ binding.

Ligand	Compound	Mass in Daltons
Succinate	Sodium Succinate Dibasic Hexahydrate	116
Malonate	Sodium Malonate Dibasic Monohydrate	102
Glutamate	L-Glutamic Acid monosodium salt monohydrate	147
Alpha-ketoglutarate (2-oxoglutarate)	Alpha-Ketoglutaric Acid	146
Fumarate	Fumaric Acid	114
Oxaloacetate	Oxaloacetic Acid	130
Malate	D-Malic Acid	132
2- phosphoglycerate	L-2-Phosphoglyceric Acid Disodium Salt Hydrate	186
Glucose	D-(+) Glucose	180
Pyruvate	Sodium Pyruvate	87
Phosphoenolpyruvate	Phospho(enol)pyruvic Acid Monopotassium Salt	165
ATP	Adenosine 5'-triphosphate disodium salt hydrate	507
Mannitol	Mannitol	182
Lysine	L-Lysine	146
Isoleucine	L-isoleucine	131
Succinyl-CoA	Succinyl coenzyme A sodium salt	867
Pyridoxine	Pyridoxine, Vitamin B6	169
Glucosamine	Glucosamine hydrochloride	179
D-Mannose	D-(+)-Mannose	180
5-hydroxy-L-lysine	DL-5-hydroxylysine hydrochloride	162
D-talose	D-(+)-talose	180
D-galactose	D-(+)-galactose	180
D-gulose	D-(+)-gulose[1]	180
D-idose	D-idose[1]	180
7-8-dihydroneopterin	7-8-dihydroneopterin[2]	255
D-allose	D-allose[1]	180

All compounds were acquired from Sigma Aldrich unless otherwise specified.
[1] Carbosynth (United Kingdom)
[2] Toronto Research Chemicals (Canada)

performed against compounds that are more likely to interact with by RsbU; namely human metabolites and metabolites associated with *Chlamydia trachomatis*.

Over 100,000 compounds were computationally screened, and a final library of 26 potential ligands was selected for further testing. This library was composed of the top scoring compounds from the human and chlamydial metabolite libraries supplemented with TCA cycle intermediates or derivatives present in *Chlamydia* (Table 2.3). The addition of the TCA cycle intermediates or derivatives was included in order to fully investigate the possibility of the chlamydial RsbU protein binding to a molecule of similar structure and function as the DctB ligand.

Binding studies support TCA cycle intermediates as RsbU ligands. Surface plasmon resonance (SPR) was selected as a method of screening the library of potential ligands for binding to the $RsbU_{45\text{-}313}$ periplasmic domain due to its sensitivity and ability to determine estimates of binding kinetics (Jason-Moller, Murphy et al. 2006). In initial screening with the 26 potential ligands at 100 μM and 1 mM concentration, binding was only observed for alpha-ketoglutarate, malate, and oxaloacetate (Figure 2.8). Subsequently, dose-dependent binding studies of these three potential ligands were performed. K_D values were estimated to be 419 ± 76 μM, 459 ± 91 μM, and 396 ± 69 μM for alpha-ketoglutarate, malate, and oxaloacetate, respectively (Table 2.4).

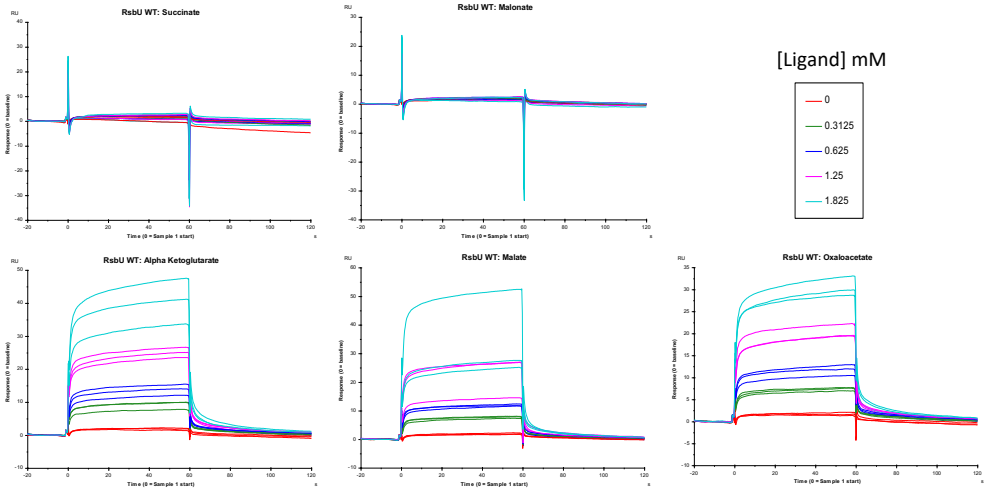
RsbU WT: Succinate
RsbU WT: Malonate
[Ligand] mM
0
0.3125
0.625
1.25
1.825
RsbU WT: Alpha Ketoglutarate
RsbU WT: Malate
RsbU WT: Oxaloacetate

Figure 2.8 SPR dose-dependent binding curves. Alpha-ketoglutarate, malate, and oxaloacetate show dose-dependent binding to $RsbU_{45-313}$, while succinate and malonate, the ligands found to bind to DctB, do not appear to be binding by SPR.

Table 2.4 Binding kinetic estimations (μM) for RsbU proteins

	Alpha-ketoglutarate		Malate		Oxaloacetate	
Protein	K_D	SD	K_D	SD	K_D	SD
WT $RsbU_{45-313}$	419	76	459	91	396	69
R134A	526	84	601*	62	379	57
Q137A	548	112	666	233	459	96
K140A	597*	120	836*	54	569*	144
K140A/R134A	558*	68	741*	49	580*	97

SD = Standard deviation

* p-value < 0.05 when compared to wild-type protein binding by a two-tailed student's t-test.

Docking with the alpha-ketoglutarate, malate, and oxaloacetate to RsbU identified specific residues at the putative binding site that could be coordinating ligand binding (Figure 2.9). Residues R134, Q137, and K140 were predicted to interact with alpha-ketoglutarate, malate, and oxaloacetate. R248 is also in proximity to the ligands. Based on these predicted residue interactions, individual alanine substitutions in the $RsbU_{45\text{-}313}$ protein were created for R134, Q137, and K140, as well as a double-substitution with R134 and K140. SPR was performed with the alanine-substituted proteins compared to the wild-type protein. Table 2.4 shows the average estimated K_D values for the three TCA cycle intermediates with each of the protein variants. Both the signal-substitution variant, K140A, and the double-substitution variant, K140A/R134A, showed statistically-significant, albeit limited, decreases in binding affinity for the three TCA cycle intermediates. The R134A variant displayed a statistically-significant decrease in binding affinity for malate as well as lower binding capabilities to alpha-ketoglutarate (p-value 0.082). Similarly, the Q137A single-substitution also had decreases in binding affinity for alpha-ketoglutarate and malate (p-value <0.1).

Orthogonal analyses using differential scanning fluorimetry (DSF) was also performed with of potential ligands (Niesen, Berglund et al. 2007). Significant stabilizing temperature shifts were observed with 5 mM and 10 mM additions of alpha-ketoglutarate and malate (Table 2.5). Oxaloacetate only showed a significant positive temperature shift at the highest ligand concentration tested and only in one of two biological replicates. Additionally, a single trial of isothermal titration calorimetry (ITC) resulted in binding curves indicating stronger ligand

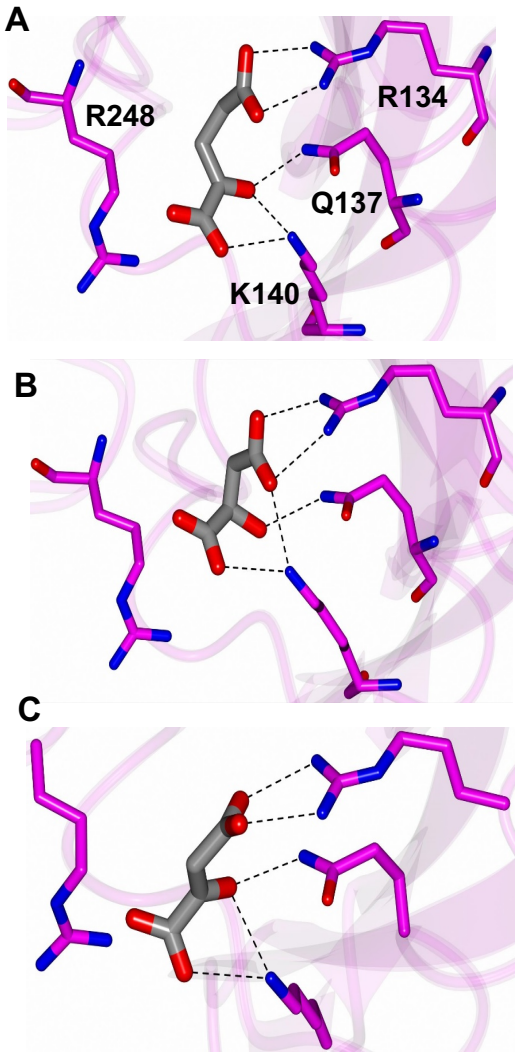
A
R248
R134
Q137
K140
B
C

Figure 2.9 Ligand docking showing the predicted binding modes of A) ketoglutarate, B) malate, and C) oxaloacetate in the binding pocket of RsbU. All the ligands are rendered as gray cylinders. Interacting residues are annotated in panel A.

Table 2.5 Average ΔTm of $RsbU_{45-313}$ with potential ligands.

	Concentration (mM)							
Ligand	1.25		2.5		5		10	
Alpha-ketoglutarate	Average ΔTm	SD	Average ΔTm	SD	Average ΔTm	SD	Average ΔTm	SD
Biological Replicate 1	-0.16	0.03	-0.17	0.07	0.15	0.17	1.64*	0.33
Biological Replicate 2	-0.05	0.11	0.11	0.42	1.42*	0.38	3.16*	0.10
Malate								
Biological Replicate 1	0.02	0.01	0.21	0.06	0.52*	0.07	2.35*	0.16
Biological Replicate 2	0.33	0.20	0.28	0.06	1.45*	0.87	1.64*	0.11
Oxaloacetate								
Biological Replicate 1	-0.05	0.05	0.05	0.07	0.27	0.07	1.75*	0.27
Biological Replicate 2	-0.02	0.03	0.11	0.51	-1.33	0.25	0.29	0.20
Malonate								
Biological Replicate 1	-0.09	0.03	-0.24	0.02	-0.27	0.04	-0.59	0.09
Biological Replicate 2	-1.27	1.19	0.04	0.25	0.10	0.49	-0.83	0.14
Succinate								
Biological Replicate 1	0.03	0.14	-0.25	0.04	-0.30	0.03	-0.57	0.01
Biological Replicate 2	-0.05	0.34	-0.25	0.21	-1.50	0.78	-0.20	0.34

Values in green are positive temperature shifts. Technical triplicates were performed for each biological replicate.
* p-value < 0.05 by two way ANOVA with Dunnett's multiple comparisons test post hoc

binding with alpha-ketoglutarate, malate, and oxaloacetate (K_D values of 25.8 μM, 22.0 μM, 55.5 μM, respectively), but not succinate or malonate (data not shown). Overall, all three of these binding studies support the binding of the RsbU periplasmic domain to TCA cycle intermediates alpha-ketoglutarate, malate, and oxaloacetate.

Nonsense mutation in *rsbU* gene suggests importance of Rsb pathway in chlamydial growth. Based on the three ligands and the potential for the regulation of ATP generation (oxidative phosphorylation), it was hypothesized that the absence of this sensing system could be detrimental to the growth of *Chlamydia*. To evaluate this hypothesis, a *C. trachomatis* L2 EMS mutant (CTL2M401) was obtained (Dr. R. Valdivia; Duke University) that contained a SNP causing a nonsense mutation at W284 in the *ct588* gene coding for the RsbU protein (Nguyen and Valdivia 2012, Kokes, Dunn et al. 2015). This nonsense mutation occurs towards the C-terminal end of the periplasmic domain resulting in a truncated protein lacking the cytoplasmic domain. Western blot analysis using antibodies raised against the periplasmic domain supported the absence of the full-length RsbU, as well as any lack of truncated product, in this mutant strain and is deemed a null mutant (RsbU*; Figure 2.10A). Growth of this RsbU* null mutant strain was assessed with DNA harvested at 0, 12, 24, 36, 48, and 72 hours post-infection. Genome copy numbers were compared between *Chlamydia* (*secY)* and host (*rpp30*) (Figure 2.10B). Striking differences in the growth pattern of the mutant were observed compared to wild-type *Chlamydia*, with the mutant strain displaying

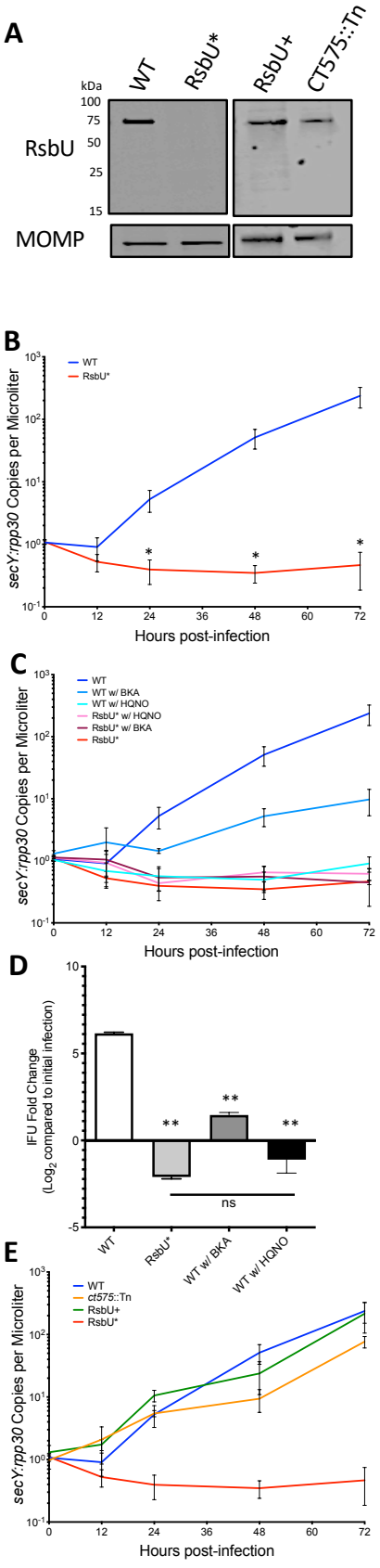
A
WT
RsbU*
RsbU+
CT575::Tn
kDa
100
75
50
25
15
RsbU
MOMP
B
WT
RsbU*
secY:rpp30 Copies per Microliter
Hours post-infection
C
WT
WT w/ BKA
WT w/ HQNO
RsbU* w/ HQNO
RsbU* w/ BKA
RsbU*
secY:rpp30 Copies per Microliter
Hours post-infection
D
IFU Fold Change
(Log2 compared to initial infection)
ns
WT
RsbU*
WT w/ BKA
WT w/ HQNO
E
WT
ct575::Tn
RsbU+
RsbU*
secY:rpp30 Copies per Microliter
Hours post-infection

Figure 2.10. The Rsb pathway affects normal growth of *Chlamydia*. (A) Western blot of WT and RsbU* expression of RsbU protein at 24 hours post-infection. No RsbU protein fragment is detected in the RsbU* mutant strain. MOMP is used as a loading control. (B) *Chlamydia* genome copy numbers (*secY*) were compared to host cell genome copy numbers (*rpp30*) over 72 hours after the initial infection. RsbU* appears to begin replicating around 72 hours post-infection (* p-value <0.05 with student's T-test). (C) Growth curves with chemical inhibitors, HQNO and BKA, show significant differences between WT and WT +BKA after 24 hours, as well as RsbU* and WT +BKA (p-value >0.05). With HQNO added, both WT and RsbU* were not statistically different from RsbU* without any inhibitors. (D) Progeny assay looking at the difference in IFUs produced after 36 hpi compared to the IFUs in the initial infection. The decrease in IFUs produced by the RsbU* strain, as well as WT treated with HQNO, suggest that the chlamydial cells are largely in the RB form at this point in the infection rather than the EB form capable of propagating the infection to new host cells. While all three experimental conditions were significantly different from the WT untreated condition (**p-value <0.001 with student's T-test), the RsbU* mutant compared to the HQNO treated infection shows no significant difference (p-value = 0.3). (E) The RsbU+ recombinant strain, with WT RsbU expression but retaining the majority of the other EMS-induced SMPs, restores growth to WT levels.

minimal replication capabilities and generation of detectable infectious progeny (Figure 2.10B and D).

Whole genome sequencing of this RsbU* mutant confirmed the truncating SNP in *ct588* (*rsbU*). Thirty-two additional SNPs were also determined (Table 2.6). Of these SNPs, seven are silent mutations and four are in intergenic regions. The remaining 21 SNPs were evaluated for their potential effect on their respective coding regions with the majority predicted to have no obvious effect on protein function based on their likelihood to alter secondary structures or active domains as predicted by EMBOSS secondary structure prediction or BLASTp domain predictions. Two SNPs are predicted to alter secondary structures: a G105E mutation in CT259 and a Q204* mutation in CT163. The mutation in CT259 is predicted to form an alpha helix spanning E99 to F113 not predicted in the wild-type CT259 and has been associated with reduced phosphatase activity of the protein (Claywell, Matschke et al. 2018). The most significant SNP, outside of *rsbU**, is the additional truncation in CT163, a hypothetical protein with no conserved motifs. The CT163 protein is predicted to be a membrane protein with one transmembrane domain in *C. trachomatis*. The truncation stops translation one third of the way through the large putative extracellular domain, likely altering protein function. It is unclear what effect the truncation of this protein would have on the chlamydial developmental cycle and we cannot rule out the possibility that the SNP is contributing to the growth and morphological defects that have been determined for the RsbU* null mutant.

Table 2.6 SNPs in RsbU* determined by Whole-Genome Sequencing.

Location (bp)	Locus Tag	Gene function	Change	Coverage at site	Possible Effect
52,232	CT674	YscC, type II secretion system protein	G664W	306x, 97.4%	Loses possible turn
119,402	CT727	zntA, metal transporting ATPase	silent, S102	200x, 98.5%	N/A
133,223	IGR	N/A	N/A	226x, 96%	Likely in the promotor region for ribA, may effect expression
137,588	CT734	lipoprotein	silent, P218	208x, 95.2%	N/A
363,948	**CT036**	**hypothetical protein, putative inc**	**G182S**	**291x, 96.9%**	**likely in a beta strand facing host cytosol, no obvious effect**
431,642	**CT094**	**tRNA pseudouridine synthase B**	**silent, L62**	**439x, 97.3%**	**N/A**
435,453	**CT097**	**nusA, transcription termination/antitermination protein**	**A247V**	**411x, 98.5%**	**Likely in beta strand, no obvious effect**
440,207	**IGR**	**N/A**	**N/A**	**543x, 98.3%**	**Between 2 diverging genes, potential expression effects**
448,523	CT109	hypothetical protein	A37V	420x, 97.9%	no obvious effects
449,796	CT110	GroEL, chaperonin	silent, L200	385x, 96.9%	N/A
452,840	**IGR**	**N/A**	**N/A**	**443x, 97.7%**	**Between divergent genes, possible small RNA or regulatory region**
477,508	CT138	microsomal dipeptidase	P70S	382x, 98.4%	potential lengthening of a turn region
509270	CT163	hypothetical protein	Q204*	688x, 98.75	Major truncation event, contains about 1/3 extracellular domain, in PZ
547175	**CT204**	**ybhI, sodium:sulfate symporter**	**S31F**	**455x, 98.2%**	**no obvious effect, in extracellular domain**
609746	**CT259**	**protein phosphatase**	**G105E**	**583x, 99.1%**	**possible addition of a-helix, not in active site**
616,827	CT266	hypothetical protein	silent, E105	572x, 97.0%	N/A
630,626	**CT281**	**nqrE, Na(+)-translocating NADH-quinone reductase subunit E**	**silent, L3**	**533x, 97.7%**	**N/A**
637,039	CT286	clpC, ATP-dependent Clp protease ATP-binding subunit	R204C	631x, 98.9%	no obvious effects
638,353	CT286	clpC, ATP-dependent Clp protease ATP-binding subunit	F642L	455x, 98.0%	no obvious effects
672,564	CT314	rpoC, DNA-directed RNA polymerase subunit beta'	E195K	394x, 97.7%	no obvious effects
675,519	CT315	rpoB, DNA-directed RNA polymerase subunit beta	H471Y	403x, 98.5%	no obvious effects
689,582	CT329	xseA, exodeoxyribonuclease VII large subunit	silent, Y279	486x, 99.0%	N/A
693,265	CT332	pykF, pyruvate kinase	S158N	372x,98.7%	possible introduction of a turn
789,731	CT411	lpxB, lipid-A-disaccharide synthase	L601F	583x, 97.4%	no obvious effects
798,820	CT414	pmpC	G157E	395x, 97.7%	possible shorter helix
847,452	CT454	argS, arginine--tRNA ligase	P412L	341x, 97.55	no obvious effects
869381	**CT476**	**hypothetical protein, ywqK antitoxin module subunit domain (E=3.23e-57)**	**C8Y**	**293x, 97.3%**	**maybe interferes with predicted signal cleavage site, interupts a-helix**
872,210	**CT478**	**oppC2, oligopeptide ABC transporter permease**	**R127W**	**429x, 97.9%**	**no obvious effects**
888,891	**CT493**	**polA, DNA polymerase I**	**G310E**	**394x, 98.7%**	**possibly extends helix**
906,093	**CT510**	**secY, preprotein translocase subunit**	**L146F**	**522x, 97.5%**	**no obvious effects**
929,717	**IGR**	**N/A**	**N/A**	**390x, 96.9%**	**possibly effects expression of CT544**
1,014,167	**CT615**	**rpoD, sigma-66**	**D50N**	**443x, 98.6x**	**no obvious effects**

Lines in bold indicate those SNPs that maintain the wild-type version of the gene in the RsbU+ complemented strain.

In order to more confidently attribute the growth defect and phenotype to the RsbU disruption rather than the other SNPs induced by EMS mutagenesis, complementation efforts were pursued. However, because of the extremely poor growth of the RsbU* mutant, standard transformation with a wild-type *rsbU* gene on a vector plasmid proved unsuccessful. To overcome this limitation, lateral gene transfer was performed between *C. trachomatis rsbU* (Rif^R)* and another mutant strain that has a transposon (β-lactamase) inserted in *mutL* (*ct575::Tn bla*), which is near the *rsbU* coding region (CT588). After mixed infection and dual antibiotic selection, this was expected to encourage homologous recombination between the two genomes and restore *rsbU* coding region (Figure 2.11). This was expected to also leave the majority of SNPs including the *ct163* mutant truncation. Importantly, the transposon mutant strain (*ct575*::Tn *bla*) showed growth phenotypes matching wild-type *C. trachomatis* L2 strain (Figure 2.10 and Figure 2.12).

Sequencing of amplicons from various genomic regions revealed a cross-over region in one of the resulting clones obtained following mixed infection and dual selection. Upon whole genome sequencing this complemented strain, the RsbU+ strain was revealed to be a mosaic between the RsbU* and wild-type genomes with a couple different regions of recombination apparent. In addition to a wild-type *rsbU* gene, the RsbU+ strain also has wild-type versions at 14 of the 32 SNP loci, 11 of which are in coding regions (Figure 2.11). Because the complemented strain does not retain all of the RsbU* SNPS, it does leave open the possibility that one or more of those SNPs could be playing a role in the growth defect of the null mutant that is restored in the complemented strain. In particular,

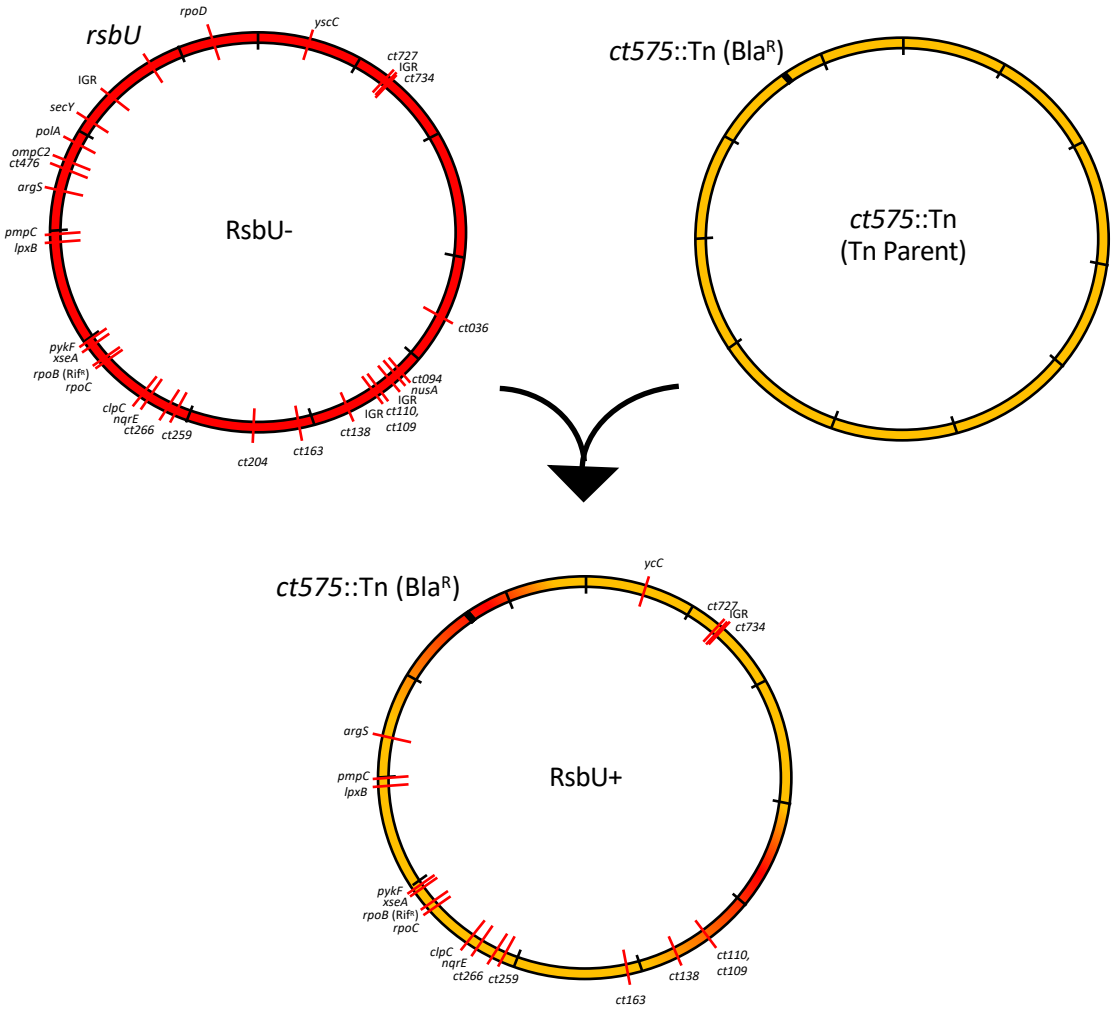
rsbU
rpoD
yscC
ct727
IGR
ct734
IGR
secY
polA
ompC2
ct476
argS
pmpC
lpxB
RsbU-
ct036
pykF
xseA
rpoB (Rifᴿ)
rpoC
clpC
nqrE
ct266
ct259
ct204
ct163
ct138
IGR
ct110,
ct109
ct094
nusA
IGR
ct575::Tn (BlaR)
ct575::Tn
(Tn Parent)
ct575::Tn (BlaR)
ycC
ct727
IGR
ct734
argS
pmpC
lpxB
RsbU+
pykF
xseA
rpoB (Rifᴿ)
rpoC
clpC
nqrE
ct266
ct259
ct163
ct138
ct110,
ct109

Figure 2.11 Chromosome schematic of cross between RsbU* EMS strain and *ct575*::Tn strain to create the complemented RsbU+ strain that retains the majority of the other SNPs induced by EMS mutagenesis. The *ct575*::Tn strain contains a beta-lactamase resistance gene in the transposon, while the RsbU* has a SNP in the *rpoB* gene that incurs rifampicin resistance. Dual selection with ampicillin and rifampicin was utilized to select for recombinants that retained the RsbU* strain backbone but a wild-type version of the *rsbU* gene. The red region on the RsbU+ chromosome represents the region of recombination between the genomes confirmed by PCR of the SNPs present in the RsbU* strain. In addition to the restoration of the *rsbU* gene, the RsbU+ strain restores three other SNPs close to the position of the transposon: two in coding regions for *secY* and *polA;* and one in an intergenic region (IGR).

the SNP in the *rpoD* gene encoding σ^{66} could effect on growth of the organism, however, the position of the SNP does not appear like it would have an effect on the structure of the protein, and is a region of the protein that does not appear to interact with the DNA binding (Paget 2015). Importantly, however, in the RsbU+ complemented strain, the non-sense mutation in the *ct163* gene is maintained, meaning that any growth difference between the mutant and complemented strain is not due to this mutation. Growth curves were done with the parental transposon strain and the RsbU+ complemented strain, revealing that the RsbU+ strain showed a restoration in growth rate (Figure 2.10).

We then hypothesized that the binding of TCA cycle intermediates to RsbU could indicate that the Rsb pathway is playing a regulatory role on TCA cycle activation in the chlamydial developmental cycle, leading to the poor growth of the RsbU* mutant. In order to test this hypothesis, we looked into chemical inhibitors targeting *Chlamydia*'s ability to produce ATP itself, as well as to steal ATP from the host cell using ATP translocases. 2-heptyl-4-hydrosyquinoline N-oxide (HQNO) has been shown to selectively inhibit at low concentrations (1 μM) the sodium-dependent NADH dehydrogenase that *Chlamydia* utilizes to produce the ion gradient that drives ATP synthesis by the chlamydial ATP synthase (Tuz, Mezic et al. 2015, Liang, Rosas-Lemus et al. 2018). Alternatively, bongkrekic acid (BKA) has been shown to inhibit ATP translocases in *Chlamydia,* limiting the ability to utilize host ATP (Winkler and Neuhaus 1999). Growth curves were repeated with wild-type *Chlamydia* and the RsbU* mutant strain with the addition of the chemical inhibitors (Figure 2.10C). BKA caused a decrease in the growth of wild-type

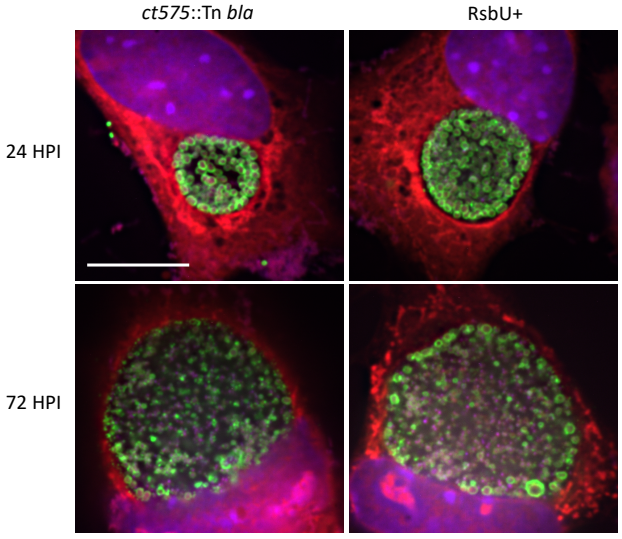
ct575::Tn *bla*
RsbU+
24 HPI
72 HPI

Figure 2.12 Immunofluorescent microscopy of *C. trachomatis ct575*::Tn parent strain and RsbU+ complemented strain. At 24- and 72-hours post-infection, the RsbU+ complemented strain does not appear to be phenotypically different from the Tn parent strain.

Chlamydia that is statistically significant from wild-type (p-value <0.05) after 24 hours, as well as from the RsbU* mutant after 24 hours. The addition of HQNO to a wild-type infection, however, was not statistically different from the RsbU* mutant growth at any time point.

Additionally, progeny production was assessed for the RsbU* mutant strain, as well as wild-type infections with the BKA and HQNO chemical inhibitors (Figure 2.10D). This assay revealed that while there is a decrease in IFUs produced in the presence of BKA compared to the untreated WT infection, viable EBs are still being produced. However, in the RsbU* and WT + HQNO conditions, there is a decrease in the number of IFUs produced compared to the initial infection, suggesting that these cells are in the RB non-infectious form rather than converting to the infectious EB form. This is consistent with the growth curves in Figure 2.10C, where genome copies can be detected for these conditions, but RB-to-EB conversion appear to be stalled in the infection.

To further investigate the poor growth by the wild-type *Chlamydia* in the presence of the sodium-dependent NADH dehydrogenase inhibitor (HQNO) and translocase inhibitor (BKA) as well as by RsbU*, confocal microscopy was carried out to view L929 cells infected with wild-type *Chlamydia* or RsbU* with and without inhibitors at 24 and 72 hours (Figure 2.13). Image analysis revealed that the wild-type *Chlamydia* at 24 hours post-infection in the presence of HQNO inhibitor formed smaller inclusions and appear to contain fewer EBs (puncta), although chlamydial RB cells appear like wild-type. At 72 hours post-infection, *Chlamydia* infected in the presence of HQNO had inclusions that were grossly under-full

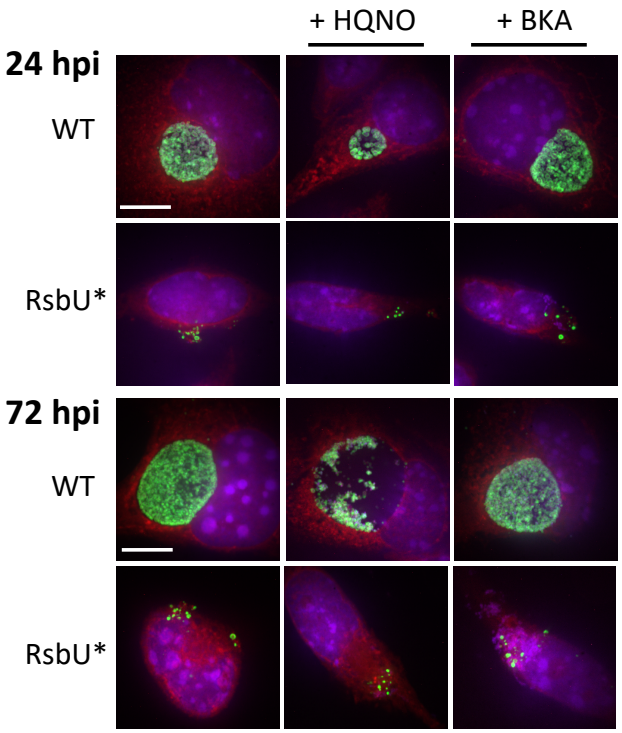
+ HQNO
+ BKA
24 hpi
WT
RsbU*
72 hpi
WT
RsbU*

Figure 2.13 Immunofluorescent microscopy of *Chlamydia* with RsbU* disruption and inhibitors of sodium-dependent NADH dehydrogenase and ATP translocase. L929 cells infected with wild-type *C. trachomatis* or RsbU* with and without the presence of inhibitor (HQNO or BKA) at 24- and 72-hours post-infection. Blue: DAPI, nucleus; Red: Evan's Blue, cytoplasm; Green: OmpA, *C. trachomatis* organisms. Images were acquired by confocal microscopy using a 150X objective and are comprised of 7 compressed Z-stacks (maximum projection) for each field.

compared to wild-type *Chlamydia* with no inhibitor. No obvious morphological abnormalities were apparent for wild-type *Chlamydia* in the presence of the BKA inhibitor. RsbU* was shown to have a severe growth defect with no defined development of an inclusion. Additionally, *Chlamydia* cells appear dispersed in the host cytosol at levels well under that seen by wild-type *Chlamydia* within inclusions at both 24- and 72-hours post-infection. RsbU* mutant infections at both 24 and 72 hpi do appear to contain both EB and RB *Chlamydia* cell forms. Addition of the HQNO and BKA inhibitors appeared to have no effect on levels of RsbU* C*hlamydia* or their dispersion within the host cell.

Overall, growth with HQNO causes a marked reduction in growth in wild-type chlamydial infections but does not have an additive effect on the growth defect observed in the RsbU* mutant. These observations support that the Rsb pathway in *Chlamydia* is linked to the ability of the bacteria to generate ATP via oxidative phosphorylation.

Transcriptional analysis of TCA cycle-associated and constitutively active genes suggestive of Rsb pathway regulation of σ^{66} activity. σ^{66} is the primary sigma factor of only three sigma factors that *Chlamydia* sp. possess and is responsible for transcription of the vast majority of genes throughout the developmental cycle. In order to further explore the proposed link between the Rsb pathway in *Chlamydia* to the regulation of σ^{66} (Thompson, Griffiths et al. 2015), transcript levels of σ^{66}-transcribed genes were assessed for differential expression between the RsbU* mutant and WT L2 *C. trachomatis* (Figure 2.14). Genes chosen for this analysis included TCA cycle associated genes (*gltT, sucA, sdhB,*

mdhC, pckA), constitutively active “housekeeping” genes, (*secY, rpoA, dnaK),* and other genes associated with dicarboxylate processing or transport (*xasA, ybhI, pdhB)* (Iliffe-Lee and McClarty 2000). All σ^{66}-transcribed genes were observed to have lower transcript counts compared to wild-type, while the σ^{28}-transcribed gene, *hctB*, did not appear to be differentially expression between the two strains. These results suggest that when the Rsb pathway is disrupted, as in the RsbU* mutant strain, there is decrease in transcription of these genes under regulation of σ^{66} activity.

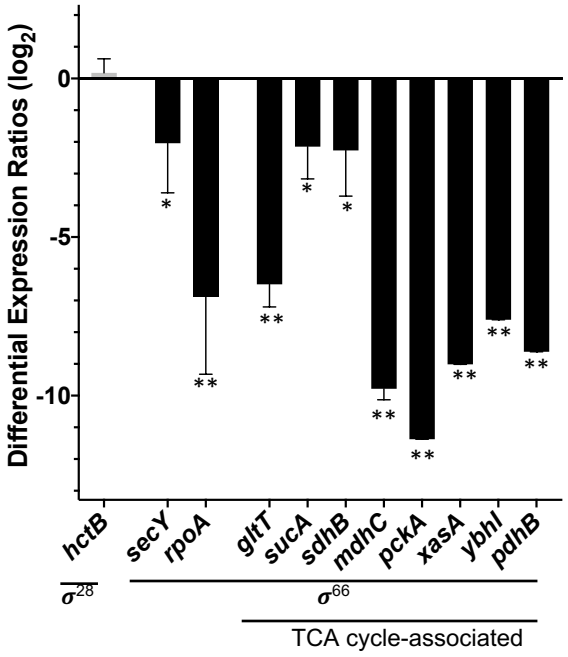
Differential Expression Ratios (log2)
0
-5
-10
hctB
secY
rpoA
gltT
sucA
sdhB
mdhC
pckA
xasA
ybhI
pdhB
σ28
σ66
TCA cycle-associated
Gene

Figure 2.14 Differential expression of TCA cycle-associated genes and other sigma-66 transcribed genes in RsbU* mutant compared to WT L2 transcript levels at 24 hpi. Genomic levels of DNA per infection were used to normalize transcript counts. Sigma-28 transcribed gene, *hctB,* shows similar transcript levels between the RsbU* mutant and WT L2, while those genes with σ^{66} promoters all show significant decreases in the level of transcripts (*p-value >0.05; **p-value >0.01 with student's T-test). Genes selected for this analysis included TCA cycle-associated genes (*gltT, sucA, sdhB, mdhC, pckA),* constitutively active genes (*secY, rpoA, dnaK),* and other genes associated with dicarboxylate processing or transport (*xasA, ybhI, pdhB),* all of which as σ^{66}-transcribed genes.

Discussion

In order to characterize the role of the Rsb phosphoregulatory partner-switching pathway in *Chlamydia*, we focused on the structure and ligand-binding capabilities of the periplasmic domain of RsbU. A 1.7 Å crystal structure for the periplasmic domain (Figure 2.5) allowed for structural comparisons to other proteins, leading to the identification of a putative binding pocket, and a possible association to the native ligand.

SPR (Table 2.4 and Figure 2.8), DSF (Table 2.5), and ITC (data not shown) experiments suggest that alpha-ketoglutarate, malate, and oxaloacetate are binding to $RsbU_{45-313}$. Dose-dependent SPR binding studies allowed for calculation of an estimated K_D value of 419, 459, and 396 μM for alpha ketoglutarate, malate, and oxaloacetate, respectively. This is a relatively high K_D value, indicative of weak binding; however, the concentrations of alpha-ketoglutarate and malate used were those similar to physiological levels in the cell (Albe, Butler et al. 1990). Similar proteins including Tlp3 from *Campylobacter jejuni* and PctA, PctB, and PctC from *Psuedomonas aeruginosa* have been shown to bind ligands at similar binding affinities (Rico-Jimenez, Munoz-Martinez et al. 2013, Rahman, King et al. 2014). Alternatively, there are several factors that could be having an effect on the $RsbU_{45-313}$ protein's ability to bind to the ligand, including the need for dimerization for ligand binding and the lack of the cytoplasmic and transmembrane portions of the protein that my help to stabilize the protein binding (Delumeau, Dutta et al. 2004, Zhou, Nan et al. 2008, Nan, Liu et al. 2010, Liu, Machuca et al. 2015). The

K_D values from the single ITC experiment were about a log lower than those values calculated from SPR, indicating tighter binding affinity. It is possible this discrepancy is due to the difference in the condition of the protein (free in solution with ITC compared to cross-linked to a surface with SPR). The K_D values from the ITC experiment are closer to the K_D determined for DctB binding to succinate, also determined by ITC (Nan, Liu et al. 2010).

The binding of multiple ligands allows for the possibility of differential responses upon binding. DctB has been shown to bind to both succinate and malonate, with a conformational change and loop closure of 2.2 Å with succinate, but not with malonate binding (Zhou, Nan et al. 2008). The aforementioned structurally similar Tlp3 and Pct proteins also have been shown to bind to multiple ligands and have differential responses based on the identity of the ligand (Rico-Jimenez, Munoz-Martinez et al. 2013, Rahman, King et al. 2014).

Determining that RsbU is binding to TCA cycle intermediates lends itself to the question of what role this protein and its related pathway are playing in the chlamydial developmental cycle. To investigate the effect of RsbU on chlamydial growth, an RsbU* mutant showed a severe deficit in growth compared to the wild-type strain supporting that the Rsb pathway plays a role in the normal pattern of chlamydial growth (Figure 2.10B) (Kokes, Dunn et al. 2015). When complementation of the *rsbU* gene was accomplished through homologous recombination with the *ct575*::Tn strain, the growth pattern returned to wild-type-like levels (Figure 2.10E).

Chlamydia has different ways that it can acquire energy. The presence of two ATP-ADP translocases allow for ATP uptake from the host cell appears to be the main source of energy when in the early stages of the developmental cycle, immediately after entry into the cell (Tjaden, Winkler et al. 1999). *Chlamydia* is then able to manufacture its own ATP utilizing a sodium-ion gradient to drive its ATP synthase activity during RB replication in midcycle time points as demonstrated by a recent publication by Liang *et al.* (Liang, Rosas-Lemus et al. 2018). Wild-type chlamydial growth with HQNO, a sodium-dependent NADH dehydrogenase inhibitor, appears to mimic the growth pattern of the RsbU* mutation, potentially stalling the RB-to-EB conversion reducing the number of infectious progeny in the late stage of the developmental cycle as well (Figure 2.10C and 7D). While it possible that the loss of the NADH-driven sodium gradient might also impact other processes that utilize the ion gradient, such as amino acid transport, when RsbU* was grown in the presence of HQNO, the growth pattern was similar to that of wild-type with HQNO. These data suggest that the inhibition of the sodium-dependent NADH dehydrogenase in the RsbU* strain does not have an additive effect on the growth defect, and that the Rsb pathway may be playing a role in *Chlamydia*'s production of ATP through oxidative phosphorylation.

The dynamic energy utilization could account for the non-lethality of the RsbU* mutation. If *Chlamydia* is able to actively scavenge ATP and other metabolites from the host in its early developmental cycle, then there is the possibility of replication as well, albeit much more slowly. Moreover, there is the possibility for redundant pathways for activation of metabolic and replicative

machinery. A second antagonist to the RsbW protein, $RsbV_2$ (CT765), is also present in *Chlamydia.* Previous studies have shown that RsbU only dephosphorylated $RsbV_1$; while RsbW phosphorylated both RsbV proteins, but has a bias towards $RsbV_1$ (Hua, Hefty et al. 2006, Thompson, Griffiths et al. 2015). This duality of RsbW antagonists could potentially mean that there is a secondary signal that has a similar, but possibly lesser effect on the repression of RsbW inhibition of the downstream target protein, and thus why the RsbU signaling disruption is not lethal.

The target protein(s) for RsbW in *Chlamydia* is debatable. Several studies have investigated the potential protein interaction partners of RsbW in order to identify its target protein. Based on the Rsb system in *B. subtilis,* the target is presumed to be a sigma factor, for which *Chlamydia* has only three [9]. However, conflicting results have been observed in interaction studies with the primary chlamydial sigma factor, σ^{66}, in addition to the alternative sigma factors, σ^{28} and σ^{54}. Douglas and Hatch demonstrated that RsbW pulled down with σ^{28} *in vitro*, while Hua and colleagues found that RsbW did not interact with any of the chlamydial sigma factors using a yeast two-hybrid system and an *in vitro* σ^{28}-dependent transcription assay (Douglas and Hatch 2000, Hua, Hefty et al. 2006). Most recently, Thompson *et al.* found using a bacterial two-hybrid system, and validated using surface plasmon resonance experiments, that RsbW binds σ^{66}, but not σ^{54} or σ^{28} (Thompson, Griffiths et al. 2015)**.** All this data combined has led to some uncertainty for any one sigma factor as the target protein, and the possibility for a non-sigma factor target has yet to be fully investigated. While the Rsb

pathway described in *B. subtilis* and other gram-positive bacteria regulates an alternative sigma factor, it is also worth considering that this pathway in *Chlamydia* may not be regulating such transcriptional machinery. In *Bordetella*, an RsbU homolog has been shown to be an important regulator of type three effector protein secretion without affecting transcription (Mattoo, Yuk et al. 2004, Kozak, Mattoo et al. 2005). Further efforts are being made to more definitively determine the target protein of the Rsb pathway and its specific role in the chlamydial developmental cycle; however, in this study, differential expression of σ^{66}-transcribed genes, TCA cycle-associated and otherwise, was also assessed (Figure 2.14). Of the genes selected for transcriptional analysis, all σ^{66}-transcribed genes appear to be down-regulated in the RsbU* mutant compared to WT L2 *C. trachomatis,* in contrast to σ^{28}-transcribed *hctB* (Yu and Tan 2003). This differential expression pattern between the RsbU* mutant and wild-type *Chlamydia* show a correlation between a disruption in the Rsb pathway and a decrease in σ^{66}-transcribed gene transcript levels.

If the Rsb pathway regulates σ^{66}, as the most recent publication and this study suggests (Thompson, Griffiths et al. 2015), the binding of alpha-ketoglutarate seems rational. *Chlamydia* is known to obtain alpha-ketoglutarate from the host cell as means for fueling its truncated TCA cycle to produce ATP through oxidative phosphorylation (Iliffe-Lee and McClarty 2000). The presence of a pool of alpha-ketoglutarate that *Chlamydia* can access could be an indicator that the bacteria is inside of the host cell and in a favorable environment for replication, and thus the activation of the primary sigma factor. The regulation of σ^{66} by the Rsb pathway

may also explain the difference in the morphology of the RsbU* mutant compared to the wild-type *Chlamydia* with the HQNO inhibitor. While the HQNO inhibitor in the wild-type infection does mimic the RsbU* growth pattern, the IFA imaging (Figure 2.13) is not an exact phenocopy. There is still an obvious inclusion present in the wild-type infection in the presence of HQNO, although the amount of *Chlamydia* is clearly less, compared to the RsbU* mutant which does not appear to be inside of an inclusion, but instead clustered together in the host cell cytoplasm. The wild-type infection in this case would still have the ability to activate σ^{66}, while the RsbU* would have σ^{66} repression, thus having a larger pleiotropic effect and be diminished in its ability to transcribe genes for the establishment and maintenance of the inclusion, TCA cycle enzymes, and effective growth and replication of the organism. Liang *et al.* were also able to show similar growth phenotype when wild-type *Chlamydia* is in the presence of monensin, a Na^+/H^+ exchanger that dissociates the Na^+ ion gradient driving the chlamydial ATP synthase (Liang, Rosas-Lemus et al. 2018).

The idea of dynamic energy utility also leads to our proposed model of how the Rsb partner-switching pathway is playing a role in the *Chlamydia* developmental cycle (Figure 2.15). When an EB enters the host cell it comes in contact with an increased level of alpha-ketoglutarate, which binds to the RsbU periplasmic domain. In the current model, upon binding to alpha-ketoglutarate, the cytoplasmic effector domain of RsbU performs its phosphatase activity on $RsbV_1$. RsbW then releases its target protein in order to re-phosphorylate the $RsbV_1$ protein. That target protein then affects the activation of the TCA cycle in *Chlamydia.* This effect

Figure 2.12 Working model of the Rsb phospho-regulatory pathway integrated with the truncated TCA cycle in *Chlamydia.* Alpha-ketoglutarate binding to the periplasmic domain of RsbU, as could be the case when an EB enters the host cell, leads to the activation of the phosphatase function of the cytoplasmic domain. RsbW then releases its target protein (black box), allowing for its normal function to be performed. That target protein then, either directly or indirectly, activates the chlamydial TCA cycle, allowing for alpha-ketoglutarate to be utilized. *Chlamydia* has been shown to be capable of creating its own ATP during mid-cycle using a truncated TCA cycle to generate electron-carrying molecules (i.e. NADH, $FADH_2$) and a sodium pumping NADH:quinone oxidoreductase (Na^+-NQR) (Liang, 2018). As malate builds up in the periplasm, through the export by the SodTi protein (Weber, 1995), it acts as an inhibitor as the concentration of alpha-ketoglutarate is depleted. The inhibition of the RsbU protein or the depletion of alpha-ketoglutarate, potentially later in the developmental cycle, could lead to a slowing of the TCA cycle as the *Chlamydia* cells prepare to convert to the EB form.

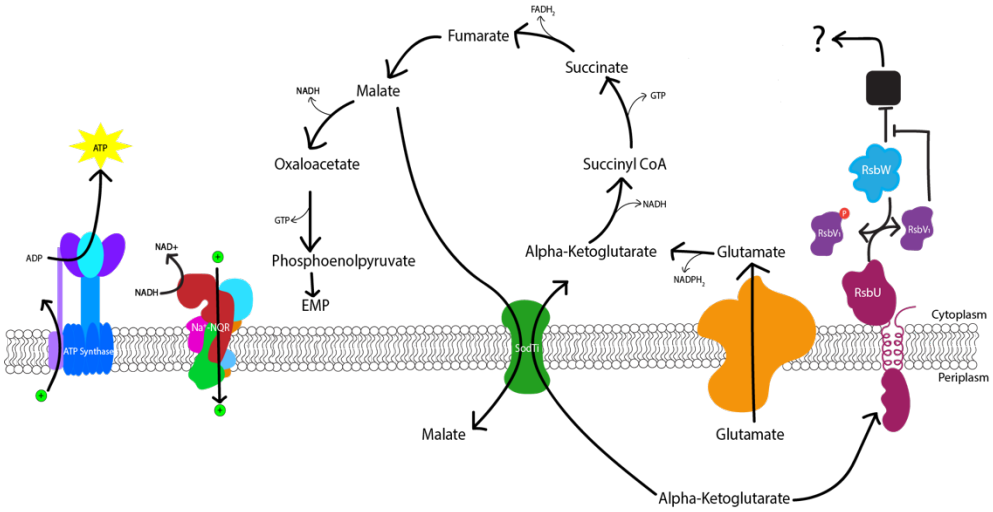
Fumarate
FADH2
Succinate
Malate
NADH
GTP
Oxaloacetate
Succinyl CoA
GTP
NADH
Phosphoenolpyruvate
Alpha-Ketoglutarate
Glutamate
NADPH2
EMP
ATP
ADP
NAD+
NADH
Na+-NQR
ATP Synthase
SodT
Malate
Glutamate
Alpha-Ketoglutarate
?
RsbW
RsbV1
P
RsbV1
RsbU
Cytoplasm
Periplasm

could be indirect, being a sigma factor, such as σ^{66}, or through the other transcriptional regulators or machinery that lead to the expression of other proteins involved in the TCA cycle; or direct, through activation of transport proteins for TCA cycle substrates or enzymes in the TCA cycle itself. Then when levels of alpha-ketoglutarate are waning, potentially towards the end of the developmental cycle, RsbU is no longer bound and the target protein is again inhibited by RsbW. Interestingly, temperature-sensitive mutants generated by Brothwell *et al.* for both *sodTi* (the putative dicarboxylate transporter) and *gltT* (the putative glutamate transporter) support that acquisition of alpha-ketoglutarate is important for chlamydial growth (Brothwell, Muramatsu et al. 2016). In addition, the levels of malate and/or oxaloacetate in the periplasm could act as an inhibitor for RsbU signaling. Malate or oxaloacetate could build up in the periplasm as it is transported out of the chlamydial cytoplasm by transporter proteins such as SodTi (Weber, Menzlaff et al. 1995). The phosphoenolpyruvate carboxylkinase (Pck) enzyme catalyzing the conversion of oxaloacetate to phosphoenolpyruvate has been shown to be differentially regulated as a mid-late stage gene, possibly leading to more malate and oxaloacetate being present in the cytoplasm to be exported into the periplasm by SodTi in exchange for alpha-ketoglutarate (Belland, Zhong et al. 2003, Nicholson, Olinger et al. 2003). Additionally, malate converted to oxaloacetate can also be used to synthesize *meso*-diaminopimelate (mDAP), a crosslinker in the A1γ-type peptidoglycan *Chlamydia* synthesizes during growth (Pilhofer, Aistleitner et al. 2013, Packiam, Weinrick et al. 2015). Peptidoglycan is only needed during growth of the *Chlamydia* cell (Liechti, Kuru et al. 2014,

Packiam, Weinrick et al. 2015), and therefore a buildup of malate could occur as the cell ceases growth in preparation for the conversion to the EB form.

Aspects of the Rsb phosphoregulatory partner-switching pathway still remain to be explored. While the transcriptional analysis supports the hypothesis that the target protein of the pathway could be σ^{66}, it does leave open the possibility of RsbW binding to a secondary transcriptional regulator. A phosphoproteomic analysis done in *Chlamydia caviae* showed that phosphorylated $RsbV_1$ and $RsbV_2$ can be detected in EBs, but not in RBs, rather than the other way around; calling into question the nature of this intermediate connection between RsbU and RsbW, and the mechanism of which these proteins communicate (Fisher, Adams et al. 2015). Furthermore, the true response of RsbU to binding either alpha-ketoglutarate, malate, or oxaloacetate; whether they are activating or inhibiting to the phosphatase activity of the RsbU cytoplasmic domain, still remains to be fully examined.

In this study, we were able to solve a 1.7Å crystal structure for the periplasmic domain of the chlamydial RsbU protein and utilize structural similarities to a dicarboxylate-binding protein to determine alpha-ketoglutarate, malate, and oxaloacetate as binding ligands. Moreover, an RsbU-null mutant was utilized to show the importance of the Rsb pathway in normal chlamydial growth. Finally, we proposed a working model for how this pathway may be sensing the aforementioned ligands to regulate the TCA cycle.

Chapter III: RsbW is an anti-sigma factor that inhibits the activity of the major sigma factor in *Chlamydia*

Abstract

The Rsb pathway consists of a cascade of proteins that inhibit the activity of alternate sigma factors mostly in Firmicutes such as *Bacillus subtilis.* The Gram-negative, intracellular pathogen *Chlamydia* also possess proteins that make up an Rsb pathway. In the chlamydial Rsb pathway, a sensor phosphatase RsbU will dephosphorylate $RsbV_1$. A protein kinase RsbW can phosphorylate $RsbV_1$, but only once it has released its binding to its target protein for which it inhibits activity. Previous studies have been conducted on the identity of the RsbW target protein; however, there has yet to be a consensus reached. Recently, it was shown that RsbU binds to TCA cycle intermediates and appears to be involved in *Chlamydia*'s ability to produce its own ATP via oxidative phosphorylation. In this study, we seek to determine the binding partners for RsbW through the use of a bacterial two-hybrid system. Additionally, we analyze the effects that overexpression of the RsbW protein in a *Chlamydia* infection has on transcription, growth, and phenotype.

Introduction

The Rsb partner-switching phosphoregulatory pathway has been described in many bacteria as a regulatory system for controlling alternate sigma factors in response to environmental or energetic stress (Hecker, Pane-Farre et al. 2007). Originally and most comprehensively studies in *Bacillus subtilis,* the Rsb pathway was shown to be responsible for the regulation of more than 150 genes during the entry of the stationary growth phase and in response to diverse stimuli including temperature extremes, salt concentration, ethanol, nutrient starvation, and a decrease in ATP (Benson and Haldenwang 1993, Boylan, Redfield et al. 1993, Boylan, Redfield et al. 1993, Voelker, Voelker et al. 1995, Mascher, Margulis et al. 2003, Zhang and Haldenwang 2005).

Chlamydia has many of the same components that make up the Rsb system from *B. subtilis* (Stephens, Kalman et al. 1998). The chlamydial RsbU protein is a transmembrane protein located in the inner membrane with a periplasmic sensor domain and a cytoplasmic phosphatase domain (Soules, Dmitriev et al. 2019). RsbU is able to dephosphorylate $RsbV_1$ which can then be re-phosphorylated by the protein kinase RsbW. In order to re-phosphorylated $RsbV_1$, RsbW must release its target protein for which it normally binds and inhibits (Douglas and Hatch 2006, Hua, Hefty et al. 2006, Thompson, Griffiths et al. 2015). In other bacterial systems, the target protein that RsbW binds to and inhibits the function of is an alternate sigma factor.

There has been some discrepancy about what is the target protein of RsbW in *Chlamydia.* Douglas and Hatch performed a pull-down assay and

showed that RsbW bound to σ^{28} (Douglas and Hatch 2006). However, Hua and colleagues were not able to detect interactions between RsbW and any of the three chlamydial sigma factors via a yeast-two hybrid study (Hua, Hefty et al. 2006). Most recently, Thompson *et al.* showed that RsbW interacted with σ^{66}, but not σ^{28} or σ^{54}, in a bacterial two-hybrid system and then confirmed these findings using surface plasmon resonance (Thompson, Griffiths et al. 2015). In their 2015 publication, Thompson *et al.* proposed that the Rsb pathway may serve to modulate σ^{66} activity, perhaps in an ATP-dependent manner (Thompson, Griffiths et al. 2015). The regulation of the Rsb pathway to control the major sigma factor in *Chlamydia* is thought to be unprecedented because there has been no evidence of such regulation of the main sigma factor in any other bacteria (Hecker, Pane-Farre et al. 2007).

In a previous study, the periplasmic domain of RsbU in *Chlamydia* was shown to bind to TCA cycle intermediates alpha-ketoglutarate, malate, and oxaloacetate (Soules, Dmitriev et al. 2019). Furthermore, an RsbU null-mutant demonstrated extremely poor growth, mimicking the growth of the *Chlamydia* in the presence of an inhibitor for *Chlamydia*-specific ATP production via oxidative phosphorylation (Liang, Rosas-Lemus et al. 2018, Soules, Dmitriev et al. 2019). These results taken together lead to the hypothesis that the Rsb pathway is affecting the regulation of the TCA cycle in *Chlamydia*, and consequently main ability for *Chlamydia* to gain ATP. Because *Chlamydia* alternates between an infectious, metabolically-inactive form known as the elementary bodies (EBs) and a metabolically-active, replicative form known as reticulate bodies (Rbs), the two

forms also have different mechanisms for obtaining ATP. *Chlamydia* has been shown to acquire ATP from the host cell in early time points during the developmental cycle, but switch to producing its own ATP during the growth and replication of RBs (Liang, Rosas-Lemus et al. 2018). If the Rsb pathway is important for the regulation of that switch between host cell ATP acquisition and ATP production through the TCA cycle in the RB form, then it is possible that the chlamydial Rsb pathway is regulating σ^{66} and thus the central metabolism of the organism.

We performed experiments to determine the target protein of RsbW in *Chlamydia.* Through the use of a bacterial two-hybrid system screening all the known components of the Rsb pathway*,* we found interacting partners for RsbW. Additionally, an RsbW-overexpression strain of *Chlamydia trachomatis* allowed us to analyze the effects of RsbW on transcription, growth, progeny production, and phenotype throughout the chlamydial developmental cycle.

Methods

Bacterial adenylate cyclase two-hybrid constructs. The following four vectors were used to insert the gene of interest: pKT25, pKNT25, pUT18, and pUT18C. The primers for the genes of interest were ligation independent primers (Table 3.1), excluding sigma54 which was used previously in the lab (Barta, Battaile et al. 2015). All of the vectors were digested with KpnI-HF restriction enzyme. RsbW was cloned into upstream (pKNT25) and downstream (pKNT25) of *B. pertussis* T25 fragment (Karimova, Pidoux et al. 1998). These constructs were cloned into DH5alpha competent cells and then electroporated into DHM1, adenylate cyclase deficient, cells. The other genes of interest were inserted upstream (pUT18) and downstream (pUT18C) of the T18 fragment and cloned into DH5alpha cells. All clones verified through sequencing.

Bacterial adenylate cyclase two-hybrid screen. In order to perform the BACTH screen, the "bait", RsbW-pKT25 and pKNT25, cells were grown overnight in 3mL of LB with kanamycin. The overnights were transferred into 50mL of LB with kanamycin and incubated until an OD_{600} of ~0.5 was reached. Incubated on ice for 15 minutes then centrifuged at 2700rpm at 4°C for 10 minutes. The pellet was suspended in 25mL of "Buffer 1" (80mM $CaCl_2$ 20mM $MgCl_2$) and centrifuged again under the same conditions. The pellet was suspended in 5mL of "Buffer 2" (100mM $CaCl_2$).

Table 3.1 Primers for BACTH constructs

Gene	Orientation	Primer
rsbW	T25-N	5'-AGGATCCCCGGGTACATGACCTTTTCTGAAGGAGAGCAAGT
		5'-GAATTCGAGCTCGGTACTGAGTTGTGAGGTTTTGTGTATAGAGTGAGAG
rsbW	T-25C	5'-AGGATCCCCGGGTACCCATGACCTTTTCTGAAGGAGAGCAAGT
		5'-CGAATTCTTAGTTACTTAGGTACTGAGTTGTGAGGTTTTGTGTATAGAGTGAGAG
rsbU	T18-N	5'-AGGATCCCCGGGTACATGGCCTATCCGGAAGCTGGC
		5'-GAATTCGAGCTCGGTACATAAGCGGAAGGTTCCTTAGGTATTTTCA
rsbU	T18-C	5'-AGGATCCCCGGGTACCATGGCCTATCCGGAAGCTG
		5'-GAATTCGAGCTCGGTACATAAGCGGAAGGTTCCTTAGGTATTTTCA
rsbV1	T18-N	5'-AGGATCCCCGGGTACATGAGTAACTTTCAGAAAGAAGAACAAGGC
		5'-GAATTCGAGCTCGGTACACTGTTTTCTTTTGCTAAAGCTTGTAGAG
rsbV1	T18-C	5'-AGGATCCCCGGGTACGGATGAGTAACTTTCAGAAAGAAGAACAAGGC
		5'-GAATTCGAGCTCGGTACACTGTTTTCTTTTGCTAAAGCTTGTAGAG
rsbV2	T18-N	5'-AGGATCCCCGGGTACATGGAATGGATAGCAAGAGAGTACAAAAATAT
		5'-GAATTCGAGCTCGGTACAAAATCGCTAAAAGATTCTTGTTCTGCT
rsbV2	T18-C	5'-AGGATCCCCGGGTACGGATGGAATGGATAGCAAGAGAGTACAAAAATAT
		5'-GAATTCGAGCTCGGTACAAAATCGCTAAAAGATTCTTGTTCTGCT
σ^{66}	T18-N	5'-AGGATCCCCGGGTACATGCGCATGGATACGCTAGA
		5'-GAATTCGAGCTCGGTACATTTTTATAACTTTTAATCTTACCCGAACCAATTTTTTCTTCT
σ^{66}	T18-C	5'-AGGATCCCCGGGTACGGATGCGCATGGATACGCTAGA
		5'-GAATTCGAGCTCGGTACATTTTTATAACTTTTAATCTTACCCGAACCAATTTTTTCTTCT
σ^{54}*	T18-N	5'-AAAAAATCTAGAGGATCCCATGTTGCATCATCAAACAGC
		5'-TTTTTTGGTACCCGGATAGTATGTCGAGAATTCTCTGT
σ^{54}*	T18-C	5'-AAAAAATCTAGAGGATCCCATGTTGCATCATCAAACAGC
		5'-TTTTTTGGTACCCGGATAGTATGTCGAGAATTCTCTGT
σ^{28}	T18-N	5'-AGGATCCCCGGGTACGGGTGAAGACTCACGATCTCGCAGA
		5'-GAATTCGAGCTCGGTACAAGCAGACTGGACAATGTACCT
σ^{28}	T18-C	5'-AGGATCCCCGGGTACGGGTGAAGACTCACGATCTCG
		5'-GAATTCGAGCTCGGTACAAGCAGACTGGACAATGTACCT
ct589	T18-N	5'-AGGATCCCCGGGTACGGATGGAAAAGAAAATCGCCATTCAAAATATTTTTCTG
		5'-GAATTCGAGCTCGGTACGATAAAGGATAAAAAGCCTACAGCTCCATCG
ct589	T18-C	5'-AGGATCCCCGGGTACGGATGGAAAAGAAAATCGCCATTCAAAATATTTTTCTG
		5'-GAATTCGAGCTCGGTACGATAAAGGATAAAAAGCCTACAGCTCCATCG

* primers were taken from a previous BACTH study (Barta 2015)

The “preys” on the pUT18 and pUT18C vectors were grown overnight in 1mL of LB with carbenicillin. A Qiagen Miniprep kit was used to purify the plasmids from these overnights. The day of the screen, the “baits” were thawed on ice, 20uL were aliquoted into a well of a 96 well block, and each well received 5uL of a different “prey” plasmid. The blocks were incubated on ice for 30 minutes, heat shocked for 1 minute and 40°C, incubated on ice for 5 minutes, and then 100uL of LB was added to each well. The blocks were incubated at 37°C, with shaking, for 1 hour. After 1 hour, 400uL of LB with both kanamycin and carbenicillin was added to each well, and the blocks were incubated at 37°C, with shaking. After 3 hours, 5uL of the cultures were then spot inoculated onto M63 minimal media plates and LB+ kanamycin/carbenicillin plates (control plates) along with pUT18 and pKT25 zip for a positive control and empty vectors for a negative control. The M63 plates were placed in the 30°C incubator for 5 days and the LB plates were placed in the 37°C incubator overnight.

5x M63 stock solution. 10g ammonium sulfate, 68g monopotassium phosphate, 2.5mg iron sulfate concentrate, and 600mL of water, were dissolved and potassium hydroxide was used to pH media to a pH of 7.0. QS to 1000mL.

M63 minimal media plates. 15g of agar and 780mL of water were autoclaved along with 200mL of 5x M63 stock solution. The following was later added to the media: 10mL 20% maltose, 1mL (50mg/mL) X-gal, 500uL (1M) IPTG, 500uL of both kanamycin and carbenicillin, 100uL of 0.5% thiamine, and 1mL $MgSO_4$.

Transformation of pL2-RsbW in *C. trachomatis.* The *rsbW* (*ctl0811/ct549*) from *C. trachomatis* L2 434/Bu (AM884176) was amplified by PCR and cloned into the pL2-tetO vector in a ligation-independent fashion at the AgeI restriction site. The pL2-tetO vector consists of the plasmid backbone from *C. trachomatis* L2 with a beta-lactamase gene and a tet-inducible promoter region upstream of the gene of interest insertion site (Wickstrum, Sammons et al. 2013). Insertion of the *rsbW* gene was confirmed by sequencing.

Purified pL2-*rsbW* expression vector plasmid was transformed into wild-type L2 *C. trachomatis*. 15 μg of vector plasmid was mixed with 100 μL 2X $CaCl_2$ buffer (20 mM Tris pH7.5, 100 mM $CaCl_2$) and 25 μL of *C. trachomatis* EBs, and diluted with water to a final volume of 200 μL. This $CaCl_2$ mixture incubated at room temperature for 30 minutes at room temperature before being diluted into 1X $CaCl_2$ buffer and added onto a confluent monolayer of L292 cells, and then centrifuged for 30 minutes at 550 x g, 20°C. Following centrifugation, the $CaCl_2$ mixture was aspirated off the monolayer and replaced with RPMI media supplemented with 5% tetracycline-free FBS, 10 μg/mL gentamycin, 1 μg/mL cycloheximide, and incubated at 37°C, 5% CO_2. After 16 hours, 1 μg/mL of ampicillin were added to the infected cells. 42 hours after the initial infection, the cells were lysed using water lysis and passaged to a new monolayer of cells, with media supplemented with 1 μg/mL of ampicillin. After an additional 48 hours, the cells were passaged again with 2 μg/mL of ampicillin. Two additional passages occur 48 hours after each previous passage, with new media containing 5 μg/mL

of ampicillin. At this point, the infection was propagated for harvesting and presence of the vector plasmid was confirmed by PCR.

Western blot analysis of RsbW overexpression. A confluent monolayer of L292 cells in a 6-well cell culture plate with tetracycline-free media was infected with pL2-*rsbW* transformed *C. trachomatis,* or an empty pL2-tetO vector control strain. At either the time of infection (0 hours) or 12 hours post-infection (hpi), 10 ng/mL of anhydrous tetracycline (ATc) was added to the RPMI media. At 24 hpi, the cell culture media was aspirated off the cells and 400 μL of a 1:1 mixture of PBS (Corning, NY) and Laemmli sample buffer (Bio-Rad, Hercules, CA) was added to each well. The wells were then cell scraped, and the well content was collected. Western blot analysis was performed on the collected samples using a rabbit anti-RsbW primary antibody at a 1:5000 dilution, and a donkey anti-rabbit secondary antibody (LI-COR, Lincoln, NE) at a 1:5000 dilution. Goat anti-MOMP primary antibody (Virostat, Westbrook, ME) was used for a loading control, with a donkey anti-goat secondary antibody (LI-COR, Lincoln, NE).

Transcriptional analysis of select genes with RsbW overexpression in *C. trachomatis.* L292 cells in a 6-well tissue culture plate with tetracycline-free media were infected with pL2-*rsbW* transformed *C. trachomatis,* or an empty pL2-tetO vector control strain. At 16 hpi the *Chlamydia* was induced with 10 ng/mL ATc. Then at 20 hpi the infections were harvested with 1 mL per well TRIzol. 200 μL of chloroform was added to each 1 mL TRIzol cell lysate,

vortexed, and centrifuged for 8 minutes at 10,000 g. The aqueous layer of the TRIzol/chloroform mixture was collected in a new tube, and a 1:1 ratio of isopropanol was added before incubating at -20°C for 30 minutes, followed by room temperature for 15 minutes. The precipitated nucleic acids were pelleted by centrifugation for 8 minutes, the supernatant was decanted, and the pellet was washed with 1 mL 70% ethanol. After another 5-minute centrifugation, the pellet was air dried and resuspended in 80 μL of RNAse-free Molecular Biology Grade water (Corning, NY). DNA depletion was performed by adding 10 μL of TURBO DNAse Buffer and 10 μL of TURBO DNAse (Thermo Fisher, Waltham, MA) to each 80 μL of sample and incubated in a 37°C water bath for 30 minutes. Immediately following DNA depletion, the samples were taken through the RNeasy Mini Kit (Qiagen, Hilden, Germany) and eluted into 50 μL of RNase-free water.

cDNA was generated using the High-Capacity cDNA Reverse Transcription Kit (Applied Biosystems, Foster City, CA) including control reactions excluding the reverse transcriptase, which was then used to assess the presence of residual gDNA contamination. Following cDNA generation, droplet digital PCR (ddPCR) was used to determine an absolute quantification for the number of transcripts present for the genes of interest. The QX200 Digital Droplet PCR system (Bio-Rad, Hercules, CA) with all the suggested Bio-Rad consumables, including QX200 EvaGreen Supermix, were utilized in the set up and reading of the ddPCR run. Primers for specific genes of interest used for ddPCR are listed in Table 3.2. Data was analyzed using the QuataSoft Analysis

Pro Software, version 1.0 (Hindson, Ness et al. 2011). The data was normalized to the quantification of genome copies from the infections and converted to $\log_2$ scale compared to the number of transcripts in the empty pL2 vector control induced with ATc.

Growth curves with RsbW overexpression. Infections of host cells and RNA isolation was as described in the previous section. Induction of RsbW overexpression was either at the time of infection (0 hpi) or at 12 hpi. RNA was harvested from the infections at 0, 12, 24, 36, 48, and 72 hpi. Number of transcripts of a *Chlamydia*-specific gene, *secY,* were compared to the number of transcripts of a host-specific gene, *rpp30.* This analysis was performed in triplicate.

Progeny assay. Infection of host cells and induction of RsbW were performed as previously described. At 24, 36, and 48 hpi, the infections were lysed by water lysis and used to infection a new monolayer of cells in a 96-well microtiter plate in a serial dilution. 24 hours after infecting the 96-well plate, the cells were fixed with methanol for 10 minutes and stained using the MicroTrack *C. trachomatis* culture confirmation test (Syva Co., Palo Alto, CA) and 10nM 4', 6-diamidino-2-phenylindole (DAPI) in PBS. Infection forming units (IFUs) were then counted and compared to the number of IFUs of the initial infection.

Immunofluoresent microscopy. L929 cells were grown to ~75% confluency in an 8-well ibiTreat µ-Slide (Ibidi, Martinsried, Germany) and were infected with *C.*

trachomatis L2 mutant or vector control strains. ATc was added at 10 ng/mL at either the 0 or 12 hpi. At 24, 36, and 48 hpi, the cells were fixed with methanol for 10 minutes and then stained with MicroTrack *C. trachomatis* culture confirmation test (Syva Co., Palo Alto, CA) and 10nM 4', 6-diamidino-2-phenylindole (DAPI) in PBS. A final overlay of Vectashield antifade mounting medium (Burlingame, CA) was added. Slides were images on an EVOS M7000 Imaging System (ThermoFisher, Waltham, MA).

Table 3.2 Primers for RsbW overexpression transcriptional profile.

Gene	Primer Direction	Sequence 5' -->3'
hctB	Forward	CATAAACATACTGCAGCTTGTG
	Reverse	ACGCCAGCTGTGAGC
ct620	Forward	ATTCTAGAAGATGCTCTTGTCTCAG
	Reverse	CTAACTAGCCAGTTTTCTTGTTAAACC
secY	Forward	TCAAGGTCTTCCTTTGGGGC
	Reverse	TACACAATGAATAGGGTAACTTTGC
rpoA	Forward	ATGTCGGATAGTTCACACAATTTAC
	Reverse	TTCCCAAGGTGTGCCCC
xasA	Forward	ATGCATCATCGCAAATCTTCTAC
	Reverse	GCGTTTTCCTAAGGCATCTC
pykF	Forward	ATGATCGCTAGAACGAAAATTATTTGTAC
	Reverse	CTTGGCCTAAACGAATTTCGG
gltT	Forward	CTAACCATGTTGAGGAAGGATATCC
	Reverse	GTAGGAAGTGCAGGAGTCC
mcdH	Forward	CAAAGATACGCTAGCTTTTTCCTG
	Reverse	CAATATATCAGCCAAAAGAAGGAGAATG
ybhI	Forward	ATGAATAAACACAAACGCTTCTTATCG
	Reverse	AAATCCGGACAAAGCTTGATC
sucA	Forward	ATGGATTCAGACTTTGCTAGGC
	Reverse	TATCATCAAAAGACTGTGTGCTTTTTTC
pdhB	Forward	ATGCCTAATTTTGTTACACTCGAAATC
	Reverse	TGGGCGAAGTCCAGTTAG

Results

Bacterial two-hybrid system screen supports σ^{66} as binding partner for RsbW. In order to determine the possible binding partner of RsbW, a two-hybrid system was utilized. Previously, a yeast two-hybrid (Y2H) was used to identify the interactions between RsbW and chlamydial sigma factors (Hua, Hefty et al. 2006). Although Y2H systems are widely used, a bacteria model organism is more relevant in order to study bacterial protein-protein interactions. With this in mind, the bacterial adenylate cyclase two-hybrid (BACTH) system was chosen to study the binding partner of RsbW. This system relies on two fragments, T18 and T25, of the adenylate cyclase protein from *Bordetella pertussis*. When cleaved, this protein is unable to convert ATP to cyclic AMP, which is necessary to bind to CAP and turn on a reporter gene, in this case the *lac* and *mal* genes (Karimova, Pidoux et al. 1998). The RsbW gene was cloned onto plasmids containing the T25 fragment at two different orientations (pKT25 and pKNT25). This is referred to as the "bait" protein. The "prey" proteins (RsbU, $RsbV_1$, $RsbV_2$, σ^{66}, σ^{54}, σ^{28}, and CT589) were cloned onto the T18 fragment also at two different orientations (pUT18C and pUT18). A BACTH screen was performed on these "baits" and "preys", and out of the fourteen target proteins tested, two showed a positive interaction with RsbW (Table 3.3). These interactions occurred with RsbU and σ^{66} at specific orientations.

Currently, there are no studies suggesting that RsbU and RsbW interact, however, the BACTH screen performed showed a very distinct interaction represented by the blue colonies through the production of beta-galactosidase (Figure 3.1). These interactions occurred at one orientation (RsbW-T25C and RsbU-T18C), which could suggest that folding of RsbW or RsbU prevented the interaction at other orientations from occurring. Also, this reiterates the necessity for proteins to be tested at varying orientations on the adenylate cyclase protein fragments. The data from this two-hybrid assay could suggest that RsbU is forming a complex with RsbW, perhaps when the phosphorylation event takes place.

Previously, Thompson *et al.* reported, through a bacterial two-hybrid system, that RsbW interacts with a sigma factor, specifically σ^{66} (Thompson, Griffiths et al. 2015), which mimics the data from the BACTH assay performed (Figure 3.1). It was hypothesized that RsbW's target protein could be a sigma factor that, when released by RsbW, would switch on essential genes in *Chlamydia*. Previous studies in the lab did support this hypothesis through a mutated RsbU protein (Soules, Dmitriev et al. 2019). When mutated, RsbU was unable to receive the appropriate compound, the signaling of the Rsb pathway would not be carried out. Consequentially, RsbW would then be unable to release its target protein and re-phosphorylate $RsbV_1$. Soules *et al*. saw a reduced ability of this mutant to establish an infection in cells, which is likely due to RsbW and its unreleased target protein (Soules, Dmitriev et al. 2019). These findings suggest that RsbW's target protein is likely a sigma factor responsible for

Table 3.3 RsbW interaction BACTH

T18-N	T25-N RsbW	T25-C RsbW
RsbU	-	-
$RsbV_1$	-	-
$RsbV_2$	-	-
σ^{66}	-	-
σ^{54}	-	-
σ^{28}	-	-
CT589	-	-
T18-C	**T25-N RsbW**	**T25-C RsbW**
RsbU	-	+
$RsbV_1$	-	-
$RsbV_2$	-	-
σ^{66}	-	+
σ^{54}	-	-
σ^{28}	-	-
CT589	-	-

The results are shown as a “+” or “-” indicating whether or not an interaction occurred.

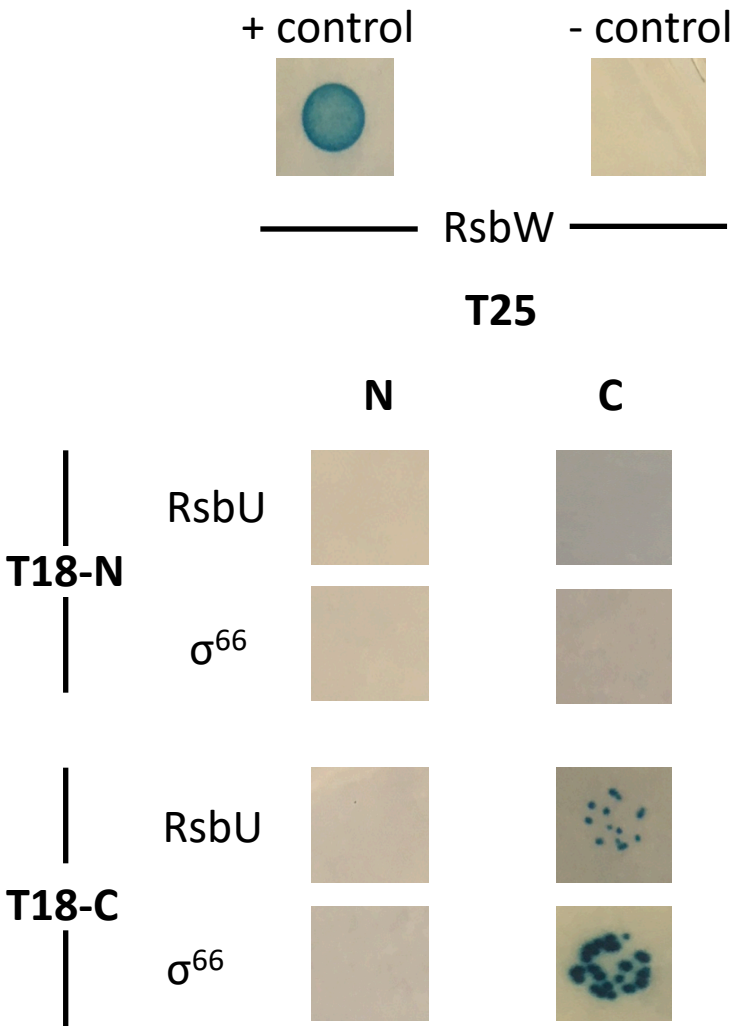
+ control
- control
RsbW
T25
N
C
T18-N
RsbU
σ66
T18-C
RsbU
σ66

Figure 3.1 BACTH assay results of the two proteins that showed positive interactions with RsbW. Both interactions occurred with the protein of interest on the C-terminus of the adenylate cyclase protein. A positive control (pKT25/pUT18 zip) and a negative control (empty pKT25/pUT18) were used as references.

regulating important genes essential for establishing a healthy inclusion inside the host cell. Those findings are supported by this bacterial two-hybrid study, that showed an interaction occur between RsbW and σ^{66} (Figure 3.1). Once again, the interaction occurred at a specific orientation (RsbW-T25C and σ^{66}-T18C). The previous work by Thompson *et al.* and Soules *et al*., along with these current data verify the hypothesis that RsbW's target protein is likely σ^{66} (Thompson, Griffiths et al. 2015, Soules, Dmitriev et al. 2019).

It has been shown that RsbW does interact with $RsbV_1$ and $RsbV_2$ in order to re-phosphorylate those protein (Hua, Hefty et al. 2006, Thompson, Griffiths et al. 2015), however, this BACTH study did not verify those interactions. This is likely due to both $RsbV_1$ and $RsbV_2$ not being dephosphorylated by RsbU. Since this step does not occur in the assay, there is no need for RsbW to interact with $RsbV_1$ or $RsbV_2$ in order to add a phosphate.

Overexpression of RsbW in *Chlamydia* affects transcription of σ^{66}-regulated genes. The gene encoding RsbW (*ctl0811/ct549*) was cloned into a tet-inducible vector and transformed into *Chlamydia* under ampicillin selection (Wickstrum, Sammons et al. 2013). Overexpression of the RsbW protein in a *Chlamydia* infection was evaluated by Western blot (Figure 3.2). Following confirmation that the RsbW protein was being overexpressed in *Chlamydia,* transcription levels of selected genes were evaluated. For evaluation of transcript levels, the infections were induced for a small window of time (16 to 20 hpi) to limit off-target effects. At 20 hpi, the RNA was harvested from the infections. ddPCR was used to

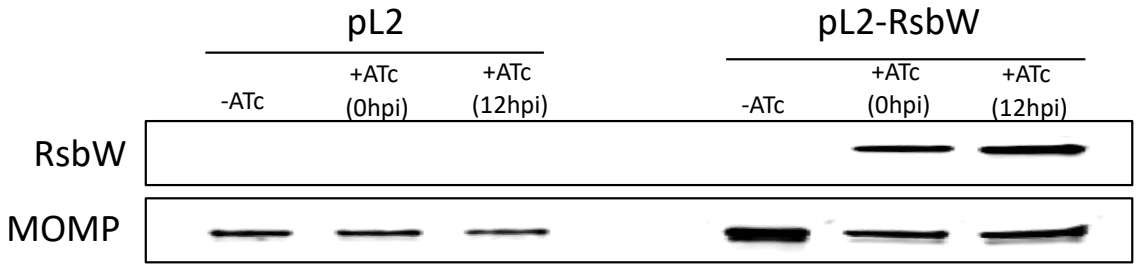
pL2
pL2-RsbW
-ATc
+ATc (0hpi)
+ATc (12hpi)
-ATc
+ATc (0hpi)
+ATc (12hpi)
RsbW
MOMP

Figure 3.2 Western blot confirmation of the overexpression of RsbW. ATc induction (10 ng/mL) was added either at the time of infection (0 hpi) or at 12 hpi. All infections were harvested at 24 hpi and run on an SDS-PAGE gel before being transferred to a membrane for Western blotting. An empty pL2 vector and no ATc controls were included as a baseline indicator. MOMP was used as a loading control.

quantify the transcript levels, normalizing to genome levels from each infection, and comparing the pL2 vector control transcript levels to the pL2-RsbW transcript levels for each gene (Figure 3.3). Known σ^{66}-regulated, constitutively active genes *secY* and *rpoA* transcript levels were both significantly down-regulated compared to the vector control (Belland, Zhong et al. 2003, Nicholson, Olinger et al. 2003). Additionally, TCA cycle-associated genes were also down-regulated, with the exception of the gene encoding glutamate transporter, *gltT.* Genes under σ^{28}- and σ^{54}-mediated control, *hctB* and *ct620,* respectively, were also evaluated (Mathews and Timms 2000, Yu and Tan 2003). These genes that are not regulated by σ^{66} do not appear to be differentially regulated with the overexpression of RsbW. These data support that RsbW inhibits the ability for σ^{66} to initiate transcription.

Phenotypic analyses of *C. trachomatis* with RsbW overexpression shows inhibited growth and progeny production. Overexpression of RsbW with the tet-inducible plasmid transformed into *Chlamydia* was evaluated for its effect on the phenotype and growth pattern of the bacteria. *Chlamydia* infections with the RsbW overexpression vector or pL2 vector control were evaluated at 0, 12, 24, 36, 48, and 72 hpi looking at chlamydial genome copies compared to host cell genome copies by ddPCR (Figure 3.4). ATc was added to induce overexpression of the RsbW gene at either the time of infection (0 hpi) or 12 hpi in order to assess if the timing of the induction had an appreciable effect on the growth of the organism. Compared to the vector control conditions (green, blue, and purple

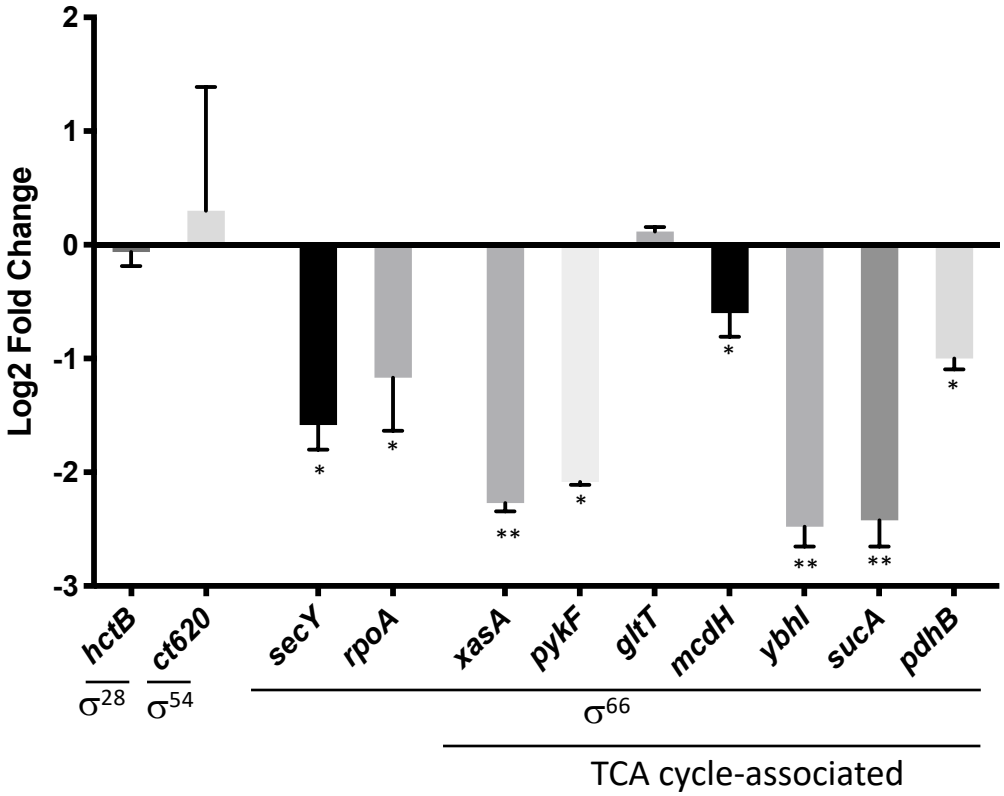
Log2 Fold Change
2
1
0
-1
-2
-3
*
*
*
**
*
*
**
**
*
hctB
ct620
secY
rpoA
xasA
pykF
gltT
mcdH
ybhI
sucA
pdhB
σ28
σ54
σ66
TCA cycle-associated

Figure 3.3 Comparison of transcript counts for select genes supports connection between RsbW overexpression and σ^{66}-regulated transcription. RsbW overexpression strain of *Chlamydia* has a significantly lower transcript counts for σ^{66}-regulated genes such as *secY* and *rpoA* and TCA cycle-related genes, with the exception of *gltT*. σ^{28}-regulated *hctB* and σ^{54}-regulated *ct620* transcript levels were unaffected by the overexpression of RsbW. * p-value <0.05; ** p-value <0.001

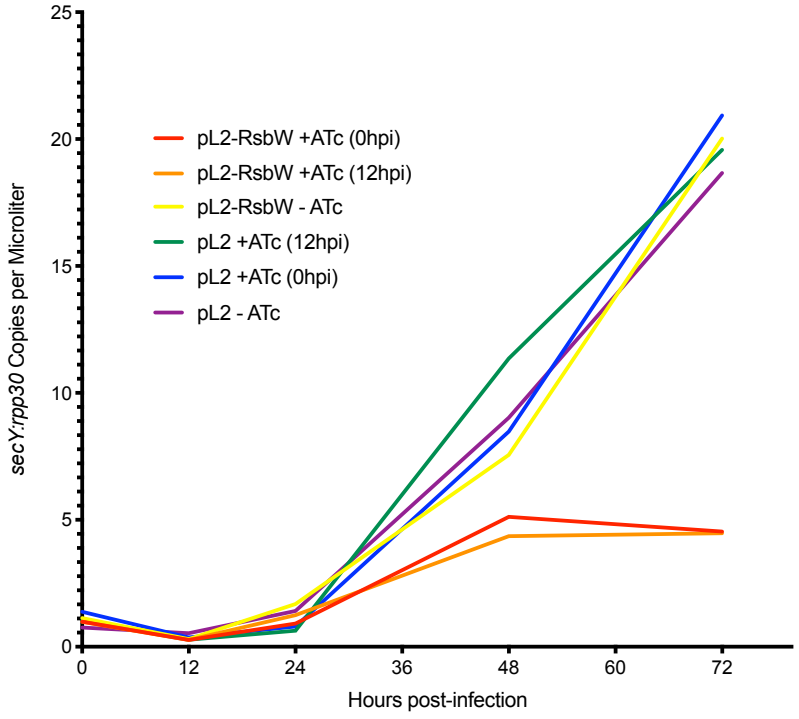
25
20
15
10
5
0
secY:rpp30 Copies per Microliter
pL2-RsbW +ATc (0hpi)
pL2-RsbW +ATc (12hpi)
pL2-RsbW - ATc
pL2 +ATc (12hpi)
pL2 +ATc (0hpi)
pL2 - ATc
0
12
24
36
48
60
72
Hours post-infection

Figure 3.4 Growth curve analysis stunting of chlamydial growth with overexpression of RsbW shows. Genome copies of *C. trachomatis* and host cells were compared at 0, 12, 24, 36, 48, and 72 hpi. After 36 hpi, there is a slowdown in the infections with induction of RsbW overexpression (red and orange lines). This growth pattern analysis was performed in triplicate; however, error bars were omitted from this graph for simplicity and ease of readability.

lines) and the uninduced control (yellow line), both induction schemes for RsbW overexpression have a decrease in growth rate after 36 hpi. After 48hpi, the overexpression of RsbW appears to stop replication altogether, in comparison to the growth pattern of the infections with native RsbW expression that continue to increase in genome copies all the way through 72hpi.

In parallel to the growth curves, a progeny assay was performed to assess the relative number of infectious progeny produced throughout the chlamydial infections (Figure 3.5). Mirroring the results of the growth curve, it was observed that at 36 and 48 hpi there were significantly less, at lease a log fold decrease, infectious progeny present in the infections with the induction of RsbW (p-value <0.001). With the induction at 12 hpi, there was also a significant decrease in infectious progeny at 24 hpi compared to the vector control conditions (p-value <0.05); however, this decrease was not observed with in addition of the inducing agent at the time of infection (0 hpi).

IFA imaging was also used to visualize the chlamydial inclusions throughout the developmental cycle (Figure 3.6). With induction of RsbW overexpression the chlamydial inclusions appear smaller in size at all three time points (24, 36, and 48 hpi), as compared to the vector control and uninduced conditions. These images are representative of the inclusions found in each infection conditions and complement the results from both the progeny assay and the growth curve analyses shown in Figure 3.4 and Figure 3.5.

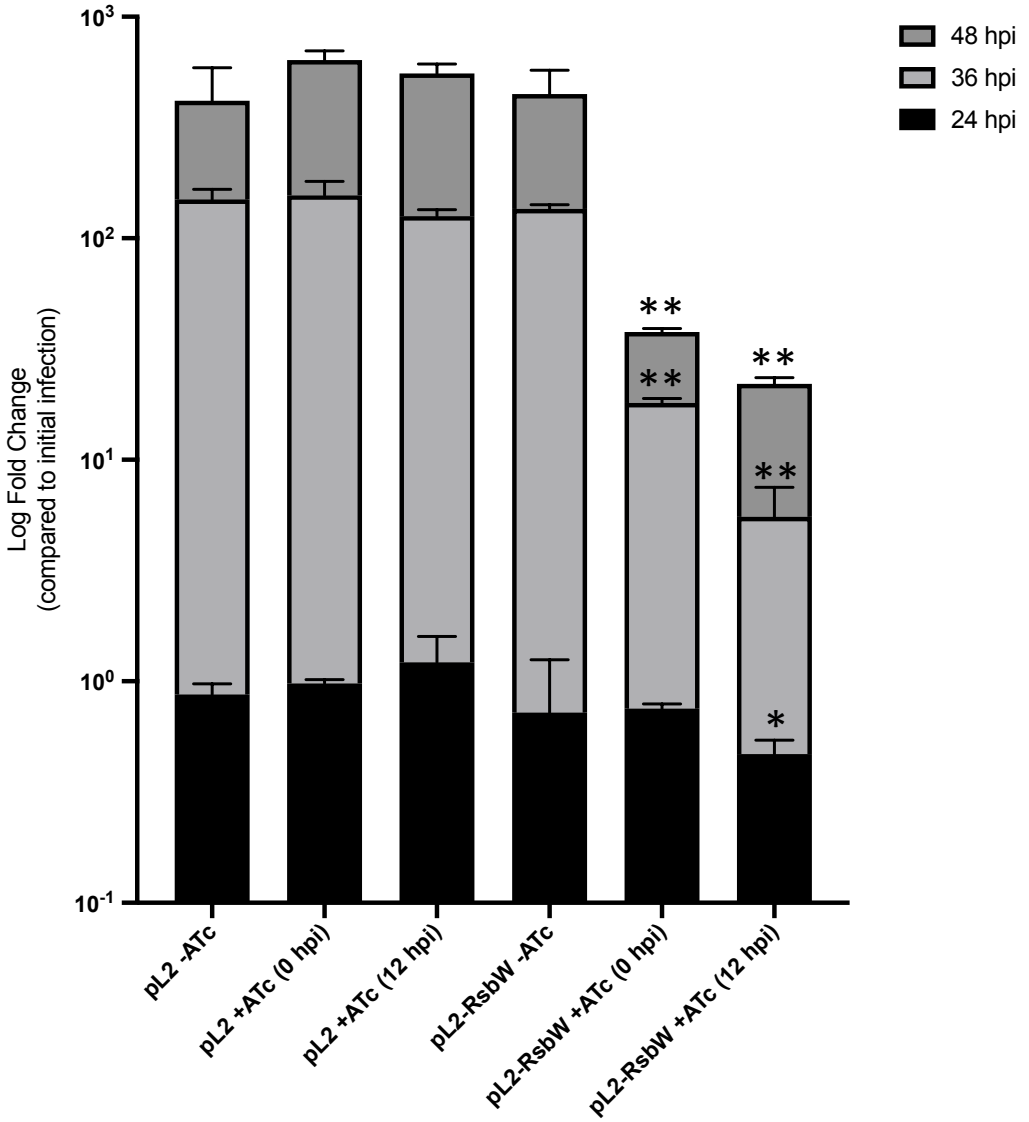
48 hpi
36 hpi
24 hpi
Log Fold Change
(compared to initial infection)
10^3
10^2
10^1
10^0
10^{-1}
**
**
**
**
*
pL2 -ATc
pL2 +ATc (0 hpi)
pL2 +ATc (12 hpi)
pL2-RsbW -ATc
pL2-RsbW +ATc (0 hpi)
pL2-RsbW +ATc (12 hpi)

Figure 3.5 Progeny assay shows decreased infectious chlamydial EBs produced with RsbW overexpression. Infectious progeny production was evaluated at 24, 36, and 48 hpi. Significant decreases in progeny production were observed when RsbW is overexpressed when compared to the pL2 vector control. * p-value <0.05; ** p-value <0.001

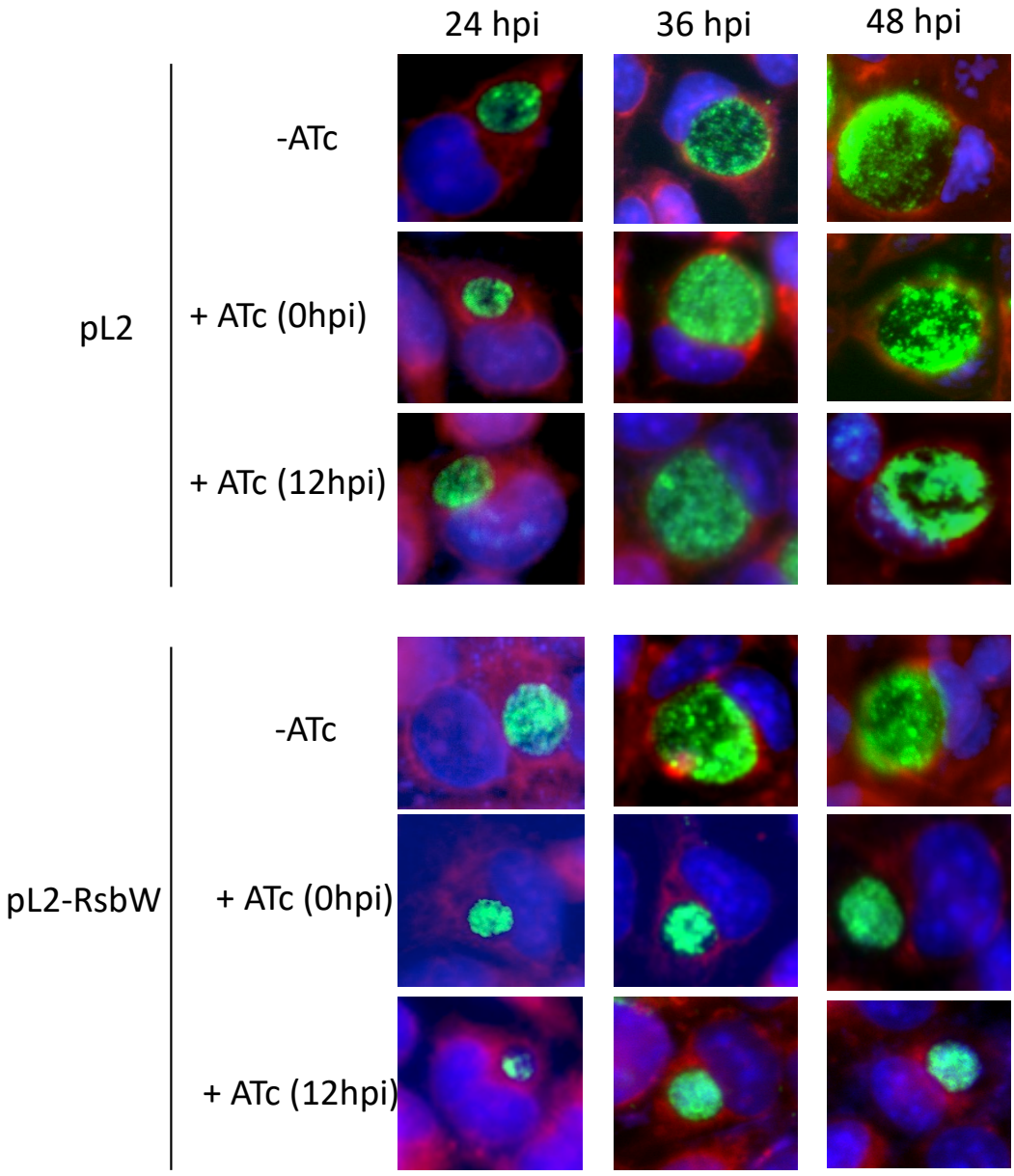
24 hpi
36 hpi
48 hpi
pL2
-ATc
+ ATc (0hpi)
+ ATc (12hpi)
pL2-RsbW
-ATc
+ ATc (0hpi)
+ ATc (12hpi)

Figure 3.6 IFA imaging allows visualization of smaller chlamydial inclusions with the overexpression of RsbW. Infections were induced with ATc for RsbW overexpression at either 0 or 12 hpi; then fixed and stained at 24, 36, or 48 hpi. With the overexpression of RsbW, inclusions are smaller in size at all observed time points. Blue: DAPI, nucleus; Red: Evan's Blue, cytoplasm; Green: OmpA, *C. trachomatis* organisms.

Discussion

The target protein regulated by the Rsb pathway in *Chlamydia* has been a point of debate with several studies showing contradictory results. Alternate sigma factors have been found to be controlled by Rsb-type pathways in some other bacterial systems (Hecker, Pane-Farre et al. 2007). *Chlamydia* only has three sigma factors in total: one major sigma factor, σ^{66}; and two alternate sigma factors, σ^{28} and σ^{54} (Stephens, Kalman et al. 1998). Following that same theme as has been found in other bacteria, Douglas and Hatch showed that σ^{28} was the binding partner for the anti-sigma factor RsbW (Douglas and Hatch 2006). Later that same year, Hua and colleagues disputed those findings with a yeast-two hybrid screen that did not find any interaction between RsbW and any of the three chlamydial sigma factors (Hua, Hefty et al. 2006). Recently, Thompson *et al.* performed a bacterial two-hybrid assay that indicated an interaction between RsbW and σ^{66}, which they subsequently confirmed with surface plasmon resonance (Thompson, Griffiths et al. 2015) .

While the regulation of a major sigma factor by such a mechanism as a Rsb system may seem unprecedented, a previous publication looking at a null-mutation of the sensor kinase protein RsbU at the beginning of this cascade pathway in *Chlamydia* showed a detrimental effect on the growth of the organism (Soules, Dmitriev et al. 2019). This previous study hypothesized that the Rsb pathway is instrumental in the regulation of the commencement of the TCA cycle as the *Chlamydia* convert from the EB form to the RB from and begins to produce its own ATP through oxidative phosphorylation (Liang, Rosas-Lemus et

al. 2018, Soules, Dmitriev et al. 2019). The model proposed in that previous study suggests that as the bacteria enters the host cell and gains access to a pool of alpha-ketoglutarate, which the *Chlamydia* utilizes as a main carbon source to fuel its truncated TCA cycle, this triggers the RsbU to start the signal cascade to activate central metabolism in the chlamydial cell. This model fits with the idea that the Rsb system could be regulating the major sigma factor for *Chlamydia.*

We sought in this current study to find the binding partners of RsbW and the effects of RsbW overexpression on chlamydial growth to provide evidence for a target protein for the Rsb pathway. In a bacterial adenylate cyclase two-hybrid (BACTH) screen with the components of the Rsb pathway, we observed positive interactions between RsbW with σ^{66} (Figure 3.1). Additionally, we used an RsbW-overexpression strain in *Chlamydia* to show that only σ^{66}-regulated genes are differentially expressed, while σ^{28}- and σ^{54}-regulated genes *hctB* and *ct620* were not affected (Figure 3.3). Growth and progeny production were both stunted by the overexpression of RsbW as well, suggesting that there is a defect in the ability of the bacteria to perform the normal metabolic activities.

Interestingly, transcription of the gene encoding the glutamate transporter protein GltT did not appear to be affected by the overexpression of RsbW (Figure 3.3). While this has yet to be fully investigated, it could be speculated that the *gltT* gene is regulated differently than the other genes associated with the TCA cycle (Iliffe-Lee and McClarty 2000). Glutamate does not enter into the TCA cycle directly but must first be converted into alpha-ketoglutarate. This may act as a

redundant measure for when alpha-ketoglutarate is less accessible and be under a secondary level of regulation that has not been addressed by these experiments.

Redundancy in the Rsb pathway and *Chlamydia* metabolism are suggested in other aspects as well. *Chlamydia* has many mechanisms for gaining ATP in addition to oxidative phosphorylation, including acquisition through the use of ATP translocases and substrate level phosphorylation (Abdelrahman and Belland 2005, Elwell, Mirrashidi et al. 2016, Liang, Rosas-Lemus et al. 2018). Even with inhibition of one mechanism of ATP acquisition, *Chlamydia* is still able to survive, albeit with a severely stunted growth, suggesting that there is not one sole mechanism for acquiring energy (Liang, Rosas-Lemus et al. 2018, Soules, Dmitriev et al. 2019). There is also the possibility of redundancy in the Rsb pathway itself. The second RsbV protein, $RsbV_2$, has been shown to be phosphorylated by RsbW, although with a lesser affinity than for $RsbV_1$, but not acted on by RsbU (Thompson, Griffiths et al. 2015). This leaves open the possibility for a whole secondary pathway that could be signaled by a completely separate set of conditions. Additionally, CT589, which based on sequence similarity appears to be a paralog of the chlamydial RsbU, has yet to be appraised as a player in the pathway as well.

Additional investigations are needed in order to further validate the interactions between RsbW and σ^{66}. Tandem affinity pull-down experiments are currently being refined in order to more directly show interaction between these proteins. A selection of amino acid crosslinkers are being evaluated to determine

ideal conditions for the procedure. While BACTH showed interactions between RsbW and σ^{66}, the results are binary and may permit for false positives (Karimova, Pidoux et al. 1998). Likewise, the BACTH screen also showed an interaction between RsbW and RsbU. An interaction between these two proteins has not been previously observed, in *Chlamydia* nor other homologous bacterial systems. This is an interesting observation and could suggest that there is a complex forming between the members of the Rsb pathway.

Moreover, utilizing the BACTH system further to gain additional knowledge about chlamydial Rsb pathway is being explored. Because *Chlamydia* is an obligate intracellular bacterium, evaluating the effects of adding or subtracting components from the culture media is difficult due to the added complexity of the host cell. It may be possible to utilize *E. coli* as a surrogate system for recapitulating the chlamydial Rsb pathway in a way that would be easier to manipulate in a logistical sense. Using the BACTH system as a reporter mechanism for interaction with RsbW and σ^{66}, with the addition of RsbU and RsbV to complete the full pathway, we may be able to show the effects of the compounds shown to bind to RsbU previously (Soules, Dmitriev et al. 2019). Efforts are currently focused on finding and cloning all the different components of the Rsb pathway into compatible vectors for transformation into *E. coli.*

In this study, we touched on the role of RsbW in the greater scheme of *Chlamydia* biology. While there are still gaps in our full understanding of the chlamydial Rsb pathway, the evaluations of potential RsbW binding partners and

the overexpression of RsbW in *Chlamydia*, suggests that Rsb pathway is interacting with the major chlamydial sigma factor, σ^{66}.

Chapter IV: Sigma 54 controls membrane reorganization and type III secretion effectors during conversion to infectious forms of *Chlamydia trachomatis*.

Abstract

Chlamydia are obligate intracellular bacteria with a phylum defining bi-phasic developmental cycle that is intrinsically linked to its ability to cause disease. The progression of the chlamydial developmental cycle is regulated by the temporal expression of genes predominantly controlled by RNA polymerase sigma (σ) factors. Sigma 54 (σ^{54}) is one of three sigma factors encoded by *Chlamydia* for which the role and regulon are unknown. CtcC is part of a two-component signal transduction system that is requisite for σ^{54} transcriptional activation. CtcC activation of σ^{54} requires phosphorylation, which relieves inhibition by the CtcC regulatory domain and enables ATP hydrolysis by the ATPase domain. Prior studies with CtcC homologs in other organisms have shown that expression of the ATPase domain alone can activate σ^{54} transcription. Biochemical analysis of CtcC ATPase domain supported ATP hydrolysis in the absence of the regulatory domain, as well as an active site residue essential for ATPase activity (E242). Using recently developed genetic approaches in *Chlamydia* to induce expression of the CtcC ATPase domain, a transcriptional profile was determined that is expected to reflect the σ^{54} regulon. Computational evaluation revealed that the majority of the differentially expressed genes were preceded by highly conserved

σ^{54} promoter elements. Reporter gene analyses using these putative σ^{54} promoters reinforced the accuracy of the proposed regulon. Investigation of the gene products included in this regulon supports that σ^{54} controls expression of genes that are critical for conversion of *Chlamydia* from replicative reticulate bodies into infectious elementary bodies.

Introduction

Sigma-54 (σ^{54}) is a widely distributed and unique subunit of RNA polymerase (RNAP) holoenzyme that is associated with stringent regulation of gene products connected with various critical biological functions in bacteria (Kustu, Santero et al. 1989, Merrick 1993, Francke, Groot Kormelink et al. 2011). Sigma 54, otherwise referred to as σ^{N}, was originally characterized as responding to nitrogen levels in *E. coli* and *Salmonella* (Keener and Kustu 1988, Kustu, Santero et al. 1989). It has since been shown that σ^{54} regulons are diverse and include responses to antibacterial compounds, toxic heavy metals, metabolism of alternate carbon sources, and biosynthesis of pilin and type III secretion systems (Ferro-Luzzi Ames and Nikaido 1985, Ishimoto and Lory 1989, Kohler, Harayama et al. 1989, Kustu, Santero et al. 1989, Gardan, Rapoport et al. 1995, Martin-Verstraete, Stulke et al. 1995, Arora, Ritchings et al. 1997, Pearson, Pesci et al. 1997, Robichon, Gouin et al. 1997, Dalet, Briand et al. 2000, Hendrickson, Guevera et al. 2000, Hutcheson, Bretz et al. 2001, Jagannathan, Constantinidou et al. 2001, Leonhartsberger, Huber et al. 2001, Chatterjee, Cui et al. 2002, Jacobi, Schade et al. 2004, Niehus, Gressmann et al. 2004). While these signals and responses are variable, transport and biosynthesis of components that comprise the exterior of the bacteria and host cell interactions are themes that appear to be shared among bacterial σ^{54} regulation (Francke, Groot Kormelink et al. 2011).

There are many aspects of σ^{54} transcriptional initiation that are highly conserved between bacterial phyla and distinct from σ^{70} family members

(Danson, Jovanovic et al. 2019). A primary difference is that the promoter recognized by σ^{54} is centered at the -12 and -24 position upstream of the transcriptional start site, rather than the typical -10 and -35 position (Morett and Buck 1989, Barrios, Valderrama et al. 1999). Unlike σ^{70}-type sigma factors which are able to spontaneously separate double-stranded DNA and initiate transcription after forming the RNAP holoenzyme (Merrick 1993, Mooney, Darst et al. 2005), Sigma 54 is incapable of transitioning from the closed- to open-complex on the DNA without the assistance of an ATP-hydrolyzing response regulator, typically referred to as NtrC.

Sigma 54 response regulators are typically composed of three domains: a DNA-enhancer binding domain; an effector ATPase domain with a conserved glutamate-242 residue that polarizes the ATP molecule allowing for hydrolysis to occur; and a receiver domain that is phosphorylated by a sensor kinase (NtrB) in response to an environmental cue (Ninfa and Magasanik 1986, Keener and Kustu 1988, Schumacher, Joly et al. 2006, Snider, Thibault et al. 2008). Phosphorylation of this receiver domain relieves inhibition of the ATPase domain and allows NtrC to hydrolyze ATP, enabling σ^{54}-RNA holoenzyme to form an open DNA complex and initiate transcription (Kustu, Santero et al. 1989, Schumacher, Joly et al. 2006). Previous studies have shown that in the absence of the receiver domain, the ATPase domain alone can initiate σ^{54}-directed transcription (Huala, Stigter et al. 1992, Xu, Gu et al. 2004, Samuels, Frye et al. 2013). The regulatory cue that triggers the signaling cascade activating σ^{54} differs in various bacteria species, as does the regulon of genes that σ^{54} is responsible

for transcribing. Despite the variation in activating signals and subsets of genes being regulated in different bacteria, this mechanism of regulation provides tight control of the σ^{54} regulon that is expressed only under specific conditions (Kustu, Santero et al. 1989).

Chlamydia are obligate intracellular bacteria that encode for a σ^{54} homolog, along with two σ^{70} family factors (σ^{66} and σ^{28}). σ^{66} and σ^{28} have previously been shown to be important for controlling various stages of temporal gene expression during the developmental cycle of *Chlamydia* (Abdelrahman and Belland 2005, Elwell, Mirrashidi et al. 2016); however the role of σ^{54} has yet to be determined. The metabolically active and replicative form of *Chlamydia* is termed the reticulate body (RB) for which σ^{66} directs transcription of most encoded genes (~80%) and products are associated with metabolism, replication, and maintenance of the intracellular environment (Belland, Zhong et al. 2003, Nicholson, Olinger et al. 2003). As the developmental cycle progresses, RBs will asynchronously convert into the infectious, spore-like form of *Chlamydia*, termed the elementary body (EB). During this stage of the developmental cycle, when RB-to-EB conversion is occurring, global gene expression profiling supports about 20% of the genome is upregulated (Belland, Zhong et al. 2003, Nicholson, Olinger et al. 2003). Expression of many of these genes have been shown to be regulated by σ^{66}, with additional factors, such as DNA topology and supercoiling, expected to contribute to this differential expression mechanism (Hefty and Stephens 2007, Cheng and Tan 2012, Orillard and Tan 2016). σ^{28} has been shown to regulate few, but critical, genes during the RB-to-EB conversion

process, including the formation of the condensed DNA structure that is unique to EBs (Yu and Tan 2003, Yu, Di Russo et al. 2006, Yu, Kibler et al. 2006, Yu, Lu et al. 2015, Rosario and Tan 2016).

Chlamydial EBs are transcriptionally silent due to a highly condensed nucleoid, have limited metabolic activity, and an extensive network of disulfide cross-linked outer-membrane proteins for osmotic stability. In spite of the minimal metabolic activity, EBs have extensive infectious capabilities that enable host cell adherence, invasion, and the establishment of the intracellular environment (Moulder 1991). EBs have been shown to bind to host cells using multiple membrane proteins (OmcB, OmpA, and Pmps) and subsequently invade and establish an intracellular vacuolar environment (i.e. inclusion) through the use of type III secretion system and pre-formed effector proteins, such as TarP, Incs, and others (Jewett, Fischer et al. 2006, Moore and Ouellette 2014). Because EBs have minimal metabolic activity, the proteins needed for these critical infection processes need to be pre-packaged before the RB-to-EB conversion and exit from an infected cell (Albrecht, Sharma et al. 2010). Therefore, at the late stages of the developmental cycle, the transcription of genes for membrane remodeling and structural transition to the EB and the arming of necessities for reinfection must occur. While many aspects of the temporal regulation of the developmental cycle have been determined, there are still gaps in the understanding of important details, including how the chlamydial cells regulate the equipping of the EB with the necessary components for survival in the extracellular environment and the next round of host cell infection.

In this study, the regulon of σ^{54} in the human pathogen *Chlamydia trachomatis* is determined using the ATPase domain of the NtrC homolog and response regulator protein, CtcC. Computational investigation of σ^{54} promoter elements and reporter gene expression analyses supported the accuracy of this determined regulon. From the proposed regulon, σ^{54} is hypothesized to regulate transcription of genes involved in the RB-to-EB transition including many membrane proteins and type III secretion effector proteins known to be important for early stages of EB infection.

Materials and Methods

Overexpression and purification of recombinant CtcC protein variants. The *ctl0728* (*ctcC*) gene was amplified via PCR from *C. trachomatis* (L2 434/BU) genomic DNA, either the full-length open reading frame or the ATPase domain-only (a.a. L142 through L386). The gene was inserted into the pTBSG vector in frame and immediately downstream of a sequence encoding an N-terminal hexahistidine tag and TEV protease recognition site. The E242A residue substitution was introduced via site-directed mutagenesis using the Q5 Site-Directed Mutagenesis Kit (New England Biolabs, Ipswich, MA).

After confirming sequence, the vector was transformed into BL21 (DE3) *E. coli* competent cells, which were then grown at 37°C in Terrific Broth supplemented with 100 μg/mL carbenicillin to an OD_{600} of approximately 0.8. Protein expression was induced with the addition of IPTG (isopropyl1-thio-β-D-galactopyranoside) to a final concentration of 0.5 mM for 10 hours at 17°C. Following *E. coli* collection by centrifugation (10,000 x g, 20 minutes), cells were resuspended in washing buffer (10 mM HEPES pH 7.2, 5 mM EDTA, 0.1% Triton-X 100) with the addition of phenylmethane sulfonyl fluoride to a final concentration of 1 mM, and 1000U of benzonase endonuclease (EDM Millipore, Burlington, MA). Cells were lysed by sonication and centrifuged for 30 minutes at 14,000 x g. The supernatant after this centrifugation was decanted and the insoluble protein pellet was resuspended in wash buffer and centrifuged again. This wash step was repeated one additional time, for a total of three washes and centrifugations. After the final wash, the supernatant is again decanted, and the

pellet is resuspended in denaturing buffer (6 M guanidine hydrochloride PBS pH 8.0) and rocked overnight at 4°C. The denatured cell mixture was centrifuged at 20,000 x g for 30 minutes, and then the supernatant was applied to a gravity flow HisPur Cobalt Resin (ThermoFisher, Waltham, MA) column. After applying the protein to the column, it was washed with three column volumes of the denaturing buffer followed by three volumes of washing buffer (8 M urea, 100 mM NaH_2PO_4, 10 mM Imidazole pH 8.0). Three column volumes of elution buffer (8 M urea, 100 mM NaH_2PO_4, 250 mM Imidazole at pH 3.0) were used to elute the protein off the column. Dialysis was performed on the eluted protein into refolding buffer (250 mM NaCl, 50 mM NaH_2PO_4, 5 mM DTT, 5% glycerol pH 10.0) with gradually lower concentrations of urea at 6, 3, 2, 1.5, 1, 0.5, 0.25 and 0 M, changing buffers with a minimum of 3 hours between each concertation. Proteins concentrations were confirmed using a Bradford assay.

***In vitro* ATPase activity assay with purified recombinant CtcC protein variants.**

Quantification of the ATPase activity was measured using the protocol and reagents provided by the ADP-Glo Kinase Assay Kit (Promega, Madison, WI). All proteins were initially suspended in the same buffer (50mM NaH_2PO_4, 250mM NaCl, 5mM DTT, 5% Glycerol at pH 10.00) and warmed to 37°C. Each were then added in a 45:45:10 volume ratio to warmed activity buffer (50 mM Tris Base pH 8.0, 100 mM KOAc, 27 mM NH_4OAc, 8 mM MgOAc, 25 μM EDTA, 1 mM DTT) with 4 mM Mg-ATP and incubated at 37°C for 30 minutes. Luminescence was

then measured on a plate-reading luminometer (Infinite M200 Pro, Tecan, Mannedorf, Switzerland). All conditions were performed in triplicate in a 96-well plate format.

Construction of *ctcC* expression constructs and *Chlamydia* transformation. The *ctl0728* (*ctcC*) gene was amplified via PCR from *C. trachomatis* (L2 434/BU) genomic DNA, either the full-length open reading frame or the ATPase domain-only (residues L142 through L386). The gene was inserted into the pL2-tetO overexpression plasmid using ligase-independent cloning methods at the AgeI restriction enzyme site and transformed in DH5α competent *E. coli* cells (Wickstrum, Sammons et al. 2013). After confirming sequence and protein expression in *E. coli* cells, vector plasmid was isolated using Qiagen Plasmid MiniPrep Kit. The E242A substitution was introduced via site-directed mutagenesis using the Q5 Site-Directed Mutagenesis Kit (New England BioLabs, Ipswich, MA).

Purified *ctcC* expression vector plasmid was transformed into wild-type L2 *C. trachomatis*. Briefly, 15 μg of vector plasmid was mixed with 100 μL 2X $CaCl_2$ buffer (20 mM Tris pH7.5, 100 mM $CaCl_2$) and 25 μL of *C. trachomatis* EBs, and diluted with water to a final volume of 200 μL. This $CaCl_2$ mixture incubated at room temperature for 30 minutes at room temperature before being diluted into 1X $CaCl_2$ buffer and added onto a confluent monolayer of L292 cells, and then centrifuged for 30 minutes at 550 x g, 20°C. Following centrifugation, the $CaCl_2$ mixture was aspirated off the monolayer and replaced with RPMI media

supplemented with 5% tetracycline-free FBS, 10 μg/mL gentamycin, 1 μg/mL cycloheximide, and incubated at 37°C, 5% CO_2. After 16 hours, 1 μg/mL of ampicillin were added to the infected cells. The infection was allowed to incubate for 42 hours after the initial infection at which point the cells were lysed using water lysis and passaged to a new monolayer of cells, with media containing 1 μg/mL of ampicillin. After an additional 48 hours, the cells were passaged again with 2 μg/mL of ampicillin. Two additional passages occur 48 hours after each previous passage, with new media containing 5 μg/mL of ampicillin. At this point, the infection was propagated for harvesting and presence of the vector plasmid was confirmed by PCR.

Western blot of CtcC overexpression in *C. trachomatis*. L929 host cell monolayers were infected with *C. trachomatis* transformed with the different tet-inducible *ctcC* construct variant plasmids and incubated in RPMI media supplemented with 5% tetracycline-free FBS, 10 μg/mL gentamycin, 1 μg/mL cycloheximide at 37°C, 5% CO_2. Infections were induced with 10 ng/mL of anhydrotetracycline (ATc) at 16 hours post-infection. At 20 hours post-infection, infections were harvested by applying a 1:1 ratio of PBS (Corning, NY) and 2X Laemmli sample buffer with 2-mercaptoethanol (Bio-Rad, Hercules, CA) directly to the cell monolayer and cell scraping was done to collect the contents of the tissue culture plate well. The collected sample was used for Western blot analysis. Rabbit anti-CtcC primary antibody and goat anti-MOMP primary antibody (ViroStat, Westbrook, ME) were used to probe for the protein of interest

and a loading control protein, respectively. IRDye donkey anti-rabbit 680LT and donkey anti-goat secondary 800CW antibody (LI-COR, Lincoln, NE) were used to visualize the Western blot.

Progeny assay with induction of CtcC protein variant overexpression. L929 host cell monolayers in 6-well tissue culture plates were infected with *C. trachomatis* transformed with different tet-inducible *ctcC* variant plasmids or empty pL2 vector control plasmid using RPMI supplemented with 5% tetracycline-free FBS, 10 μg/mL gentamycin, 1 μg/mL cycloheximide. At 12 hours post-infection, 10 ng/mL of ATc was added to induce overexpression of CtcC protein variant. At 30 hours post infection, the infected monolayer was lysed using water lysis technique and passaged onto new monolayer of host cells in a 96-well plate format to determine infectious titer. At 24 hours after the passage, the 96-well plate was fixed and stained using the MicroTrack *C. trachomatis* culture confirmation test (Syva Co., Palo Alto, CA). Wells were then quantified for the number of inclusions and the compared to the number of inclusion-forming units in the initial infection. This procedure was repeated in triplicate for each condition.

Immunofluoresent microscopy of *C. trachomatis* infected cells following expression induction of CtcC variants. L929 cells were grown to ~75% confluency in an 8-well ibiTreat μ-Slide (Ibidi, Martinsried, Germany) and were infected with respective *C. trachomatis* L2 mutants. At 12 hpi, 10 ng/ml ATc was

added to respective wells, and at 24 hpi wells were fixed with methanol for 10 minutes and then washed with Hank's Balanced Salt Solution (HBSS). Cells were washed with HBSS and then stained with MicroTrack *C. trachomatis* culture confirmation test (Syva Co., Palo Alto, CA) and 10nM 4', 6-diamidino-2-phenylindole (DAPI) in PBS. A final overlay of Vectashield antifade mounting medium (Burlingame, CA) was added and slides were immediately imaged. Cells were visualized on an Olympus IX81/3I spinning disk confocal inverted microscope at 150X magnification and captured on an Andor Zyla 4.2 sCMOS camera (Belfast, Northern Ireland). Microscope and camera were operated using SlideBook 6 software (Intelligent Imaging Innovations, Denver, USA). Images are representative of at least 5 different fields/inclusions per condition. Exposure time remained consistent for all fields captured, with exposure for DAPI (DNA) at 1 second, FITC (OmpA) for 3 seconds, and Cy5 (cytoplasm) for 3 seconds. Three Z-stack images at 0.3µm apart were taken per field imaged. Images were processed in SlideBook 6 and No Neighbors Deconvolution with a subtraction constant of 0.4 was applied to all images. Images represent an average projection over the Z-axis of the three Z-stacks for each field shown.

RNA purification and RNAseq. L929 cells in a 6-well tissue culture plate with tetracycline-free RPMI media were infected with the pL2-tetO *ctcC* ATPase only construct or the pL2-tetO vector control. The infection was induced with a final ATc concentration of 10 ng/mL at 16 hpi. A relatively small window of induction was chosen to reduce the pleiotropic effect of over-activating σ^{54}. At 20 hpi, the

infection was harvested as described in the previous section using TriZol and subsequent chloroform RNA extraction. As per the procedure for RNA-sequencing intracellular bacteria by Marsh, Humphrys, and Myers, following TURBO DNase treatment (Thermo Fisher, Waltham, MA) and purification using the RNeasy kit (Qiagen, Hilden, Germany), both host and chlamydial ribosomal RNA was depleted using the Ribo-Zero Magnetic Core Kits (Illumina, San Diego, CA) specific for Human/Mouse/Rat rRNA and Gram-negative bacteria rRNA (Marsh, Humphrys et al. 2017). A final purification step was performed using the RNeasy Mini kit (Qiagen, Hilden, Germany). rRNA depletion was assessed by running samples on a 2% agarose gel. RNA quality was assessed using Qubit quantification and TapeStation gel analysis. The RNA library was made using the NEBNext Ultra II Direactional RNA Library Prep Kit for Illumina (New England BioLabs, Ipswich, MA) and was sequenced with NextSeq 550 High Output Single Read 50 bp Sequencing (NX-HO-SR50). Geneious Prime (Version 2019.1.1) was used for the data analysis. Reads were aligned to *Chlamydia trachomatis* 434/Bu genome (NC010287). Transcript levels were normalized to reads per million. Genes with an average differential expression ratio two standard deviations away from the mean differential expression ratio for the entire genome were considered to be significantly up-regulated and were included as part of the σ^{54} regulon and listed in Table 4.3 or Table 4.4, depending on the presence or absence of a predicted σ^{54} promoter region upstream of the open reading frame.

Droplet digital PCR quantification of RNA transcripts with CtcC protein variant overexpression. L292 cells in a 6-well tissue culture plate with tetracycline-free media were infected with the different *ctcC* construct plasmids or empty pL2 control vector transformed *C. trachomatis* were induced with 10 ng/mL ATc at 16 hours post-infection, and then harvested with 1 mL per well TRIzol. 200 μL of chloroform was added to each 1 mL TRIzol cell lysate, vortexed, and centrifuged for 8 minutes at 10,000 g. The aqueous layer of the TRIzol/chloroform mixture was collected in a new tube, and a 1:1 ratio of isopropanol was added before incubating at -20°C for 30 minutes, followed by room temperature for 15 minutes. The precipitated nucleic acids were pelleted by centrifugation for 8 minutes, the supernatant was decanted, and the pellet was washed with 1 mL 70% ethanol. After another 5-minute centrifugation, the pellet was air dried and resuspended in 80 μL of RNAse-free Molecular Biology Grade water (Corning, NY). DNA depletion was performed by adding 10 μL of TURBO DNAse Buffer and 10 μL of TURBO DNAse (Thermo Fisher, Waltham, MA) to each 80 μL of sample and incubated in a 37°C water bath for 30 minutes. Immediately following DNA depletion, the samples were taken through the RNeasy Mini Kit (Qiagen, Hilden, Germany) and eluted into 50 μL of RNase-free water.

cDNA was generated using the High-Capacity cDNA Reverse Transcription Kit (Applied Biosystems, Foster City, CA) including control reactions excluding the reverse transcriptase, which was then used to assess the presence of residual gDNA contamination. Following cDNA generation, droplet

digital PCR (ddPCR) was used to determine an absolute quantification for the number of transcripts present for the genes of interest. The QX200 Digital Droplet PCR system (Bio-Rad, Hercules, CA) with all the suggested Bio-Rad consumables, including QX200 EvaGreen Supermix, were utilized in the set up and reading of the ddPCR run. Primers for specific genes of interest used for ddPCR are listed in Table 4.1. Data was analyzed using the QuataSoft Analysis Pro Software, version 1.0 (Hindson, Ness et al. 2011). The data was normalized to the quantification of *secY* transcript copies, and converted to $\log_2$ scale compared to the number of transcripts in the empty pL2 vector control induced with ATc (Belland, Zhong et al. 2003, Nicholson, Olinger et al. 2003).

Miller Assays. β-galactosidase activity was used to assess the ability of σ^{54} to activate transcription of a downstream gene (*lacZ)* from promoter regions taken from those genes found to be upregulated in the RNAseq analysis. Promoter regions were amplified using primers listed in Table 4.2 and cloned into the pAC-lacZ vector at the BamHI restriction site upstream of the *lacZ* gene (Hefty and Stephens 2007). The chlamydial genes encoding σ^{54} and the CtcC ATPase domain (residues 142-386), with and without the E242A amino acid substitution, were cloned into the pRSF-Duet vector at the NcoI and NdeI restriction sites, respectively, putting the transcription of both these genes under IPTG-inducible regulation. All insertions were confirmed by sequencing. *E. coli* cells were co-transformed with the pAC-lacZ plasmid containing the various promoter regions

in combination with the different pRSF-Duet plasmids. IPTG-induced expression of σ^{54} and the CtcC ATPase domain were assessed via Western Blot. Overnight cultures were grown in LB broth supplemented with 50 μg/ml of chloramphenicol and kanamycin (only chloramphenicol was used when just the pAC-lacZ vector was present). Cultures were then diluted 1:100 in fresh broth and grown at 37°C until the culture reach mid-log phase. Cultures were induced with 1mM IPTG for 1 hour before being centrifuged. Pellets were washed and resuspended in Z-buffer [0.06M Na_2HPO_4, 0.04M NaH_2PO_4, 0.01M KCl, 0.001M $MgSO_4$, 0.05M β-mercaptoethanol, pH 7.0). Permeabilization was perform with 10% volume chloroform and 5% volume 0.1% sodium dodecyl sulfate for 10 minutes at room temperature. 100 μL of the aqueous layer of the mixture was then aliquoted in triplicate into a microtiter plate, followed by 20 μl of *ortho*-nitrophenyl-β-galactoside (4mg/ml) was added. 50 μl of Na_2CO_3 was added to each well after 10 minutes to stop the reactions. OD_{420} and OD_{550} was then measure for each reaction, as well as OD_{600} of samples taken prior to cell permeabilization, in order to calculate Miller units (Miller 1972, Hefty and Stephens 2007).

Table 4.1 ddPCR Primers

Gene	Direction	Sequence (5' --> 3')
ct084	Forward	TTTTTCAAACTTGTCGTGATAGCG
ct084	Reverse	AATAATGTTCAGCTTAGTTTCCCTTTTTG
ct105	Forward	GTATGCCAGCAACCTACG
ct105	Reverse	CACAAGGCTTTGCACATTAG
ct142	Forward	ATGAGTGATTCTGACAAAATTATTAATGATTG
ct142	Reverse	ACTGGTTGGGAGTCTTTCTC
ct229	Forward	CGTTGATACAATGCGACAAATG
ct229	Reverse	TTTATATTCTTCCTCAAGCTCCTC
ct394	Forward	ATGGAAAATAGAATAGAAATGTCCCAAC
ct394	Reverse	TTTCGTATCGTTGCCGAAC
ct444	Forward	GTAGTTGTTGTCGTATCGTTG
ct444	Reverse	TTGTCTGCATTTGCCGTC
ct456	Forward	CAACTTTTACATCATCAACCACTTC
ct456	Reverse	ATCGCTTGATGAGGTAGAGC
ct494	Forward	TTTTTCGATTTTTATTAAAAGGTTTTTTATCCG
ct494	Reverse	CAACTCCTTGAGCGTTGG
ct576	Forward	CCTGTTCCTACGGAAGAG
ct576	Reverse	CAAAAGCGGCTTCATCATAC
ct619	Forward	GAGTATTTCCTGGAGGAGACTG
ct619	Reverse	TTCGACGATACACCAGCTAC
ct620	Forward	ATTCTAGAAGATGCTCTTGTCTCAG
ct620	Reverse	CTAACTAGCCAGTTTTCTTGTTAAACC
ct646	Forward	GTAACCCAAAGTGCAGAAAAC
ct646	Reverse	GTCTCCTGTCCTTGTAAGG
ct683	Forward	GGAAAAGCATTTAGCGAAAGAG
ct683	Reverse	ACGTAAATAGCTGTCTCCAG
ct711	Forward	CCATTTCTTTAACTAAGAATATAACGGC
ct711	Reverse	TTTACTCGTTGTTCCCGTAG
ct814	Reverse	CTGCAAATTCTCGTGTGTG
ct814.1	Forward	ATGATTTATTTTTTTGTTTTTATGACCCCC
ct814.1	Reverse	TCGACTGACAAGTTTCATAATCTTATG
ct841	Forward	TGTTGCTTATGGTTGCGAG
ct847	Forward	AAATACTGTCATACCAGACTCTAC
ct847	Reverse	TAACAAGGGGATGTTGATTAGTTC
ct875	Forward	GAATCCCTTCTCATAATGGGG
ct875	Reverse	GGTGCTCTCGATCATAGAGC
rpoA	Forward	ATGTCGGATAGTTCACACAATTTAC
rpoA	Reverse	TTCCCAAGGTGTGCCCC
secY	Forward	TCAAGGTCTTCCTTTGGGGC
secY	Reverse	TACACAATGAATAGGGTAACTTTGC

Table 4.2 Primers for cloning

Vector	Name	Restriction site	Sequence(5' --> 3')
pRSF-Deut			
	RpoN Forward	NcoI	GTTTAACTTTAATAAGGAGATATACCATGATGTTGCATCAGCATCAAACAG
	RpoN Reverse	NcoI	GGTGATGATGGTGATGGCTGCTGCCCATGTTAGATAGTATGTCGAGAATTCTCTGTGC
	CtcC ATPase Forward	NdeI	GTTAAGTATAAGAAGGAGATATACATAATGCTGATCGCCGAAAGTCCTTC
	CtcC ATPase Reverse	NdeI	CCGGCCGATATCCAATTGAGATCTGCCATATTATAAGAGAGCGAGCATAGAAGG
pACYC-lacZ			
	ct620 Promoter Forward	BamHI	CATACCCATGGGCTCTGGATCCCAAAGCTACAGCTAAACGTC
	ct620 Promoter Reverse	BamHI	GTCATCGTCATCACCGGATCCTCAACTAATGTCTTTTATAAAAAGATTACC
	ct142 Promoter Forward	BamHI	CATACCCATGGGCTCTGGATCATCCGACTCCTTACGGATAC
	ct142 Promoter Reverse	BamHI	GTCATCGTCATCACCGGATCTTAATTGTTTCCAAGTTTTTATTTTGAATAAAAAG
	ct814.1 Promoter Forward	BamHI	CATACCCATGGGCTCTGGATCGTCGGGTATCTTTACCAACAAC
	ct814.1 Promoter Reverse	BamHI	GTCATCGTCATCACCGGATCGTTTTCGATAATTATTTTCTTACTTCTTATTTAAAAAG
	ct084 Promoter Forward	BamHI	CATACCCATGGGCTCTGGATCCCCCCCATGATCCTGAATG
	ct084 Promoter Reverse	BamHI	GTCATCGTCATCACCGGATCGATTTTTTACGGCTATTTATTTTCTTTTAATTAAAAAC
	ct494 Promoter Forward	BamHI	CATACCCATGGGCTCTGGATCGGCTCTTTAGTTTACCAAGGAC
	ct494 Promoter Reverse	BamHI	GTCATCGTCATCACCGGATCGCAAACCCTAATAAATCTATTAATCGC
	ct394 Promoter Forward	BamHI	CATACCCATGGGCTCTGGATCCGGAGAGCTTCTCCGTAG
	ct394 Promoter Reverse	BamHI	GTCATCGTCATCACCGGATCAAGTCGGTGTCATTATAAGAAAACC
	hctB Promoter Forward	BamHI	CATACCCATGGGCTCTGGATCGTCGACACTAACCATTTTTTATTAAAGTTTTTC
	hctB Promoter Reverse	BamHI	GTCATCGTCATCACCGGATCGGTACCTCCCCTAATTAGACAGG
	ct229 Promoter Forward	BamHI	CATACCCATGGGCTCTGGATCAAAACCTCAGTTTTTCTGAGAGG
	ct229 Promoter Reverse	BamHI	GTCATCGTCATCACCGGATCTTATTTCCCCTAAAACTTAATGCC
	ct444 Promoter Forward	BamHI	CATACCCATGGGCTCTGGATCCCCTCCGATTCTTGTATTATATAG
	ct444 Promoter Reverse	BamHI	GTCATCGTCATCACCGGATCAACTTCCAGACTCCTTTCTAG
	ct456 Promoter Forward	BamHI	CATACCCATGGGCTCTGGATCCAAGTAATTTAGTTGTAGCATTTTTAGC
	ct456 Promoter Reverse	BamHI	GTCATCGTCATCACCGGATCAACTACAAATTAAATAAAAACAACAGCCG
	ct620 Site-Direcet Mutagenesis Promoter Bashing Forward		TAAAAACCGAGCAAGGATTGGCG
	ct620 Site-Direcet Mutagenesis Promoter Bashing Reverse		AAAACAAAGCACGGCCAGCC
pTBSG			
	Full CtcC Forward	SspI	CCGTTATCCACTTCCAATATGTCGATAGAACACATTCTTATTATTGAC
	CtcC Reverse	SspI	CCGTTATCCACTTCCAATTTATAAGAGAGCGAGCATAGAAGGAGTGA
	CtcC ATPase Forward	SspI	CCTGTACTTCCAATCCAATCTGATCGCCGAAAGTCCTTCCATG
pL2-tetO			
	Full CtcC Forward	AgeI	CTTTAAGAAGGAGATACCGGATGTCGATAGAACACATTCTTATTATTGAC
	CtcC ATPase domain Forward	AgeI	CTTTAAGAAGGAGATACCGGATGCTGATCGCCGAAAGTCCTTC
	CtcC Reverse	AgeI	CACTTCACAGGTCAACCGGTTATAAGAGAGCGAGCATAGAAGG
	CtcC E242A Site Directed Mutagenesis Forward		GCACTCTTTTACTAGATGCAATCACAGAAATTC
	CtcC E242A Site Directed Mutagenesis Reverse		CTTGGTGGGCGAGTTCAAATCTTCCTAC

Results

Effector (ATPase) domain of chlamydial σ^{54}-activator protein, CtcC exhibited ATP hydrolysis in the absence of regulatory domain. CtcC consists of an N-terminal regulatory domain and a C-terminal effector ATPase domain but lacks a DNA-binding domain (Figure 4.1A). Figure 4.2 shows an amino acid alignment of the chlamydial CtcC protein with homologous response regulatory proteins from other bacterial species. Without the DNA-binding domain, the chlamydial CtcC protein has the highest sequence identity with AtoC from *E. coli* at 42.2% (62% sequence similarity) (Koo and Stephens 2003). Multiple features are conserved between CtcC and other NtrC homologs, including the E242 residue important for ATP hydrolysis (Figure 4.2, red arrow), the predicted σ^{54}-interaction site (Figure 4.2, red box), and the site of phosphorylation by the sensor kinase protein (Figure 4.2, red asterisk) (Neuwald, Aravind et al. 1999).

The response regulator CtcC (CT466) has previously been shown to be phosphorylated *in vitro* by the sensor kinase CtcB (CT467) (Koo and Stephens 2003); however, ATPase activity or the inhibitory effect of the regulatory domain has yet to be investigated. To assess this, *in vitro* ATPase activity was evaluated for CtcC full-length, ATPase domain (a.a.142-386), and ATPase domain with an active site substitution (E242A). The full-length CtcC protein exhibited very low ATPase activity with less than 10% depletion of total ATP (Figure 4.1). In contrast, the ATPase domain reduced ATP levels by over 40%. When an active site substitution (E242A) was introduced into the ATPase domain, ATPase

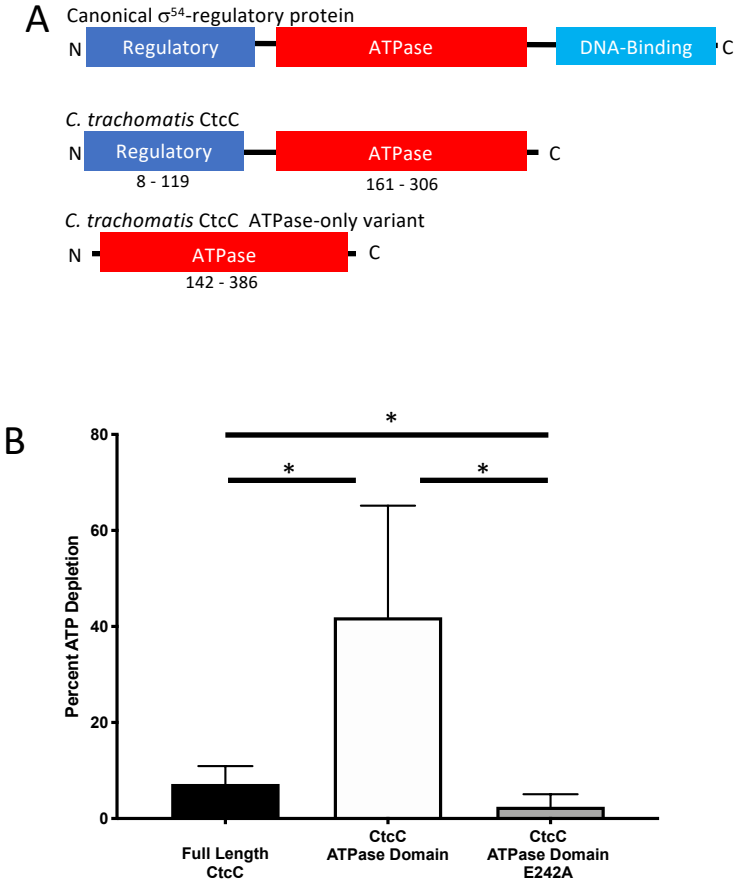
A
Canonical σ54-regulatory protein
N
Regulatory
ATPase
DNA-Binding
C
C. trachomatis CtcC
N
Regulatory
8 - 119
ATPase
161 - 306
C
C. trachomatis CtcC ATPase-only variant
N
ATPase
142 - 386
C
B
Percent ATP Depletion
80
60
40
20
0
*
*
*
Full Length CtcC
CtcC ATPase Domain
CtcC ATPase Domain E242A

Figure 4.1 *C. trachomatis* CtcC domain organization and *in vitro* ATPase activity of CtcC protein constructs. (A) Graphic domain structure of the canonical σ^{54}-regulatory protein shows that the native chlamydial homolog, CtcC, does not contain a DNA-binding domain, and that the ATPase domain-only variant eliminates the regulatory domain. (B) Triplicate ATPase hydrolysis activity of full-length, ATPase domain, and active site defective σ^{54}-regulatory protein, CtcC. The ATPase domain-only recombinant protein depleted approximately four times as much ATP on average compared to the full-length CtcC protein. When the E242A substitution was introduced into the ATPase domain, there was a significant decrease in the amount of ATP depletion compared to the full-length CtcC, supporting the hypothesis that this single amino acid substitution disrupts the ability for the protein to perform its normal activity. * p-value < 0.05 by student's t-test.


Regulatory Domain
ATPase Domain
DNA Binding Domain
CtCtcC
SmDctD
StNtrC
PaNtrC
EcAtoC

Figure 4.2 Clustal W sequence alignment of CtcC from *Chlamydia trachomatis* (Ct) with other σ^{54}-regulatory proteins from *Sinorhizobium meliloti* (Sm), *Salmonella* Typhimurium (St), *Pseudomonas aeruginosa* (Pa), and *Escherichia coli* (Ec) shows that the overall domain structure is conserved among bacterial species. The residues involved in σ^{54} interaction are highly conserved (red box), as is the E242 residue (red arrow) responsible for polarization of the ATP molecule allowing for hydrolysis and the D54 residue that is phosphorylated by the sensor kinase protein.

activity was severely affected. Overall, these data support that the absence of the regulatory domain enables ATPase activity of the ATP domain of CtcC.

Expression of ATPase domain revealed σ^{54} regulon in *C. trachomatis.*

Previous studies expressing only the ATPase effector domain of NtrC homologs have demonstrated constitutive activation of σ^{54}-directed transcription in *Salmonella* Typhimurium and *Sinorhizobium meliloti* (Xu, Gu et al. 2004, Samuels, Frye et al. 2013). Given the observations that the CtcC ATPase domain exhibited ATP hydrolysis activity, expression of this domain in *Chlamydia* was hypothesized to activate σ^{54}-RNAP and enable the discovery of a cognate regulon. Before evaluating the transcriptional profile, protein induction of full-length CtcC, ATPase domain, or E242A ATPase-inactive variant was evaluated in *Chlamydia* (Figure 4.3) (Wickstrum, Sammons et al. 2013). Limited but equal expression of wild-type CtcC could be detected in vector control samples (Figure 4.3B). Full-length CtcC was strongly induced; however, CtcC levels were considerably higher than native expression prior to induction, indicating leaky expression (Figure 4.3B). Importantly, induced expression of ATPase domain and E242A variant were evident (Figure 4.3B).

To discover a potential σ^{54} regulon in *Chlamydia*, RNA was isolated from infected samples with vector-only or construct encoding the ATPase domain after four hours of induction (16-20 hpi). Stranded RNAseq analysis was performed on RNA from two biological replicates revealing that transcripts for 64 genes were significantly and reproducibly upregulated in both samples following induced

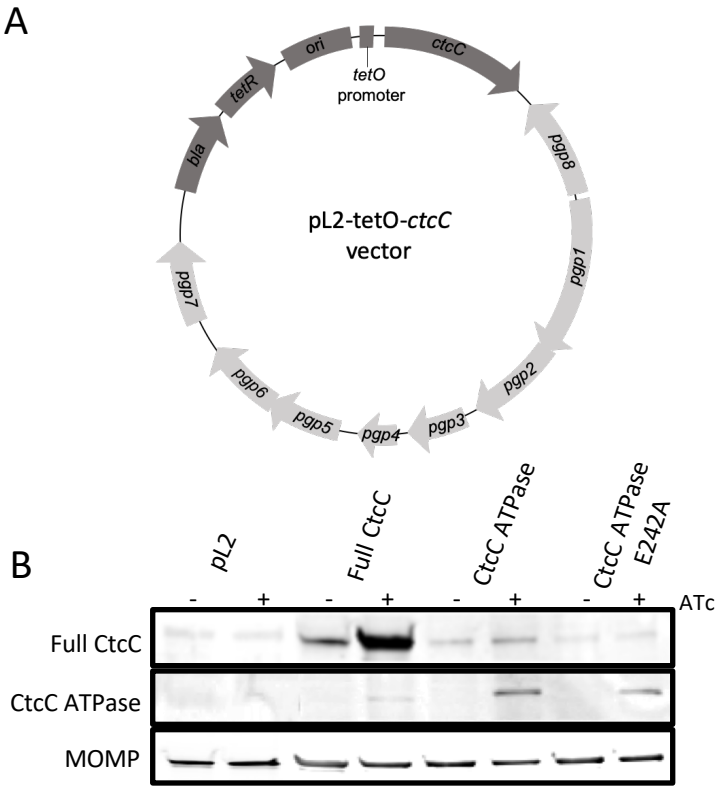
A
ori
ctcC
tetO
promoter
tetR
bla
pgp8
pgp1
pgp2
pgp3
pgp4
pgp5
pgp6
pgp7
pL2-tetO-ctcC
vector
B
pL2
Full CtcC
CtcC ATPase
CtcC ATPase E242A
- + - + - + - +
ATc
Full CtcC
CtcC ATPase
MOMP

Figure 4.3 CtcC constructs overexpression with inducible vector. A) Vector map of with *ctcC* gene variants under ATc-inducible promoter on *C. trachomatis* native plasmid backbone (light gray) (Wickstrum *et al*., 2013). B) Western blot showing overexpression of full-length, ATPase domain-only, and ATPase-domain with E242A substitution induced with addition of ATc to infection at 12 hpi and harvested at 24 hpi.

expression of the CtcC ATPase domain (Tables 4.3 and 4.4). An initial and striking observation related to this potential regulon was that all of the genes upregulated following ATPase domain induction are normally up-regulated during the middle-late stages of the *Chlamydia* developmental cycle (Belland, Zhong et al. 2003, Nicholson, Olinger et al. 2003). These stages coincide with the RB-to-EB conversion, as well as other late infection and exit events. Twenty-four genes are classified as mid-late stage genes, which are normally upregulated after 16 to18 hpi during the developmental cycle and 40 genes are late stage genes, normally upregulated after 24 hpi (Belland, Zhong et al. 2003, Nicholson, Olinger et al. 2003). Of the 64 genes, 41 (64%) are hypothetical proteins with no known or only putative functions, and 23 (36%) are functionally annotated. Nineteen genes encode for membrane proteins, 6 of which are predicted to be inclusion membrane proteins. Twenty-eight genes were for type 3 secretion system (T3SS)-associated proteins, including effector proteins such as TarP.

To validate this expression profile, ddPCR was performed on newly isolated RNA for a subset of 19 genes selected from the σ^{54}-overactivation RNAseq data (Table 4.3 and Table 4.4). All of these genes displayed an upregulation following induction of the CtcC ATPase domain (Table 4.6). Several genes evaluated by ddPCR were found to have expression ratios greater than twice as high as with RNAseq. This difference is possibly due to the additional processing that RNA prepared for RNAseq must go through, including exonuclease treatment and ribosomal RNA depletion steps; although RNA stability and loss for each step has not been evaluated (Humphrys, Creasy et al.

Table 4.3 Direct σ54-regulated genes

CT number	Locus Tag	Gene Name	Protein Role	RNAseq Average Differential Expression	Distance from start codon
Midlate genes [a]					
CT051	CTL0307	hyp	putative secreted, pmp-like protein	6.58	67
CT105[d]	CTL0360	hyp	hypothetical	3.12	178[c]
CT142	CTL0397	hyp	T3SS exported protein	4.81	95
CT143	CTL0398	hyp	T3SS exported protein	4.79	operon
CT144	CTL0399	hyp	T3SS exported membrane protein	3.99	operon
CT455[d]	CTL0715	*murA*	T3SS secreted protein; UDP-N-acetylglucosamine 1-carboxyvinyltransferase	3.01	16
CT494	CTL0755	*sohB*	exported protease	5.02	105
CT575	CTL0838	*mutL*	DNA mismatch repair protein	4.76	56
CT635	CTL0003	hyp	putative T3SS chaperone	5.48	248
CT683	CTL0052	hyp	tetratricopeptide repeat protein	3.59	40
CT849.1	CTL0222	hyp	hypothetical	4.18	43
Late genes[a]					
CT005	CTL0260	inc	inclusion membrane protein	3.61	42
CT050	CTL0306	hyp	secreted, pmp-like protein	6.1	186
CT082	CTL0338	hyp	putative T3SS effector	3.4	116
CT083	CTL0338A	hyp	putative T3SS secreted protein; putatitve thymidylate kinase	3.96	operon
CT084	CTL0339	PLD	phosphatidylcholine-hydrolyzing phospholipase D (PLD) protein	4.68	176
CT229[b]	CTL0481	inc	inclusion membrane protein	3.67	37
CT394	CTL0650	hrcA	heat-inducible transcriptional repressor	4.5	18
CT395	CTL0651	*grpE*	HSP-70 cofactor	3.59	operon
CT443[d]	CTL0702	*omcB*	membrane protein	3.09	operon
CT444	CTL0703	*omcA*	membrane protein	4.6	165
CT489	CTL0750	*glgC*	glucose-1-phosphate adenylyltransferase	4.79	136
CT493	CTL0754	*polA*	DNA polymerase A	5.03	16
CT619	CTL0883	hyp	putative T3SS effector	5.66	36[c]
CT620	CTL0884	hyp	putative T3SS effector	6.48	198
CT622	CTL0886	hyp	T3SS effector; putative cell surface protein	3.51	42
CT702	CTL0071	hyp	hypothetical	4.29	2
CT711	CTL0080	hyp	putative T3SS effector	4.36	83[c]
CT814	CTL0185	hyp	putative membrane protein	3.55	66
CT814.1	CTL0186	hyp	putative membrane protein	5.24	102
CT841[d]	CTL0213	*ftsH*	membrane reorganization protease	3.1	28
CT847	CTL0219	hyp	putative T3SS effector	4.03	133
CT875	CTL0255	hyp	T3SS effector	3.83	180[c]

[a] Expression pattern classifications were taken from previous microarray studies Belland et al. (2003) and Nicholson et al. (2003). Late stage genes are upregulated at 24hpi; midlate genes are upregulated at 18 hpi.

[b] Expression pattern shows an enrichment of transcripts in EBs according to Albrecht et al. (2009), as well as temporal transcript levels evaluated by ddPCR Table 4.5)

[c] Transcript reads from RNAseq data suggest different transcriptional start site compared to current C. trachomatis 434/Bu genome (NC010287). Figure S3 shows PCR confirmation of alternate transcriptional start site.

[d] Upregulated above two standard deviations from the average differential expression in only one of the two trials of RNAseq

Table 4.4 Indirect σ^{54}-regulated genes.

CT number	Locus Tag	Gene Name	Protein Role	RNAseq Average Differential Expression
Midlate genes[a]				
CT049	CTL0305	hyp	secreted, pmp-like protein	4.63
CT132	CTL0387	hyp	putative membrane protein	3.89
CT157[d]	CTL0413	PLD	T3SS secreted protein; Phospholipase D	4.16
CT196[d]	CTL0448	hyp	putative inclusion membrane protein	3.11
CT218	CTL0470	*surE*	5-nucleotidase	3.49
CT382.1[d]	CTL0638	hyp	hypothetical	3.09
CT547[d]	CTL0809	hyp	putative exported protein	2.91
CT646[b]	CTL0014	hyp	hypothetical	4.32
CT647	CTL0015	hyp	putative exported protein (lipoprotein)	4.84
CT648	CTL0016	hyp	putative membrane protein	3.90
CT798	CTL0167	*glgA*	glycogen synthase; secreted protein	4.14
CT837	CTL0209	hyp	puttative inclusion membrane protein	4.54
CT849[d]	CTL0221	hyp	T3SS secreted protein	3.56
Late genes[a]				
CT046	CTL0302	*hctB*	histone-like protein	3.31
CT073	CTL0329	hyp	putative outer membrane protein	3.18
CT080	CTL0336	*ltuB*	late transcription unit B protein	5.23
CT181[d]	CTL0433	hyp	putative exported protein	3.29
CT288	CTL0540	hyp	putative inclusion membrane protein	5.73
CT356	CTL0610	hyp	thioredoxin domain-containing protein	4.15
CT365[d]	CTL0619	hyp	putative inclusion membrane protein	2.98
CT392[d]	CTL0648	hyp	hypothetical	3.39
CT456	CTL0716	*tarp*	translocated actin-recruiting phosphoprotein	4.75
CT546	CTL0808	hyp	putative outer membrane protein	3.35
CT565[d]	CTL0828	hyp	putative membrane protein	3.36
CT576	CTL0839	*scc2*	T3SS chaperone	4.83
CT577	CTL0840	hyp	putative cytosolic protein	5.10
CT578	CTL0841	*copB*	putative T3SS membrane protein	4.53
CT579	CTL0842	*copD*	putative T3SS protein	3.93
CT682[d]	CTL0051	*pbpB*	penicillin-binding protein	2.97
CT694	CTL0063	hyp	putative T3SS effector	3.39
CT848	CTL0220	hyp	T3SS-secreted protein	3.72

[a] Expression pattern classifications were taken from previous microarray studies Belland et al. (2003) and Nicholson et al. (2003). Late stage genes are upregulated at 24 hpi; midlate genes are upregulated at 18 hpi.

[b] Expression pattern evaluated for differentially regulated transcript levels evaluated by ddPCR (Table S2)

[d] Upregulated above two standard deviations from the average differential expression in only one of the two trials of RNAseq

Table 4.5 Temporal gene expression level evaluation of *ct229* and *ct646*

	Average Normalized Transcript Counts			
Gene	12 hpi	18 hpi	24 hpi	30 hpi
rpoA	338.52 +/- 18.16	323.67 +/- 10.06	350.13 +/- 17.82	357.65 +/- 20.01
ct229	29.4 +/- 17.85	31.5 +/- 11.45	36.08 +/- 11.48	116.08 +/- 36.72
ct646	82.82 +/- 9.31	207.65 +/- 17.18	224.93 +/- 10.15	282.57 +/- 79.94

2013). To determine if pleiotropic transcription effects should be considered, expression ratio was determined for *rpoA* which encodes the alpha subunit of RNA polymerase and is transcribed by σ^{66}-holoenzyme. Expression levels of *rpoA* were unchanged following induction of CtcC ATPase domain. To demonstrate that transcription induction was specific to CtcC ATPase domain activity, ratios were also determined following induction of the E242A ATPase domain. Transcription of the 19 σ^{54} regulon genes and *rpoA* following induction of the ATPase defective form were unchanged relative to the vector control sample (Table 4.6). When the full-length CtcC construct was induced, transcript ratios for most of the 19 genes were considerably lower than those observed with the ATPase domain, supporting that the regulatory domain is still inhibiting ATPase activity *in vivo,* similar to the observations of the *in vitro* ATPase depletion study (Figure 4.1). Interestingly, many genes (*ct456*, *ct619*, *ct620*, *ct683*, *ct711*, and *ct875*) were transcribed at ratios twice those observed for the ATPase defective domain (E242A) whereas *rpoA* levels were unchanged. Overall, RNAseq and ddPCR validation studies support the identification of a putative σ^{54} regulon in σ^{54} in *C. trachomatis* that is associated with mid-late stage gene expression and RB to EB conversion components.

These observations would suggest that CtcB/C activation of σ^{54} occurs during the middle and late stages of gene expression, requiring the presence of these components during these stages. Using ddPCR, transcript levels of *rpoN* (σ^{54}), *ctcB*, and *ctcC* were calculated at 12, 18, 24, and 30 hpi. Transcript levels for σ^{54} are relatively constant, while *ctcC* and *ctcB* levels increase throughout the

Table 4.6 Average differential expression ratio (ATPase vs vector control).

	CtcC ATPase		E242A ATPase[a]	CtcC Full Length
Gene	RNAseq	ddPCR	ddPCR	ddPCR
ct084	4.68	28.78	1.42	1.51[b]
ct105	3.12	3.41	-1.17	1.43[b]
ct142	4.81	13.14	1.29	1.51[b]
ct229	3.67	9.11	1.18	1.47[b]
ct394	4.50	9.67	1.50	1.98[b]
ct444	4.60	22.16	1.02	1.77[b]
ct456	4.75	4.66	-1.47	2.70[c]
ct494	5.02	27.35	1.04	1.76[b]
ct576	4.83	5.10	1.09	1.31[b]
ct619	5.66	3.53	1.00	4.71[c]
ct620	6.48	27.61	1.40	5.92[b]
ct646	4.32	2.98	1.01	1.55
ct683	3.59	4.65	1.06	2.21[b]
ct711	4.36	7.19	1.15	5.42[c]
ct814	3.55	6.08	1.13	1.32[b]
ct814.1	5.24	12.47	-1.39	1.21[b]
ct847	4.03	8.00	1.79	1.66[b]
ct875	3.83	3.17	1.07	2.39
hctB	3.31	2.99	1.00	2.70
rpoA	-1.33	-1.08	1.12	1.05

[a] All genes analyzed by ddPCR for the CtcC ATPase E242A mutant had significantly different transcription levels, with the exception of the *rpoA* control (p-value <0.05).
[b] Significant differences in transcript counts for selected genes between the Full-length CtcC and the CtcC ATPase domain-only expression variants by ddPCR analysis (p-value <0.05).
[c] Significant differences in transcript counts for selected genes between the Full-length CtcC and the CtcC ATPase E242A mutant expression variants by ddPCR analysis (p-value <0.05).

developmental cycle (Figure 4.4). Interestingly, the sensor kinase CtcB has very low levels of transcription early in the developmental cycle before rising above those of σ^{54} after 24 hpi. These results mirror those in prior studies in support of the timing and function of this gene regulatory system (Mathews, Volp et al. 1999, Belland, Zhong et al. 2003, Nicholson, Olinger et al. 2003).

Computational analysis identified σ^{54} promoter sequences upstream of 33 σ^{54} regulon genes. One study has investigated the presence of σ^{54} promoters in *Chlamydia* indicating that nine genes are preceded by a consensus sequence (Mathews and Timms 2000). Given that 64 genes appear to be part of the σ^{54} regulon, a broader computational investigation for putative σ^{54} promoters in the *C. trachomatis* genome was applied. The σ^{54} consensus sequence TGG-N_9-TGC, allowing for one mismatch and a variable length of linker region between eight and ten nucleotides, within 400 bases upstream of a putative σ^{54} gene target was used for the search (Barrios, Valderrama et al. 1999). Of the 64 putative σ^{54}-regulated genes, 28 were found to be preceded by a σ^{54} promoter consensus sequence and are considered to be direct σ^{54} targets (Table 4.3 and Figure 4.5). Five genes that are included in the σ^{54} regulon are not preceded by σ^{54} promoters but are expected to be contained within an operon that is controlled by σ^{54} promoter (Table 4.3; operon). These 28 promoters were used to generate a consensus *Chlamydia* σ^{54} promoter that reflects the diversity of nucleotides at individual sites (WebLogo; Figure 4.6A) (Crooks, Hon et al. 2004).

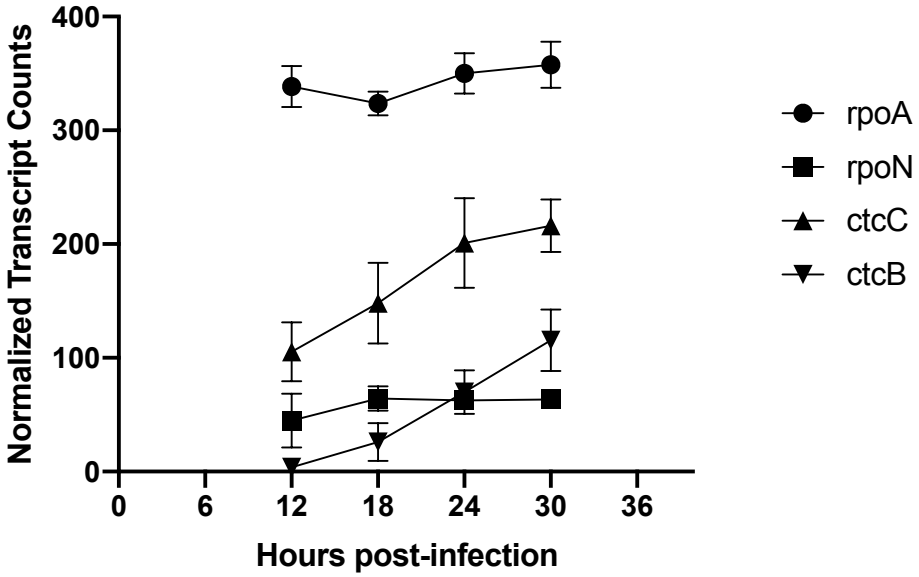
Normalized Transcript Counts
400
300
200
100
0
0
6
12
18
24
30
36
Hours post-infection
rpoA
rpoN
ctcC
ctcB

Figure 4.4 Temporal analysis of *ctcC, ctcB* and *rpoN* transcript levels throughout the chlamydial developmental cycle. RNA was isolated at 12, 18, 24, and 30 hpi from a wild-type L2 infection. Transcript counts were determined by ddPCR and normalized to *secY* transcript counts. *rpoA* was used as a constitutively-active control.

CT005	(0.93)	CTT **TGG** TTA-N_2-TTA **TAC** TAG
CT050	(0.93)	TAA **TGG** AGG-N_3-TGA **TAC** CTC
CT051	(0.94)	TCA **TGG** CTT-N_4-TTT **TTC** ATT
CT082	(0.94)	GCA **AGG** CCC-N_4-CCT **TGC** GTT
CT084	(0.93)	CGC **TGG** CAT-N_3-TAT **TTC** CCA
CT105	(1.00)	ATT **TGG** TAT-N_3-TAG **TGC** TTG
CT142	(0.93)	CCC **AGG** CTT-N_3-TAT **TGC** TCT
CT229	(0.94)	TTA **TGT** TAT-N_4-TTT **TGC** CAA
CT394	(0.93)	CGG **TGG** AGA-N_2-GTT **TTC** TTA
CT444	(0.93)	TGT **TTG** CTT-N_2-ATT **TGC** TAA
CT455	(0.93)	CGT **TTG** TGA-N_2-AAA **TGC** AAT
CT489	(0.94)	GTA **TGG** GTC-N_4-TTT **TGT** CAA
CT493	(0.93)	TTG **TGG** TAC-N_3-GGT **TGA** GGC
CT494	(0.93)	ACC **TGG** AGT-N_3-TAT **TTC** CAG
CT575	(0.94)	GCT **TGG** ACT-N_4-CTT **TTC** TCT
CT619	(0.93)	AAC **TCG** CAA-N_2-CCT **TGC** TCG
CT620	(0.93)	GCT **TGG** GTT-N_3-AAA **TCC** GAG
CT622	(0.94)	TGT **GGG** CTT-N_4-TAT **TGC** CTT
CT635	(0.93)	TGC **TGG** GGC-N_3-ATG **TGA** GCC
CT683	(1.00)	GAT **TGG** CAT-N_3-TTT **TGC** TCC
CT702	(0.93)	TCT **TGG** AGA-N_3-TAA **TCC** CTA
CT711	(0.93)	TTC **TGG** ATG-N_3-TCG **TGT** CAA
CT814	(1.00)	TTG **TGG** AGC-N_3-ACT **TGC** CGC
CT814.1	(0.93)	ATC **TGG** GTA-N_2-AAT **AGC** TTA
CT841	(0.93)	TAT **TGA** ATA-N_3-ATC **TGC** CTG
CT847	(1.00)	ATC **TGG** TCT-N_3-AAA **TGC** TTC
CT849.1	(0.93)	TTT **TCG** CAG-N_2-GGC **TGC** GAG
CT875	(0.93)	GGT **TGG** TTT-N_3-ATG **AGC** ATC

Figure 4.5 Alignment of σ^{54} promoters upstream of differentially regulated genes. Predicted σ^{54} promoters for each gene are shown along with the computational promoter prediction scores indicated in parentheses. These alignments show that the canonical TGG-N_9-TGC σ^{54} promoter sequence is conserved in these predicted promoter regions.

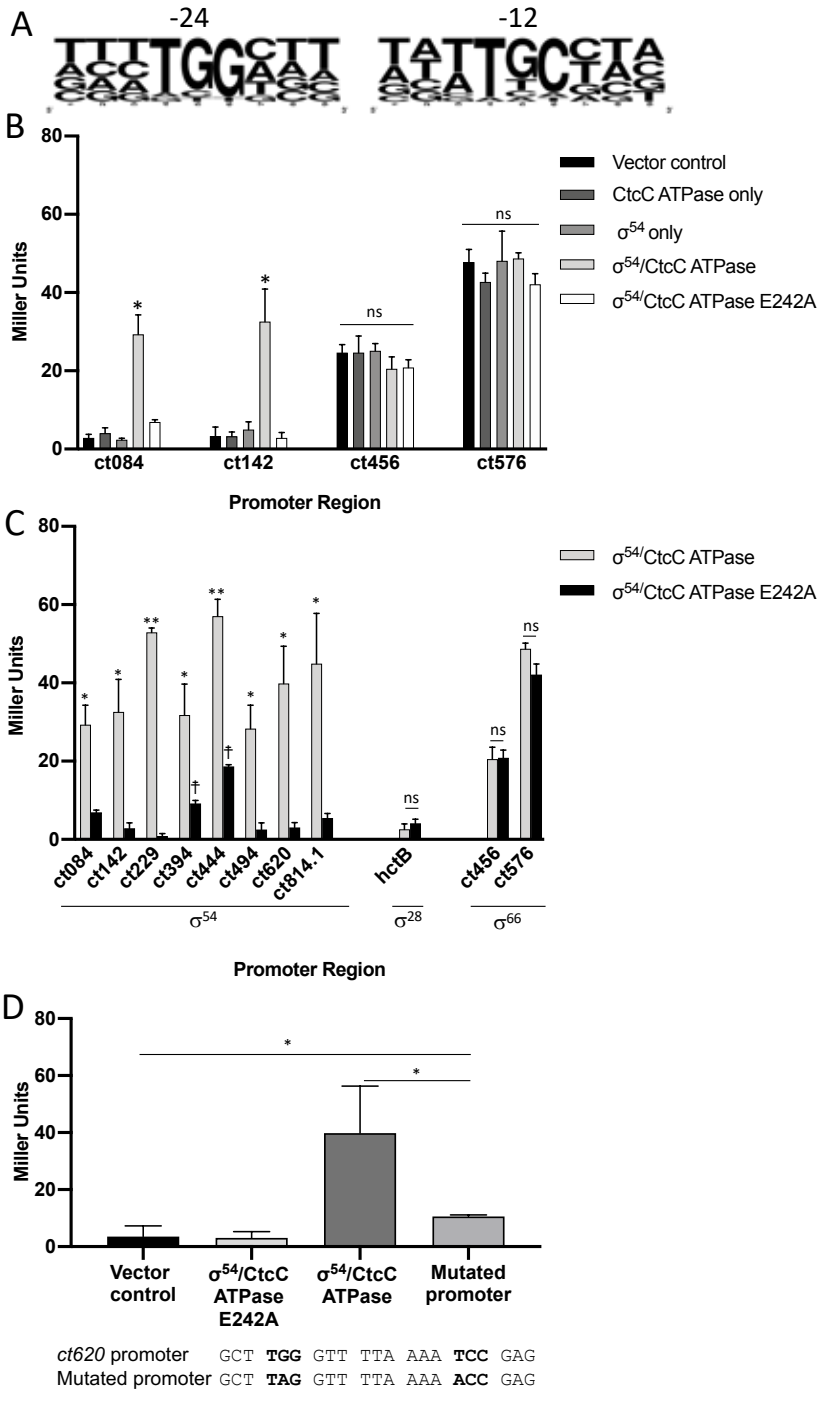
A
-24
-12
B
Miller Units
Vector control
CtcC ATPase only
σ54 only
σ54/CtcC ATPase
σ54/CtcC ATPase E242A
ns
ct084
ct142
ct456
ct576
Promoter Region
C
σ54/CtcC ATPase
σ54/CtcC ATPase E242A
ct084
ct142
ct229
ct394
ct444
ct494
ct620
ct814.1
hctB
ct456
ct576
σ54
σ28
σ66
Promoter Region
D
Vector control
σ54/CtcC ATPase E242A
σ54/CtcC ATPase
Mutated promoter
ct620 promoter GCT TGG GTT TTA AAA TCC GAG
Mutated promoter GCT TAG GTT TTA AAA ACC GAG

Figure 4.6 Beta-galactosidase assays of σ^{54}- and CtcC-dependent activation on select promoters. Promoter regions upstream of select σ^{54} regulated genes were tested for their ability to induce expression of *lacZ* on the pACYC vector with or without the chlamydial *rpoN* (σ^{54}) and *ctcC ATPase* genes (pRSF-DUET). A) WebLogo alignment of the -12/-24 promoter elements shows the relative frequency of nucleotides of the predicted σ^{54} promoter regions upstream of the genes that were found to be differentially regulated by RNAseq. B) Promoters were used to test the induction of *lacZ* expression without either σ^{54} or CtcC present (vector control) and with each protein expressed individually in order to assess the system for induction from the *E. coli* σ^{54}. C) Additional promoters were tested from the predicted σ^{54} regulon, looking at the difference between the constitutively active CtcC ATPase and the inactivated E242A mutant. The predicted regulatory sigma factor is indicated below the promoter region. Experiments performed in triplicate with * p-value <0.05; ** p value <0.01 by student t-test comparing the CtcC ATPase to the E242A ATPase mutant; † p-value <0.05 comparing the CtcC E242A ATPase mutant to a promoter-less pACYC-*lacZ* negative control. D) Two point mutations were introduced into the *ct620* promoter(alignment below graph). The level of LacZ activity decreases significantly compared to the wild-type promoter, but still significantly increased from the inactive conditions. * p-value < 0.05 by student t-test. All beta-galactosidase assays were performed in triplicate.

Interestingly, four genes (*ct105, ct619, ct711,* and *ct875*; all hypothetical proteins) have predicted σ^{54} promoters inside the currently annotated open reading frame; however, based on the RNAseq transcript reads, the transcriptional start site (TSS) appears to be downstream from the start codon, and is in line with the σ^{54} promoter (Figure 4.7). In order to investigate if the transcripts start internal of the annotated start codon and validate the σ^{54} promoter for these genes, primers were designed to lie on either side of the alignment of the RNAseq reads (Table 4.7). PCR of cDNA confirmed that transcripts only occurred with the internal primers for all four genes, indicating that the transcripts start internal to the annotated start codon for these genes. A new start codon for these genes was selected as the next in-frame ATG, and the location of that start codon is indicated as the distance from the σ^{54} promoter indicated in Table 4.3. These observations support that 33 genes are direct gene targets of σ^{54} (Table 4.3). This also suggests that 31 genes are indirect σ^{54} gene targets and regulated by unknown factor(s) (Table 4.4).

Reporter gene assays supported σ^{54} and ATPase dependent regulation of selected σ^{54} gene promoters. To provide further support for direct targets of σ^{54}-mediated transcription, β-galactosidase assays were performed in *E. coli* with inducible *Chlamydia* σ^{54} and CtcC ATPase domain. Induction of *Chlamydia* σ^{54} and CtcC ATPase proteins resulted in β-galactosidase activity when *ct084* and *ct142* promoter regions preceded *lacZ* (Figure 4.6B). Both of these genes were upregulated with σ^{54} activation and predicted to have σ^{54} promoters (Table 4.3

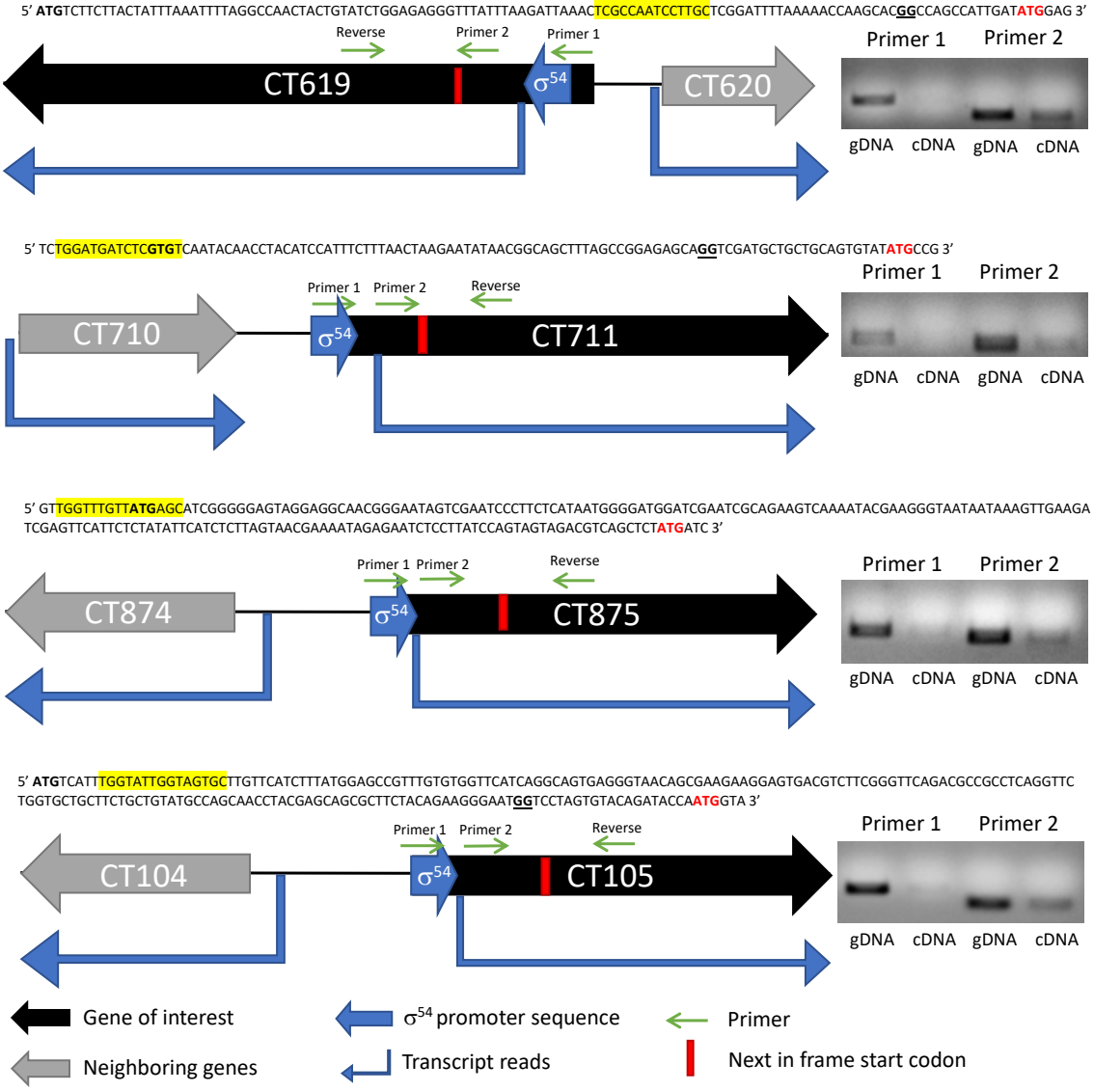
5′ ATGTCTTCTTACTATTTAAATTTTAGGCCAACTACTGTATCTGGAGAGGGTTTATTTAAGATTAAACTCGCCAATCCTTGCTCGGATTTTAAAAACCAAGCACGGCCAGCCATTGATATGGAG 3′
Reverse
Primer 2
Primer 1
CT619
σ54
CT620
Primer 1
Primer 2
gDNA cDNA gDNA cDNA
5′ TCTGGATGATCTCGTGTCAATACAACCTACATCCATTTCTTTAACTAAGAATATAACGGCAGCTTTAGCCGGAGAGCAGGTCGATGCTGCTGCAGTGTATATGCCG 3′
Primer 1
Primer 2
Reverse
CT710
σ54
CT711
Primer 1
Primer 2
gDNA cDNA gDNA cDNA
5′ GTTGGTTTGTTATGAGCATCGGGGGAGTAGGAGGCAACGGGAATAGTCGAATCCCTTCTCATAATGGGGATGGATCGAATCGCAGAAGTCAAAATACGAAGGGTAATAATAAAGTTGAAGA
TCGAGTTCATTCTCTATATTCATCTCTTAGTAACGAAAATAGAGAATCTCCTTATCCAGTAGTAGACGTCAGCTCTATGATC 3′
Primer 1
Primer 2
Reverse
CT874
σ54
CT875
Primer 1
Primer 2
gDNA cDNA gDNA cDNA
5′ ATGTCATTTGGTATTGGTAGTGCTTGTTCATCTTTATGGAGCCGTTTGTGTGGTTCATCAGGCAGTGAGGGTAACAGCGAAGAAGGAGTGACGTCTTCGGGTTCAGACGCCGCCTCAGGTTC
TGGTGCTGCTTCTGCTGTATGCCAGCAACCTACGAGCAGCGCTTCTACAGAAGGGAATGGTCCTAGTGTACAGATACCAATGGTA 3′
Primer 1
Primer 2
Reverse
CT104
σ54
CT105
Primer 1
Primer 2
gDNA cDNA gDNA cDNA
Gene of interest
Neighboring genes
σ54 promoter sequence
Transcript reads
Primer
Next in frame start codon

Figure 4.7 PCR analysis of transcriptional start site comparing the current annotated open reading frame to the transcript read alignments observed by RNAseq for four hypothetical proteins with predicted σ^{54} start sites that would affect the open reading frame of the transcribed gene. Primers were designed to sit just on either side of the transcript read alignment (blue arrow below gene), with primer 1 amplifying a region that would capture transcripts for the annotated ORF and primer 2 amplifying a region internal of the transcript alignments. The same internal reverse primer was used for PCR amplification with both primer 1 and primer 2. The approximate location of the next in frame start codon downstream from the σ^{54} promoter is represented by the red box. Above each schematic is the DNA sequence corresponding to the region including the σ^{54} promoter (highlighted in yellow), the originally annotated start codon (bold), and the next in frame ATG downstream of the σ^{54} promoter (red) with a possible ribosomal binding site within a reasonable distance (underlined, if present). To the right is the gel images showing PCR products for genomic DNA or cDNA made from isolated chlamydial RNA for each primer set. With these four genes encoding hypothetical, they show amplification only with the primer internal to the RNAseq transcript alignment supporting that the transcriptional start site is downstream from the currently annotated start codon for the gene.

Table 4.7 Primers for TSS position confirmation.

Gene	Primer Name	Sequence 5' -->3'
ct619	Primer 1	CTGGAGAGGGTTTATTTAAGATTAAAC
	Primer 2	GAGTATTTCCTGGAGGAGACTG
	Reverse	TTCGACGATACACCAGCTAC
ct711	Primer 1	TTAGAAAAACAATAGTTTTCTGGATG
	Primer 2	CCATTTCTTTAACTAAGAATATAACGGC
	Reverse	TTTACTCGTTGTTCCCGTAG
ct875	Primer 1	TGGGTTGGTTTGTTATGAGC
	Primer 2	GAATCCCTTCTCATAATGGGG
	Reverse	GGTGCTCTCGATCATAGAGC
ct105	Primer 1	ATGTCATTTGGTATTGGTAGTGC
	Primer 2	GTATGCCAGCAACCTACG
	Reverse	CACAAGGCTTTGCACATTAG

and Figure 4.5). σ^{54} or the inactive CtcC ATPase domain, alone or in combination, were unable to initiate transcription (Figure 4.6B) supporting the specificity and functionality of this surrogate system. Promoter regions for two genes, *ct456* and *ct576*, did not enable transcription with or without σ^{54} and/or the CtcC ATPase present. These genes were not predicted to have σ^{54} promoters but were upregulated with σ^{54} activation. Interestingly, both *ct456* and *ct576* promoters result in β-galactosidase activity without additional factors, supporting that these promoters are active in *E. coli*, which corresponds with a prior study [37].

Six additional putative σ^{54} promoters were selected for further investigation using this surrogate system and displayed CtcC ATPase dependent activation (Figure 4.6C). *Ct456* and *ct576* promoters again displayed CtcC ATPase independent transcriptional activity. Transcription of *hctB* was upregulated by the CtcC ATPase domain by both RNAseq and ddPCR (Table 4.4 and Table 4.6). This gene has been shown to be under σ^{28}-regulation in late stages of the chlamydial developmental cycle (Brickman, Barry et al. 1993, Yu and Tan 2003, Yu, Di Russo et al. 2006, Yu, Kibler et al. 2006) and lacks a σ^{54} promoter. The *hctB* promoter region did not exhibit *lacZ* activation in the presence or absence of the σ^{54} (Figure 4.6C); however, when the gene encoding σ^{28} (*fliA*) was added in conjunction, there was a significant increase in LacZ activity (Figure 4.8), showing that the cloned-in promoter region is functional.

The upstream regions for *ct394* and *ct444* showed a significant increase in β-galactosidase activity with the CtcC ATPase E242A mutant as compared to the

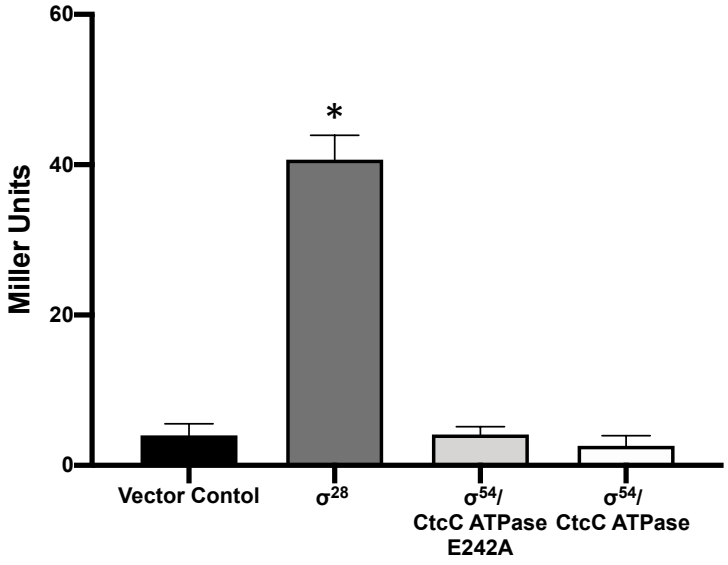
60
40
20
0
Miller Units
*
Vector Contol
σ28
σ54/
CtcC ATPase
E242A
σ54/
CtcC ATPase

Figure 4.8 Beta-galactosidase assays for additional investigation of upstream regions of *hctB*. The *hctB* upstream region does not show activation of the *lacZ* gene with expression of σ^{54} and CtcC; however, when σ^{28} is present, LacZ activation is detected. * p-value < 0.05 by student t-test.

promoter-less pACYC-*lacZ* control (Figure 4.6C). While β-galactosidase activity with CtcC ATPase was significantly greater than with inactive protein, a closer analysis of the upstream regions for *ct394* and *ct444* revealed that both a σ^{54} and a σ^{66} promoter sequence are present for these genes (Figure 4.9). Interestingly, for *ct394* the σ^{54} promoter lies inside the σ^{66} promoter, allowing for the possibility for σ^{54} to act as an inhibitor of transcription for this gene when no CtcC activation occurs. For both genes, these dual promoters could account for the slight β-galactosidase activity when no σ^{54}/CtcC ATPase proteins are present.

To further validate the σ^{54} consensus sequence, two conserved bases in the *ct620* promoter were mutated and β-galactosidase activity evaluated. The central G in the -24 and the T at position -13 were both mutated to A. β-galactosidase activity promoted by this mutated sequence was significantly lower than *lacZ* driven by the wild-type promoter. The β-galactosidase levels for the mutated promoter were still higher than that of the vector control and with the E242A CtcC ATPase mutant (p-value = 0.0339) (Figure 4.6D) supporting that the promoter is still functional. These data suggest that the predicted promoter sequence is necessary for σ^{54}-initiated transcription.

Overexpression of CtcC protein variants in *Chlamydia* resulted in abnormal phenotype and lower progeny production. Progeny production was evaluated with *Chlamydia* infected L929 cells at 30 hpi either with or without 18 hours of protein induction. Addition of ATc alone had no effect on progeny formation nor did the induction of the inactive ATPase domain (Figure 4.10A). Full-length CtcC

ct394 (hrcA)

CTAAAATTCTTGACCGGTGGAGACGGTTTTCTTATAATGACACCGACTTATGGAAAATAG

ct444 (omcA)

GTTTGCTTTGATTTGCTAATTACCTGTTATTAGACGATTTGTTTTAAAAAACAATTGATATAATTTTTATTTTATAATGTAATATT – N_{92} -- GTTATGAAAA

Figure 4.9 Upstream regions for *ct394* and *ct444* show both σ^{54} and σ^{66} promoter regions present. Promoter sequences are highlighted in yellow with the downstream start codon for the gene underlined. Interestingly, the σ^{54} promoter lies inside of the σ^{66} promoter for *ct394.*

induction resulted in a 1.4 log-fold decrease in progeny production while the ATPase domain caused a 1.6 log-fold lower progeny production. When no ATc is added to the pL2-*ctcC* ATPase-only construct chlamydial strain, there is also a significant, 0.5 log-fold decrease in progeny when compared to the vector control strain. This decrease is likely due to minimal uninduced production of the CtcC ATPase domain-only protein.

In order to evaluate the bacterial cellular morphology and inclusion composition, immunofluorescent microscopy was performed on L929 cells infected with or without 12 hours of induction (12-24 hpi). Similar to progeny production (Figure 4.10A), no observable abnormal bacterial or inclusion morphology was apparent in vector control or ATPase-inactive samples (Figure 4.10B). Overexpressing the full-length CtcC protein or ATPase domain resulted in a noticeable decrease in *C. trachomatis* bacterial cells within the interior of the inclusion, as most organisms were observed almost exclusively around the inclusion membrane (Figure 4.10B). Furthermore, bacterial cells expressing the ATPase domain appeared to be larger with more diverse sized reticulate bodies. These data further support the observations associated with progeny production that irregular expression of CtcC ATPase or full-length CtcC, along with the expected σ^{54} gene expression, causes distortion in normal growth and formation of infectious EBs. The absence of this growth effect with the E242A ATPase defective mutant supports that ATPase activity and σ^{54} gene expression is the likely cause of these defects.

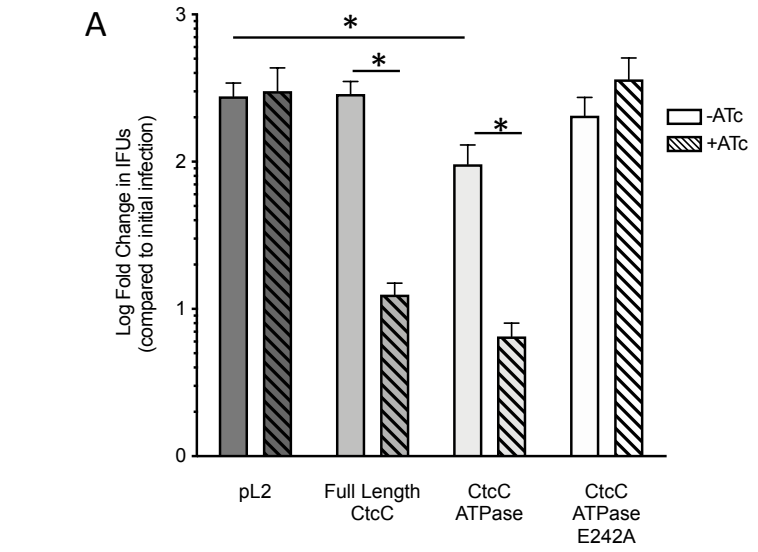
A
Log Fold Change in IFUs
(compared to initial infection)
3
2
1
0
*
*
*
-ATc
+ATc
pL2
Full Length CtcC
CtcC ATPase
CtcC ATPase E242A

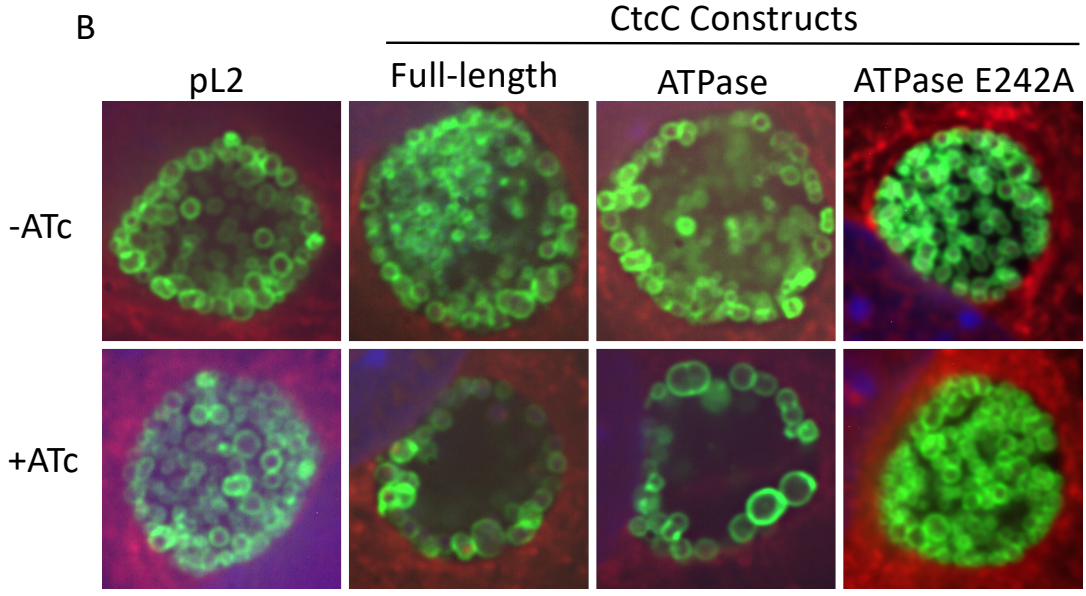
B
CtcC Constructs
pL2
Full-length
ATPase
ATPase E242A
-ATc
+ATc

Figure 4.10 Phenotypic analysis of CtcC variant overexpression during host cell infection. (A) Progeny assays performed in triplicate show a significant decrease in progeny production with the overexpression of the full-length and ATPase-only CtcC protein variants. Vector control, pL2, shows no difference in progeny production with the addition of ATc induction of full-length CtcC at 12 hpi resulted in a decrease in the number of progeny passaged at 30 hpi when compared to the pL2 control and the uninduced conditions. Overexpression of the CtcC ATPase domain-only construct produced less progeny as well. Additionally, the uninduced CtcC ATPase domain-only infection produced a significant difference in progeny produced compared to the pL2 vector control. No difference in progeny production was observed with the E242A substitution in the ATPase domain. * p-value < 0.05 by student's t-test. **(B)** Immunofluoresent microscopy of *C. trachomatis* infected cells following expression induction of CtcC variants. Induction of full-length CtcC appears to affect observable chlamydial cell density inside the center of the inclusion. Overexpression of the ATPase domain-only variant causes the chlamydial cells to have an enlarged appearance, in addition to having fewer cells apparent in center of the inclusion. Infections were induced at 12 hpi, and the infected cell monolayers were fixed and stained at 24 hpi. Green (OmpA), Red (Host cytosol), Blue (DAPI - DNA).

Discussion

In this study, the σ^{54} regulon has been determined which supports a role in controlling RB to EB conversion processes, especially many components associated with infectious capabilities. As observed with other NtrC homologs, the absence of the CtcC regulatory domain enabled ATPase activity (Figure 4.1B). This activity appears to have enabled the induction of σ^{54} transcription in the absence of CtcC phosphorylation by CtcB. This is evidenced by RNAseq profiling (Tables 4.3 and 4.4), presence of σ^{54} promoters (Figure 4.5), and surrogate reporter gene analyses (Figure 4.5). A major observation was that all genes within the resulting σ^{54} regulon were upregulated during the middle and late stages of the developmental cycle, supporting that σ^{54} is critical for controlling gene expression during these developmental phases. Investigation of the gene products encoded in the σ^{54} regulon further supports a role in preparing EBs for the next round of infection through remodeling the outer membrane and packaging numerous type III secretion effectors proteins. Overall, these observations provide comprehensive support for the previously unknown and critical role of σ^{54} in *Chlamydia*.

All of the genes making up the chlamydial σ^{54} regulon were normally upregulated during mid-late (16 to 18 hpi) or late (24 hpi) stages of the developmental cycle. Interestingly, *omcA* and *omcB* were both found among the genes with σ^{54} promoters and appear to be direct σ^{54} targets. OmcA and OmcB are cysteine-rich proteins that make up a large portion of the highly cross-linked EB cellular envelope whose genes are translated late in the developmental cycle

(Liu, Afrane et al. 2010). Additionally found to be part of the σ^{54} regulon, *ct682* (*pdpB*), *ct455* (*murA*), and *ct841* (*ftsH*) are all cell wall modification proteins transcribed after 18 hpi (Barbour, Amano et al. 1982, McCoy, Sandlin et al. 2003, Ito and Akiyama 2005). This collection of late stage genes associated with cell membrane composition suggests that the σ^{54} regulon is involved in the RB-to-EB transition. EBs are highly condensed forms of the chlamydial cell with a large degree of disulfide bonds holding the membrane rigid against osmotic pressure outside of the host cell, compared to the fragile membrane of RBs (Hatch, Allan et al. 1984, Allan, Hatch et al. 1985, Hatch 1996). Thus, in late stages of the developmental cycle, the transcription of genes involved in this membrane recomposing and restructuring are critical for the transition between chlamydial forms.

Just under half of the σ^{54} regulon contains genes encoding T3SS-associated proteins, including secreted effectors, inclusion membrane proteins, parts of the T3SS apparatus, and chaperone proteins. The T3SS is essential for chlamydial virulence and initially establishing an infection in a host cell (Valdivia 2008, Betts-Hampikian and Fields 2010). TARP (for translocated actin recruiting phosphoprotein) associates directly with actin in the host cell at the site of EB invasion and is required for EB uptake (Clifton, Fields et al. 2004, Jewett, Fischer et al. 2006). CopB and CopD have been shown to make up the translocator of the T3SS apparatus, and are thus essential for attachment of the chlamydial cell to the host membrane (Hefty and Stephens 2007, Spaeth, Chen et al. 2009). CT229 has been shown to be an inclusion membrane protein that is critical for

the subverting the host cell defenses that would otherwise lead to destruction, and therefore is necessary for the establishment of the infection from the initial point of entry (Weber, Lam et al. 2017, Faris, Merling et al. 2019). These are just a few examples of T3SS-associated genes that were found to be regulated by σ^{54}. Because the EBs are less metabolically active than RBs, the many effectors proteins needed for establishing the chlamydial inclusion and commandeering the host cell machinery must be made before the conversion event. With a substantial number of genes in the σ^{54} regulon encoding for T3SS-associated proteins, it suggests that σ^{54} gene regulation is involved in the preparation of the chlamydial cells for propagation of the infection (Albrecht, Sharma et al. 2010).

The σ^{54} regulon is almost equally split between direct and indirect gene targets (Tables 4.3 and 4.4). This supports that other regulators participate in controlling the σ^{54} regulon. *Chlamydia* currently only has a few identified transcription factors (Tan 2006, Tan 2012). More than half of the genes (64%) in the σ^{54} regulon encode for hypothetical proteins, several of which have no predicted role or identifiable motifs. Thus, there is a possibility that there is an unknown transcriptional regulator among the genes transcribed by σ^{54} that may contribute to regulating the indirect targets in the regulon. It was interesting to observe that the well-characterized σ^{28} gene target *hctB* was reproducibly and specifically upregulated upon induction of the intact CtcC ATPase domain (Table 4.4 and S1)(Fahr, Douglas et al. 1995, Yu and Tan 2003). The level of upregulation observed here (~3 fold) is minimal relative to upregulation observed during temporal expression between 18-24 hpi (~60 fold; (Hefty and Stephens

2007)). The absence of a σ^{54} promoter element (Figure 4.5) and induction in *E. coli* (Figures 4.6 and 4.8) supports that it is an indirect target of σ^{54}. However, upregulation of this DNA condensation factor could have broader effects on gene regulation due to modified DNA topology and supercoiling, an aspect also well-established in *Chlamydia* and bacterial gene regulation(Niehus, Cheng et al. 2008, Shen and Landick 2019).

Tandem promoters for both σ^{54} and σ^{66} were found to be present upstream of *ct394* (*hrcA*) and *ct444* (*omcA*) (Figure 4.9), potentially allowing for different temporal regulation patterns (Rosario and Tan 2016). While *hcrA* has been shown to have a σ^{66} promoter *in vitro* and in the *E. coli* surrogate system (Figure 4.6C) (Wilson and Tan 2002, Hanson and Tan 2015), and a CIRCE operator element, the presence of the σ^{54} promoter directly inside of the -10/-35 sequence could disrupt the ability of σ^{66} to bind to the DNA and thus additionally inhibit transcription of the downstream gene when σ^{54}-mediated transcription is inactive. These two genes are just a couple of examples of the potential for multiple layers of regulation that could be at play for any number of genes in the chlamydial genome.

The σ^{54} regulon in *Chlamydia* has previously only been investigated in an *in silco* promoter mapping study (Mathews and Timms 2000). Mathews and Timms predicted only nine genes as being regulated by σ^{54} based on the presence of the canonical σ^{54} consensus sequence. In this current study, a less strict consensus sequence (TGG-N_9-TGC) was used to look for potential σ^{54} promoters. Two of the nine genes (*ct620* and *ct683*) previously predicted by

Mathews and Timms to be regulated by σ^{54} appeared in the RNAseq analysis as being differentially expressed when σ^{54} is overactivated. The potential for additional regulatory factors affecting the transcription of the σ^{54} -regulated gene may account for the discrepancy in those genes that were computationally predicted to have σ^{54} promoter sequences, and those that were found to be experimentally upregulated by σ^{54} overactivation. For instance, CT398 (CdsZ) has been shown to interact with σ^{54} by Barta *et al.* (2015), and is hypothesized to be a repressor of σ^{54} activity although its impact on transcription has yet to be evaluated (Barta, Battaile et al. 2015).

While this study addresses the general role of σ^{54} in *Chlamydia,* there are many questions remaining regarding σ^{54} activation. The signal that initiates the two-component regulatory cascade starting with the sensor kinase CtcB, stimulating CtcC, and subsequently activating σ^{54} in Chlamydia has yet to be determined. In bacteria such as *Salmonella* Typhimurium*,* NtrC becomes phosphorylated by NtrB under nitrogen-limiting conditions (Kustu, Santero et al. 1989). The homologous regulatory protein in *Rhizobium,* DctD, is phosphorylated by DctB in response to the availability of external dicarboxylates (Huala, Stigter et al. 1992, Xu, Gu et al. 2004). DctB in *Sinorhizobium meliloti* and *Vibrio cholerae* binds to the C_4-dicarboxylate succinate to signal for the expression of succinate transport proteins (Huala, Stigter et al. 1992, Xu, Gu et al. 2004). In *E. coli*, the sensor kinase AtoS responds to acetoacetate, leading to the transcription of genes encoding enzymes involved in short-chain fatty acid metabolism (Grigoroudis, Panagiotidis et al. 2007). While homologs of the sensor

kinase and response regulators in similar two-component regulatory systems have been identified in various bacteria, the particular environmental signal in many cases has yet to be identified. Determining the initial signal sensed by CtcB could further inform the role of σ^{54}.

A 2011 study published by Francke *et al.* looked for a common theme in σ^{54} regulons across bacteria phyla (Francke, Groot Kormelink et al. 2011). Their comparative analyses found that genes associated with flagella and cellular membrane components in response to the external environment were conserved and highly-represented in σ^{54} regulons. The chlamydial σ^{54} regulon appears to share this same theme. Based on the findings of the current study, the regulon of σ^{54} in *Chlamydia* includes genes normally upregulated after 16- or 18-hour post-infection during the developmental cycle, genes encoding mainly T3SS-associated and membrane proteins, as well as genes which have transcripts enriched in EBs. These data support the role of σ^{54} in the preparation of the chlamydial cells for RB-to-EB conversion and in the arming for subsequent host cell infection.

Chapter V: Comprehensive Discussion

In the previous chapters, I have discussed my research concerning two protein pathways connected to the regulation of *Chlamydia* metabolism and transcription. In this general discussion, I would like to highlight my thoughts on 1) how these pathways are likely how *Chlamydia* is sensing its environment to regulate its developmental cycle; 2) how the Rsb pathway is contributing to the EB-to-RB conversion; 3) how additional layers of regulation are interplaying with the protein pathways characterized in this work; 4) how the Rsb pathway and σ^{54} are contributing to the RB-to-EB conversion; and 5) how CtcB, and subsequently σ^{54}, may be responding to metabolites such as alpha-ketoglutarate as well.

The chlamydia developmental cycle is temporally and situationally regulated.

Chlamydia is an obligate intracellular Gram-negative bacterium with a unique, phylum-defining biphasic developmental cycle. The progression of the chlamydial developmental cycle is regulated by the regimented differential expression of gene at specific times. Chlamydial genes are transcribed in three main temporal classes corresponding to the stages of the developmental cycle (Shaw, Dooley et al. 2000, Belland, Zhong et al. 2003, Nicholson, Olinger et al. 2003). Early genes are first transcribed during the EB-to-RB conversion within the first few hours after entry into the host cell. Midcycle genes represent the largest temporal group of genes and are expressed during the RB stage. Late stages genes are

upregulated the end of the developmental cycle as the RB are converting to EBs. In other words, midcycle genes are expressed during growth and replication, while early and late genes are more specialized subsets of genes that are involved in the establishment and conclusion of the intracellular infection (Tan 2012).

While the majority of differential gene expression in *Chlamydia* is temporally regulated, *Chlamydia* is able to sense and respond to certain environmental conditions. An enlarged, aberrant morphology of *Chlamydia* cells has been observed when the bacteria is confronted with particular stresses. This form has been termed a “persistent state” (Panzetta, Valdivia et al. 2018). The persistent state is thought to function as a resilience pathway allowing the *Chlamydia* to deal with unfavorable conditions in order to survive adverse surroundings. There is a diverse range of stimuli that can trigger the chlamydial RBs to enter into a persistent state, including antibiotics, interferon-gamma (INFγ), deprivation of essential nutrients like iron, and heat shock (Beatty, Morrison et al. 1994, Huston, Theodoropoulos et al. 2008, Schoborg 2011).

The diversity in the environmental conditions that initiate this persistence suggests that, while the morphology appears similar under microscopic observation, the same response is not elicited in all circumstances. Further investigation into the different scenarios does reveal that the transcriptional profiles change based on the stress being combatted. Beta-lactam antibiotics, such as ampicillin, will cause entry into the persistent state by blocking the cross-linking of peptidoglycan. In *Chlamydia,* the application of beta-lactams causes

cell division to be inhibited and halts the RB-to-EB transition (Beatty, Morrison et al. 1994). Transcriptional analysis of a *Chlamydia* infection under penicillin-induced persistence revealed that late genes are down-regulated even as the infections reaches the 48 hour post-infection mark and later (Ouellette, Hatch et al. 2006). Alternatively, INFγ-induced growth inhibition provokes a distinctive transcriptional profile. INFγ is a cytokine that plays a key role in immune response and host defense against pathogens (McClarty, Caldwell et al. 2007). INFγ causes an increase in the activity of a catabolic enzyme that degrades tryptophan known as indoeamine-2,3-diocygenase (IDO). This tryptophan-starvation causes the *Chlamydia* to up-regulate its own tryptophan biosynthesis pathway gene, while simultaneously down-regulating genes involved in cell division, the TCA cycle, and other growth and replication functions (Belland, Zhong et al. 2003).

While the temporal and situational expression patterns throughout the chlamydial developmental cycle is well documented, there is little known about what triggers the conversions events between the two forms that the *Chlamydia* cells take. One study published in 2018, suggested that the RB-to-EB conversion is facilitated by successive rounds of replication resulting in size reduction of the RB cells (Lee, Enciso et al. 2018). They proposed that there is a minimal size threshold that the RBs must reach in order to convert, and that this size reduction model of control for the developmental cycle provides an intrinsic timer for the length of the developmental cycle without the need for an external signal. While the evidence presented in this previous study does suggest that there is a

reduction in size of the RB cells as the developmental cycle progresses, it could be argued that this model for the RB-to-EB conversion event is too simplistic and does not explain the differential gene expression profile that is observed in late time points of the developmental cycle. My research on the Rsb and Ctc protein pathways suggest that these pathways and the signals to which they respond are playing a critical role in the conversion events necessary for the propagation of the chlamydial infection.

The Rsb pathway is essential for the initiation of central metabolism during the early stages of the chlamydial developmental cycle.

The studies described in the previous chapters have provided data that suggests that the Rsb pathway is responsible for triggering the chlamydial cells to shift their method of ATP acquisition from foraging the host cell to autonomous production through oxidative phosphorylation. We proposed, and subsequently supported with transcriptional and protein-interaction observations, a model that the Rsb partner-switching pathway is regulating σ^{66}-mediated transcription. While this would be the first time that an Rsb-type pathway has been shown to regulate the major sigma factor in a bacteria, the unique, spore-like, semi-dormant EB form that *Chlamydia* takes does insinuate a global transcriptional silencing (Moulder 1991, Barry, Brickman et al. 1993).

Our model hypothesizes that as the *Chlamydia* are internalized into the host cell and gain access to pool of alpha-ketoglutarate, which RsbU senses the presence of, recognizing that the *Chlamydia* can utilize to drive its truncated TCA

cycle. RsbU binding to that host generated alpha-ketoglutarate signals that the bacteria has reached a favorable environment for growth and allows for the signaling cascade that eventually leads to RsbW 's release of inhibition on σ^{66}, thus allowing for the global transcription of genes to occur as the *Chlamydia* grows and divides in the RB phase of the developmental cycle. As the developmental cycle proceeds, that pool of alpha-ketoglutarate will lessen, or the concentration of later TCA cycle intermediates, such as malate and oxaloacetate, may increase and cause the RsbU protein to be inactive. This would lead to RsbW binding to σ^{66} again, and a slowdown in transcription. Malate and oxaloacetate, which have also demonstrated binding to RsbU, are towards the end of the truncated chlamydial TCA cycle, and are shuttle to other pathways to synthesize *meso*-diaminopimelate (mDAP), a crosslinker in the A1γ-type peptidoglycan *Chlamydia* synthesizes during growth (Pilhofer, Aistleitner et al. 2013, Packiam, Weinrick et al. 2015). Peptidoglycan is only needed during growth of the *Chlamydia* cell (Liechti, Kuru et al. 2014, Packiam, Weinrick et al. 2015), and therefore a buildup of malate could occur as the cell ceases growth in preparation for the conversion to the EB form.

Currently, the data that we have presented only supports that RsbU is binding to alpha-ketoglutarate, malate, and oxaloacetate, but does not show what response is provoked by the different compounds. In order to more fully explore the effect that these molecules have on the Rsb pathway, and thus *Chlamydia* metabolism, we are pursuing the use of a surrogate *E. coli* system to recapitulate the chlamydial Rsb pathway in an environment that can be more easily

manipulated without the interference of a host cell to combat. Using the BACTH reporter system to show inaction between RsbW and σ^{66}, it may be possible to introduce the compounds that have shown binding to RsbU and observe differences in the colony phenotype.

We are also currently working on optimizing Strep/FLAG tandem affinity purification (SF-TAP) protein pull-down for the Rsb pathway proteins, especially RsbW, to more definitively show evidence for protein-protein interactions between the different components of this pathway. Despite the evidence presented here and another previous study by Thompson *et al.* (2015), there may still be skepticism regarding such an essential protein like σ^{66} being regulated in this fashion (Thompson, Griffiths et al. 2015). While our data do support the interaction between σ^{66} and the Rsb pathway, there are aspects of this pathway that are still needing to be explored. The chlamydial Rsb system is unique from the canonical pathway in a couple key ways. Notably, the RsbU protein is a membrane protein instead of strictly cytoplasmic. Additionally, some proteins are missing from the chlamydial pathway that are normally present in other bacteria with homologs systems; however, in *Chlamydia* there are two additional proteins that appear to be associated with the pathway that are absent from other organisms. There is a second RsbV protein, $RsbV_2$, that has been shown to also be phosphorylated by RsbW, albeit with a lesser affinity than $RsbV_1$, but does not seem to be acted upon at all by RsbU (Thompson, Griffiths et al. 2015). The hypothetical protein CT588 also may be playing a role in this pathway as well because of its shared sequence identity to the chlamydial RsbU

(CT588). Interestingly though CT589 does not have the necessary residues conserved in order to perform the phosphatase activity, nor does it share sequence homology in the sensor domain of the protein to RsbU (Hua, Hefty et al. 2006). These additional proteins could potentially be part redundant pathways or pathways that converge on the same target protein but respond to different signals. It is possible that these proteins are part of a divergent evolutionary event in the making where overtime they started as genetic duplications but have since mutated into a new function.

The data presented here suggests that the Rsb pathway is critical for the progression of the developmental cycle. A fuller understanding the Rsb pathway and its different protein components and signals in *Chlamydia* will allow for a better understanding of what initiates the metabolic pathways in the bacteria and could also reveal how those metabolic pathways are being stalled as the cells convert from the non-infectious to the infectious form.

CtcC activates σ^{54}-mediated transcription to control the production of infectious EBs.

Through our analysis of σ^{54} regulon, we have shown data that suggests that the σ^{54}-RNAP is responsible for transcription of genes associated with the preparation and membrane reorganization of the chlamydial cells as they convert to the infectious EB form. The σ^{54} regulon that was determine consists of 64 genes. Over half of the proposed regulon are thought to be direct targets of σ^{54}-RNAP transcription with consensus sequences mapped upstream of the open

reading frame. All genes found to be differentially regulated with the overactivation of σ^{54} are transcribed after 16-to-18 hpi; many of which are known to be outer membrane proteins enriched in the EB membrane, such as OmcA and OmcB. Approximately 42% of the genes regulated by σ^{54} encode T3SS-associated proteins essential for virulence and establishment of the host cell infection from the initial stages of the developmental cycle.

Interestingly, overexpression of the CtcC, both full-length and ATPase domain-only variants, suggests a significant arrest of ability to generate progeny, including infectious progeny which is highlighted by Figure 4.10A. 12 hpi is prior to most *C. trachomatis* infectious progeny production, and therefore the *in vivo* disruption appears to be inhibiting effective bacterial cellular division. Enlargement of the bacterial cells with the overexpression of the CtcC ATPase domain-only and the lack of progeny production in both the ATPase-only and full-length CtcC strains may highlight the observation by Lee *et al.* that production of infectious progeny in *Chlamydia* requires at least 6 divisions and correlates with smaller bacteria size (Lee, Enciso et al. 2018). Incorporating these observations would suggest that the lack of infectious progeny production from the CtcC mutants may in fact be due to a lack of cellular division and lack of reduction in the size of bacteria. This lack of cellular division could be due to the overabundance of crosslinked cysteine rich proteins in the cellular membrane that are typically absent until later time points in the developmental cycle that correlate with the reduction in size of the bacterial cells, and the condensing of the DNA with the upregulation of the histone-like protein HctB as observed with

the overactivation of σ^{54}. This would then support that σ^{54} could be acting at some level as a regulator of *Chlamydia* cellular division prior to inducing conversion to the infectious EB form.

While sigma factors are global regulators of gene regulation through the chlamydial developmental cycle, there are additional layer of regulation at work through the use of transcriptional activators and repressors. CT398 has been shown previously to interact with σ^{54} by co-immunoprecipitation and BACTH (Barta, Battaile et al. 2015). Preliminary RNAseq analysis of a CT398 overexpression strain of *C. trachomatis* (data not published) revealed that there was notable overlap in genes that were down-regulated and the σ^{54} regulon (Figure 5.1). CT398 has also been shown to be associated with the T3SS proteins CdsL and FliH, possibly as a T3SS chaperone (Barta, Battaile et al. 2015). While *ct398* has been shown to be constitutively expressed throughout the developmental cycle, it is possible that its utility as a T3SS chaperone is only needed during certain times during the developmental cycle such as during the early time points while the T3SS is used to establish the intracellular niche (Barta, Battaile et al. 2015). During the early time points, levels of the σ^{54} transcriptional activator CtcC, and its signal-sensing protein kinase CtcB, are low. Then as the developmental cycle proceeds, CT398 acts to inhibit σ^{54}, while levels of CtcC and CtcB rise. This would add an additional layer of regulation to the σ^{54} regulon to more tightly control the RB-to-EB conversion.

Currently, it is not known what the signal is that initiates the CtcB/CtcC cascade. When activating an ATPase protein as part of the two-component

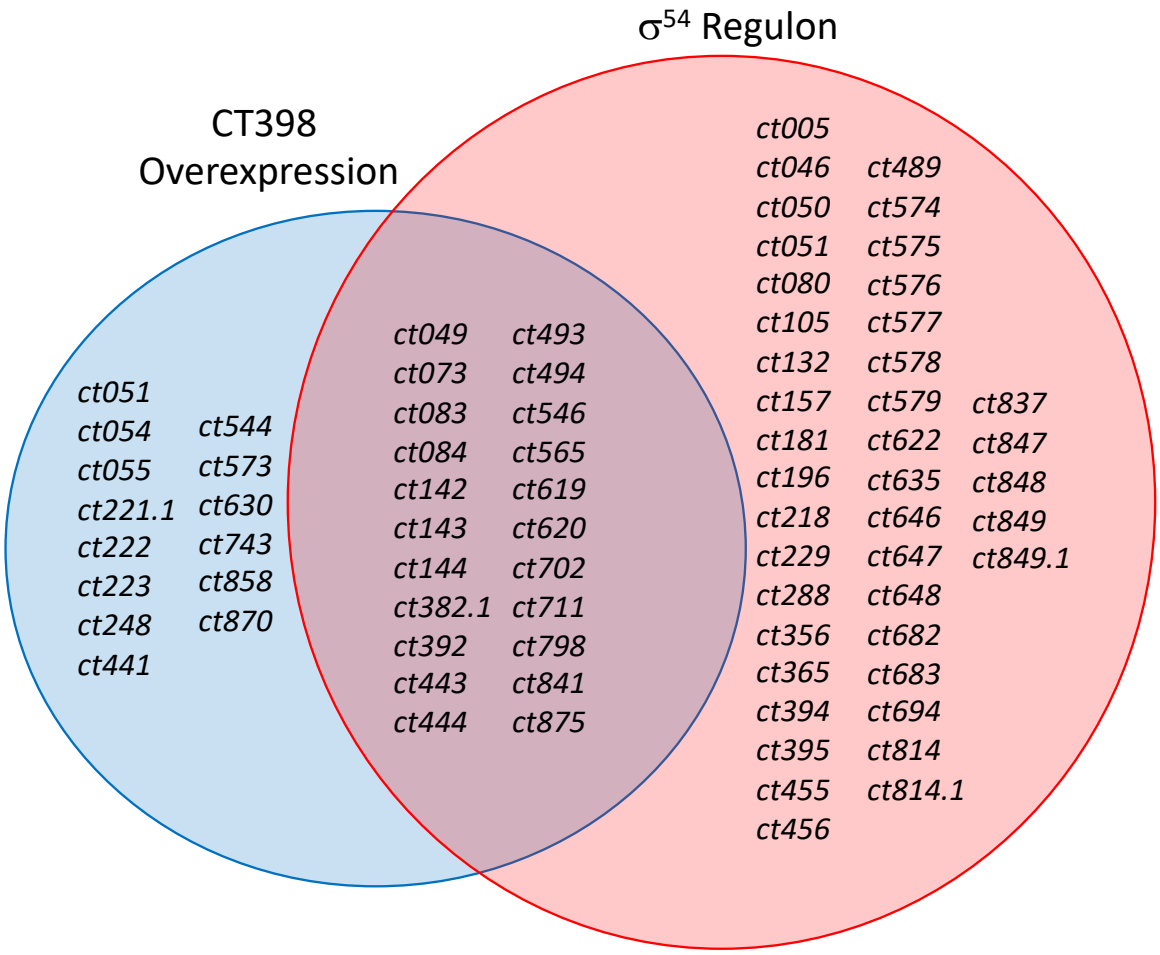
σ54 Regulon
CT398
Overexpression
ct051
ct054
ct055
ct221.1
ct222
ct223
ct248
ct441
ct544
ct573
ct630
ct743
ct858
ct870
ct049
ct073
ct083
ct084
ct142
ct143
ct144
ct382.1
ct392
ct443
ct444
ct493
ct494
ct546
ct565
ct619
ct620
ct702
ct711
ct798
ct841
ct875
ct005
ct046
ct050
ct051
ct080
ct105
ct132
ct157
ct181
ct196
ct218
ct229
ct288
ct356
ct365
ct394
ct395
ct455
ct456
ct489
ct574
ct575
ct576
ct577
ct578
ct579
ct622
ct635
ct646
ct647
ct648
ct682
ct683
ct694
ct814
ct814.1
ct837
ct847
ct848
ct849
ct849.1

Figure 5.1 Venn diagram comparison of genes found by RNAseq to be down-regulated by the overexpression of the putative σ^{54} repressor CT398 versus the σ^{54} regulon. Twenty-two genes are found in both data sets as being differentially regulated in both conditions, making up approximately 34% of the σ^{54} regulon.

regulatory system involved in σ^{54}-RNAP transcriptional initiation, the sensor kinase first binds to a signaling molecule and subsequently will undergo an autophosphorylation event, then the phosphate can be transferred to the response regulator protein. In *E. coli*, the sensor kinase AtoS responds to acetoacetate (Grigoroudis, Panagiotidis et al. 2007). DctB the sensor kinase protein in the σ^{54} activation pathway in *S. meliloti* and *V. cholerae* binds to the C_4-dicarboxylate succinate (Janausch, Zientz et al. 2002, Cheung and Hendrickson 2008, Zhou, Nan et al. 2008). It has also been shown that in some cases an additional protein can be detecting the actual environmental signal and then regulating the ability of the kinase protein transmit the signal to the response regulator ATPase protein. This is the case for NtrB in *E. coli* and *Klebsiella pneumoniae;* NtrB does not directly sense the environmental stimulus, but instead interacts with an additional signal transduction P_{II} protein which response to the level of alpha-ketoglutarate present in the cell (Jack, De Zamaroczy et al. 1999, Jiang and Ninfa 1999, Zhang, Pohlmann et al. 2005, Jiang and Ninfa 2009). In *Chlamydia,* no evidence suggests that there are additional proteins involved in the CtcB/CtcC signaling pathway; however, there has yet to be a comprehensive investigation of the CtcB protein. Protein interaction studies, such as a co-immunoprecipitation, could indicate if CtcB is interacting with another protein. Purification and structure determination of CtcB could allow for the determination of possible ligands if it is directly sensing the environmental stimuli.

Similar to homologous proteins from *E. coli, K. pneumoniae, V. cholerae,* and many other bacteria, it could be hypothesized that the CtcB protein in

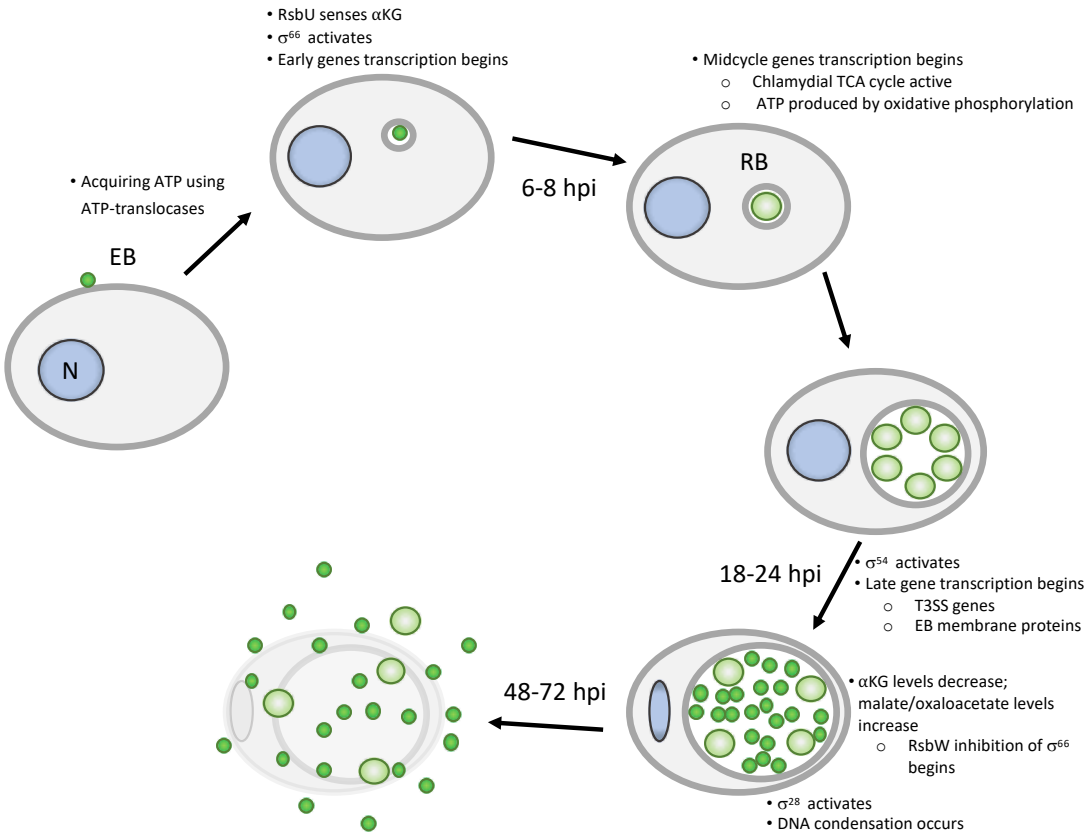
• RsbU senses αKG
• σ66 activates
• Early genes transcription begins
• Midcycle genes transcription begins
○ Chlamydial TCA cycle active
○ ATP produced by oxidative phosphorylation
• Acquiring ATP using ATP-translocases
EB
N
6-8 hpi
RB
18-24 hpi
• σ54 activates
• Late gene transcription begins
○ T3SS genes
○ EB membrane proteins
48-72 hpi
• αKG levels decrease; malate/oxaloacetate levels increase
○ RsbW inhibition of σ66 begins
• σ28 activates
• DNA condensation occurs

Figure 5.2 *Chlamydia* developmental cycle is temporally regulated by the activation of three sigma factors. Modified from Figure 1.1. Additional details regarding the proposed sequence of events that are triggered throughout the developmental cycle including the timing of transcriptional categories of genes, regulation of the Rsb pathway and how that relates to the acquisition of ATP through different means, and the activation of the three different sigma factors in relation to the stages of the cycle.

Chlamydia is responding to TCA cycle-associated compounds. As we hypothesized with the regulation of the Rsb pathway, as the truncated chlamydial TCA cycle slows down with a buildup of intermediate compounds, this could signal a reduction in replication, or a decrease in access to host-acquired resources; signaling that it is time to find a new host. In response, σ^{54} is activated to equip the cell with the machinery for establishing a new infection and the armor to survive the extracellular environment as it searches for the next host.

Adding detail to the progression of the chlamydial developmental cycle.

With the data collected regarding the Rsb partner-switching pathway and the σ^{54} regulon, additional details can be added to the current understanding of the progression of the chlamydial developmental cycle (Figure 5.2). The early transcription of genes is hypothesized to be triggered by RsbU sensing compounds inside of the host cell, such as alpha-ketoglutarate (αKG). This leads to an activation of σ^{66} that subsequently allows the *Chlamydia* to produce its own ATP through oxidative phosphorylation. As the developmental cycle reaches later time points, around 18 hpi, σ^{54} becomes active and transcribes genes associated with the preparation of the chlamydial cells to convert to the infectious EB form. Then as αKG levels decrease, or malate and oxaloacetate build up, it is hypothesized that RsbW re-establishes its inhibition on σ^{66}, limiting global transcription just as σ^{28}'s activities lead to the late stage genes that cause the condensation of the genome. At the end of the developmental cycle, many of the

chlamydial cells are in the EB form, ready to escape their current host cell and propagate the infection.

References

Abdelrahman, Y. M. and R. J. Belland (2005). "The chlamydial developmental cycle." FEMS Microbiol Rev **29**(5): 949-959.

Adams, P. D., P. V. Afonine, G. Bunkoczi, V. B. Chen, I. W. Davis, N. Echols, J. J. Headd, L. W. Hung, G. J. Kapral, R. W. Grosse-Kunstleve, A. J. McCoy, N. W. Moriarty, R. Oeffner, R. J. Read, D. C. Richardson, J. S. Richardson, T. C. Terwilliger and P. H. Zwart (2010). "PHENIX: a comprehensive Python-based system for macromolecular structure solution." Acta Crystallogr D Biol Crystallogr **66**(Pt 2): 213-221.

Akers, J. C., H. HoDac, R. H. Lathrop and M. Tan (2011). "Identification and functional analysis of CT069 as a novel transcriptional regulator in Chlamydia." J Bacteriol **193**(22): 6123-6131.

Akers, J. C. and M. Tan (2006). "Molecular mechanism of tryptophan-dependent transcriptional regulation in Chlamydia trachomatis." J Bacteriol **188**(12): 4236-4243.

Albe, K. R., M. H. Butler and B. E. Wright (1990). "Cellular concentrations of enzymes and their substrates." J Theor Biol **143**(2): 163-195.

Albrecht, M., C. M. Sharma, M. T. Dittrich, T. Muller, R. Reinhardt, J. Vogel and T. Rudel (2011). "The transcriptional landscape of Chlamydia pneumoniae." Genome Biol **12**(10): R98.

Albrecht, M., C. M. Sharma, R. Reinhardt, J. Vogel and T. Rudel (2010). "Deep sequencing-based discovery of the Chlamydia trachomatis transcriptome." Nucleic Acids Res **38**(3): 868-877.

Allan, I., T. P. Hatch and J. H. Pearce (1985). "Influence of cysteine deprivation on chlamydial differentiation from reproductive to infective life-cycle forms." J Gen Microbiol **131**(12): 3171-3177.

Arora, S. K., B. W. Ritchings, E. C. Almira, S. Lory and R. Ramphal (1997). "A transcriptional activator, FleQ, regulates mucin adhesion and flagellar gene expression in Pseudomonas aeruginosa in a cascade manner." J Bacteriol **179**(17): 5574-5581.

Bao, X., B. E. Nickels and H. Fan (2012). "Chlamydia trachomatis protein GrgA activates transcription by contacting the nonconserved region of sigma66." Proc Natl Acad Sci U S A **109**(42): 16870-16875.

Barbour, A. G., K. Amano, T. Hackstadt, L. Perry and H. D. Caldwell (1982). "Chlamydia trachomatis has penicillin-binding proteins but not detectable muramic acid." J Bacteriol **151**(1): 420-428.

Barrios, H., B. Valderrama and E. Morett (1999). "Compilation and analysis of sigma(54)-dependent promoter sequences." Nucleic Acids Res **27**(22): 4305-4313.

Barry, C. E., 3rd, T. J. Brickman and T. Hackstadt (1993). "Hc1-mediated effects on DNA structure: a potential regulator of chlamydial development." Mol Microbiol **9**(2): 273-283.

Barry, C. E., 3rd, S. F. Hayes and T. Hackstadt (1992). "Nucleoid condensation in Escherichia coli that express a chlamydial histone homolog." Science **256**(5055): 377-379.

Barta, M. L., K. P. Battaile, S. Lovell and P. S. Hefty (2015). "Hypothetical protein CT398 (CdsZ) interacts with sigma(54) (RpoN)-holoenzyme and the type III secretion export apparatus in Chlamydia trachomatis." Protein Sci **24**(10): 1617-1632.

Beatty, W. L., R. P. Morrison and G. I. Byrne (1994). "Persistent chlamydiae: from cell culture to a paradigm for chlamydial pathogenesis." Microbiol Rev **58**(4): 686-699.

Belland, R. J., G. Zhong, D. D. Crane, D. Hogan, D. Sturdevant, J. Sharma, W. L. Beatty and H. D. Caldwell (2003). "Genomic transcriptional profiling of the developmental cycle of Chlamydia trachomatis." Proc Natl Acad Sci U S A **100**(14): 8478-8483.

Benson, A. K. and W. G. Haldenwang (1993). "Regulation of sigma B levels and activity in Bacillus subtilis." J Bacteriol **175**(8): 2347-2356.

Benson, A. K. and W. G. Haldenwang (1993). "The sigma B-dependent promoter of the Bacillus subtilis sigB operon is induced by heat shock." J Bacteriol **175**(7): 1929-1935.

Berger, R. E., E. R. Alexander, G. D. Monda, J. Ansell, G. McCormick and K. K. Holmes (1978). "Chlamydia trachomatis as a cause of acute "idiopathic" epididymitis." N Engl J Med **298**(6): 301-304.

Betts-Hampikian, H. J. and K. A. Fields (2010). "The Chlamydial Type III Secretion Mechanism: Revealing Cracks in a Tough Nut." Front Microbiol **1**: 114.

Boylan, S. A., A. R. Redfield, M. S. Brody and C. W. Price (1993). "Stress-induced activation of the sigma B transcription factor of Bacillus subtilis." J Bacteriol **175**(24): 7931-7937.

Boylan, S. A., A. R. Redfield and C. W. Price (1993). "Transcription factor sigma B of Bacillus subtilis controls a large stationary-phase regulon." J Bacteriol **175**(13): 3957-3963.

Brahmachary, P., M. G. Dashti, J. W. Olson and T. R. Hoover (2004). "Helicobacter pylori FlgR is an enhancer-independent activator of sigma54-RNA polymerase holoenzyme." J Bacteriol **186**(14): 4535-4542.

Brickman, T. J., C. E. Barry, 3rd and T. Hackstadt (1993). "Molecular cloning and expression of hctB encoding a strain-variant chlamydial histone-like protein with DNA-binding activity." J Bacteriol **175**(14): 4274-4281.

Brothwell, J. A., M. K. Muramatsu, E. Toh, D. D. Rockey, T. E. Putman, M. L. Barta, P. S. Hefty, R. J. Suchland and D. E. Nelson (2016). "Interrogating Genes That Mediate Chlamydia trachomatis Survival in Cell Culture Using Conditional Mutants and Recombination." J Bacteriol **198**(15): 2131-2139.

Bryant, S. H. and S. F. Altschul (1995). "Statistics of sequence-structure threading." Curr Opin Struct Biol **5**(2): 236-244.

Burton, M. J. and D. C. Mabey (2009). "The global burden of trachoma: a review." PLoS Negl Trop Dis **3**(10): e460.

Carlson, J. H., S. Hughes, D. Hogan, G. Cieplak, D. E. Sturdevant, G. McClarty, H. D. Caldwell and R. J. Belland (2004). "Polymorphisms in the Chlamydia trachomatis cytotoxin locus associated with ocular and genital isolates." Infect Immun **72**(12): 7063-7072.

Case, E. D., J. C. Akers and M. Tan (2011). "CT406 encodes a chlamydial ortholog of NrdR, a repressor of ribonucleotide reductase." J Bacteriol **193**(17): 4396-4404.

Caspi, R., R. Billington, L. Ferrer, H. Foerster, C. A. Fulcher, I. M. Keseler, A. Kothari, M. Krummenacker, M. Latendresse, L. A. Mueller, Q. Ong, S. Paley, P. Subhraveti, D. S. Weaver and P. D. Karp (2016). "The MetaCyc database of metabolic pathways and enzymes and the BioCyc collection of pathway/genome databases." Nucleic Acids Res **44**(D1): D471-480.

Cates, W., Jr. and J. N. Wasserheit (1991). "Genital chlamydial infections: epidemiology and reproductive sequelae." Am J Obstet Gynecol **164**(6 Pt 2): 1771-1781.

CDC. (2018). "Sexually Transmitted Disease Surveillance, 2018." Retrieved January 22, 2020.

Chang, C., C. Tesar, M. Gu, G. Babnigg, A. Joachimiak, P. R. Pokkuluri, H. Szurmant and M. Schiffer (2010). "Extracytoplasmic PAS-like domains are common in signal transduction proteins." J Bacteriol **192**(4): 1156-1159.

Chatterjee, A., Y. Cui and A. K. Chatterjee (2002). "Regulation of Erwinia carotovora hrpL(Ecc) (sigma-L(Ecc)), which encodes an extracytoplasmic function subfamily of sigma factor required for expression of the HRP regulon." Mol Plant Microbe Interact **15**(9): 971-980.

Chen, A. L., A. C. Wilson and M. Tan (2011). "A Chlamydia-specific C-terminal region of the stress response regulator HrcA modulates its repressor activity." J Bacteriol **193**(23): 6733-6741.

Chen, V. B., W. B. Arendall, 3rd, J. J. Headd, D. A. Keedy, R. M. Immormino, G. J. Kapral, L. W. Murray, J. S. Richardson and D. C. Richardson (2010). "MolProbity: all-atom structure validation for macromolecular crystallography." Acta Crystallogr D Biol Crystallogr **66**(Pt 1): 12-21.

Cheng, E. and M. Tan (2012). "Differential effects of DNA supercoiling on Chlamydia early promoters correlate with expression patterns in midcycle." J Bacteriol **194**(12): 3109-3115.

Cheong, H. C., C. Y. Q. Lee, Y. Y. Cheok, G. M. Y. Tan, C. Y. Looi and W. F. Wong (2019). "Chlamydiaceae: Diseases in Primary Hosts and Zoonosis." Microorganisms **7**(5).

Cheung, J. and W. A. Hendrickson (2008). "Crystal structures of C4-dicarboxylate ligand complexes with sensor domains of histidine kinases DcuS and DctB." J Biol Chem **283**(44): 30256-30265.

Claywell, J. E., L. M. Matschke, K. N. Plunkett and D. J. Fisher (2018). "Inhibition of the Protein Phosphatase CppA Alters Development of Chlamydia trachomatis." J Bacteriol **200**(19).

Clifton, D. R., K. A. Fields, S. S. Grieshaber, C. A. Dooley, E. R. Fischer, D. J. Mead, R. A. Carabeo and T. Hackstadt (2004). "A chlamydial type III translocated protein is tyrosine-phosphorylated at the site of entry and associated with recruitment of actin." Proc Natl Acad Sci U S A **101**(27): 10166-10171.

Collado-Vides, J., B. Magasanik and J. D. Gralla (1991). "Control site location and transcriptional regulation in Escherichia coli." Microbiol Rev **55**(3): 371-394.

Coordinators, N. R. (2017). "Database resources of the National Center for Biotechnology Information." Nucleic Acids Res.

Crooks, G. E., G. Hon, J. M. Chandonia and S. E. Brenner (2004). "WebLogo: a sequence logo generator." Genome Res **14**(6): 1188-1190.

Dalet, K., C. Briand, Y. Cenatiempo and Y. Hechard (2000). "The rpoN gene of Enterococcus faecalis directs sensitivity to subclass IIa bacteriocins." Curr Microbiol **41**(6): 441-443.

Danson, A. E., M. Jovanovic, M. Buck and X. Zhang (2019). "Mechanisms of sigma(54)-Dependent Transcription Initiation and Regulation." J Mol Biol **431**(20): 3960-3974.

Darville, T. and T. J. Hiltke (2010). "Pathogenesis of genital tract disease due to Chlamydia trachomatis." J Infect Dis **201 Suppl 2**: S114-125.

De Puysseleyr, K., L. De Puysseleyr, H. Dhondt, T. Geens, L. Braeckman, S. A. Morre, E. Cox and D. Vanrompay (2014). "Evaluation of the presence and zoonotic transmission of Chlamydia suis in a pig slaughterhouse." BMC Infect Dis **14**: 560.

Delumeau, O., S. Dutta, M. Brigulla, G. Kuhnke, S. W. Hardwick, U. Volker, M. D. Yudkin and R. J. Lewis (2004). "Functional and structural characterization of RsbU, a stress signaling protein phosphatase 2C." J Biol Chem **279**(39): 40927-40937.

Desai, M., W. Wurihan, R. Di, J. D. Fondell, B. E. Nickels, X. Bao and H. Fan (2018). "A role for GrgA in regulation of sigma(28)-dependent transcription in the obligate intracellular bacterial pathogen Chlamydia trachomatis." J Bacteriol.

Dixon, R. A. (1984). "The genetic complexity of nitrogen fixation. The ninth Fleming lecture." J Gen Microbiol **130**(11): 2745-2755.

Domman, D. and M. Horn (2015). "Following the Footsteps of Chlamydial Gene Regulation." Mol Biol Evol **32**(12): 3035-3046.

Douglas, A. L. and T. P. Hatch (2000). "Expression of the transcripts of the sigma factors and putative sigma factor regulators of Chlamydia trachomatis L2." Gene **247**(1-2): 209-214.

Douglas, A. L. and T. P. Hatch (2006). The phosphorelay system in *Chlamydia trachomatis*. Chlamydial Infections: Proceedings of the Eleventh International Symposium on Human Chlamydial Infections, Niagara-on-the-Lake, Canada.

Elliott, K. T., I. B. Zhulin, J. A. Stuckey and V. J. DiRita (2009). "Conserved residues in the HAMP domain define a new family of proposed bipartite energy taxis receptors." J Bacteriol **191**(1): 375-387.

Elwell, C., K. Mirrashidi and J. Engel (2016). "Chlamydia cell biology and pathogenesis." Nat Rev Microbiol **14**(6): 385-400.

Emsley, P., B. Lohkamp, W. G. Scott and K. Cowtan (2010). "Features and development of Coot." Acta Crystallogr D Biol Crystallogr **66**(Pt 4): 486-501.

Evans, P. R. (2011). "An introduction to data reduction: space-group determination, scaling and intensity statistics." Acta Crystallogr D Biol Crystallogr **67**(Pt 4): 282-292.

Fahr, M. J., A. L. Douglas, W. Xia and T. P. Hatch (1995). "Characterization of late gene promoters of Chlamydia trachomatis." J Bacteriol **177**(15): 4252-4260.

Faris, R., M. Merling, S. E. Andersen, C. A. Dooley, T. Hackstadt and M. M. Weber (2019). "Chlamydia trachomatis CT229 Subverts Rab GTPase-Dependent CCV Trafficking Pathways to Promote Chlamydial Infection." Cell Rep **26**(12): 3380-3390 e3385.

Ferro-Luzzi Ames, G. and K. Nikaido (1985). "Nitrogen regulation in Salmonella typhimurium. Identification of an ntrC protein-binding site and definition of a consensus binding sequence." EMBO J **4**(2): 539-547.

Fisher, D. J., N. E. Adams and A. T. Maurelli (2015). "Phosphoproteomic analysis of the Chlamydia caviae elementary body and reticulate body forms." Microbiology **161**(8): 1648-1658.

Francke, C., T. Groot Kormelink, Y. Hagemeijer, L. Overmars, V. Sluijter, R. Moezelaar and R. J. Siezen (2011). "Comparative analyses imply that the enigmatic Sigma factor 54 is a central controller of the bacterial exterior." BMC Genomics **12**: 385.

Friesner, R. A., J. L. Banks, R. B. Murphy, T. A. Halgren, J. J. Klicic, D. T. Mainz, M. P. Repasky, E. H. Knoll, M. Shelley, J. K. Perry, D. E. Shaw, P. Francis and P. S. Shenkin (2004). "Glide: a new approach for rapid, accurate docking and scoring. 1. Method and assessment of docking accuracy." J Med Chem **47**(7): 1739-1749.

Friesner, R. A., R. B. Murphy, M. P. Repasky, L. L. Frye, J. R. Greenwood, T. A. Halgren, P. C. Sanschagrin and D. T. Mainz (2006). "Extra precision glide: docking and scoring incorporating a model of hydrophobic enclosure for protein-ligand complexes." J Med Chem **49**(21): 6177-6196.

Galan-Vasquez, E., B. Luna and A. Martinez-Antonio (2011). "The Regulatory Network of Pseudomonas aeruginosa." Microb Inform Exp **1**(1): 3.

Garcia, E., S. Bancroft, S. G. Rhee and S. Kustu (1977). "The product of a newly identified gene, glnF, is required for synthesis of glutamine synthetase in Salmonella." Proc Natl Acad Sci U S A **74**(4): 1662-1666.

Gardan, R., G. Rapoport and M. Debarbouille (1995). "Expression of the rocDEF operon involved in arginine catabolism in Bacillus subtilis." J Mol Biol **249**(5): 843-856.

Gottesman, S. and G. Storz (2011). "Bacterial small RNA regulators: versatile roles and rapidly evolving variations." Cold Spring Harb Perspect Biol **3**(12).

Grieshaber, N. A., S. S. Grieshaber, E. R. Fischer and T. Hackstadt (2006). "A small RNA inhibits translation of the histone-like protein Hc1 in Chlamydia trachomatis." Mol Microbiol **59**(2): 541-550.

Grigoroudis, A. I., C. A. Panagiotidis, E. E. Lioliou, M. Vlassi and D. A. Kyriakidis (2007). "Molecular modeling and functional analysis of the AtoS-AtoC two-component signal transduction system of Escherichia coli." Biochim Biophys Acta **1770**(8): 1248-1258.

Gussin, G. N., C. W. Ronson and F. M. Ausubel (1986). "Regulation of nitrogen fixation genes." Annu Rev Genet **20**: 567-591.

Hackstadt, T., W. J. Todd and H. D. Caldwell (1985). "Disulfide-mediated interactions of the chlamydial major outer membrane protein: role in the differentiation of chlamydiae?" J Bacteriol **161**(1): 25-31.

Haggerty, C. L., S. L. Gottlieb, B. D. Taylor, N. Low, F. Xu and R. B. Ness (2010). "Risk of sequelae after Chlamydia trachomatis genital infection in women." J Infect Dis **201 Suppl 2**: S134-155.

Haldenwang, W. G. and R. Losick (1979). "A modified RNA polymerase transcribes a cloned gene under sporulation control in Bacillus subtilis." Nature **282**(5736): 256-260.

Haldenwang, W. G. and R. Losick (1980). "Novel RNA polymerase sigma factor from Bacillus subtilis." Proc Natl Acad Sci U S A **77**(12): 7000-7004.

Halgren, T. A., R. B. Murphy, R. A. Friesner, H. S. Beard, L. L. Frye, W. T. Pollard and J. L. Banks (2004). "Glide: a new approach for rapid, accurate docking and scoring. 2. Enrichment factors in database screening." J Med Chem **47**(7): 1750-1759.

Hanson, B. R. and M. Tan (2015). "Transcriptional regulation of the Chlamydia heat shock stress response in an intracellular infection." Mol Microbiol **97**(6): 1158-1167.

Hatch, T. P. (1996). "Disulfide cross-linked envelope proteins: the functional equivalent of peptidoglycan in chlamydiae?" J Bacteriol **178**(1): 1-5.

Hatch, T. P., I. Allan and J. H. Pearce (1984). "Structural and polypeptide differences between envelopes of infective and reproductive life cycle forms of Chlamydia spp." J Bacteriol **157**(1): 13-20.

Hawkins, P. C., A. G. Skillman, G. L. Warren, B. A. Ellingson and M. T. Stahl (2010). "Conformer generation with OMEGA: algorithm and validation using high quality structures from the Protein Databank and Cambridge Structural Database." J Chem Inf Model **50**(4): 572-584.

Hecker, M., J. Pane-Farre and U. Volker (2007). "SigB-dependent general stress response in Bacillus subtilis and related gram-positive bacteria." Annu Rev Microbiol **61**: 215-236.

Hefty, P. S. and R. S. Stephens (2007). "Chlamydial type III secretion system is encoded on ten operons preceded by sigma 70-like promoter elements." J Bacteriol **189**(1): 198-206.

Hendrickson, E. L., P. Guevera, A. Penaloza-Vazquez, J. Shao, C. Bender and F. M. Ausubel (2000). "Virulence of the phytopathogen Pseudomonas syringae pv. maculicola is rpoN dependent." J Bacteriol **182**(12): 3498-3507.

Hindson, B. J., K. D. Ness, D. A. Masquelier, P. Belgrader, N. J. Heredia, A. J. Makarewicz, I. J. Bright, M. Y. Lucero, A. L. Hiddessen, T. C. Legler, T. K. Kitano, M. R. Hodel, J. F. Petersen, P. W. Wyatt, E. R. Steenblock, P. H. Shah, L. J. Bousse, C. B. Troup, J. C. Mellen, D. K. Wittmann, N. G. Erndt, T. H. Cauley, R. T. Koehler, A. P. So, S. Dube, K. A. Rose, L. Montesclaros, S. Wang, D. P. Stumbo, S. P. Hodges, S. Romine, F. P. Milanovich, H. E. White, J. F. Regan, G. A. Karlin-Neumann, C. M. Hindson, S. Saxonov and B. W. Colston (2011). "High-throughput droplet digital PCR system for absolute quantitation of DNA copy number." Anal Chem **83**(22): 8604-8610.

Hong, E., M. Doucleff and D. E. Wemmer (2009). "Structure of the RNA polymerase core-binding domain of sigma(54) reveals a likely conformational fracture point." J Mol Biol **390**(1): 70-82.

Hu, V. H., E. M. Harding-Esch, M. J. Burton, R. L. Bailey, J. Kadimpeul and D. C. Mabey (2010). "Epidemiology and control of trachoma: systematic review." Trop Med Int Health **15**(6): 673-691.

Hua, L., P. S. Hefty, Y. J. Lee, Y. M. Lee, R. S. Stephens and C. W. Price (2006). "Core of the partner switching signalling mechanism is conserved in the obligate intracellular pathogen Chlamydia trachomatis." Mol Microbiol **59**(2): 623-636.

Huala, E., J. Stigter and F. M. Ausubel (1992). "The central domain of Rhizobium leguminosarum DctD functions independently to activate transcription." J Bacteriol **174**(4): 1428-1431.

Hughes, K. T. and K. Mathee (1998). "The anti-sigma factors." Annu Rev Microbiol **52**: 231-286.

Hulko, M., F. Berndt, M. Gruber, J. U. Linder, V. Truffault, A. Schultz, J. Martin, J. E. Schultz, A. N. Lupas and M. Coles (2006). "The HAMP domain structure implies helix rotation in transmembrane signaling." Cell **126**(5): 929-940.

Humphrys, M. S., T. Creasy, Y. Sun, A. C. Shetty, M. C. Chibucos, E. F. Drabek, C. M. Fraser, U. Farooq, N. Sengamalay, S. Ott, H. Shou, P. M. Bavoil, A. Mahurkar and G. S. Myers (2013). "Simultaneous transcriptional profiling of bacteria and their host cells." PLoS One **8**(12): e80597.

Huston, W. M., C. Theodoropoulos, S. A. Mathews and P. Timms (2008). "Chlamydia trachomatis responds to heat shock, penicillin induced persistence, and IFN-gamma persistence by altering levels of the extracytoplasmic stress response protease HtrA." BMC Microbiol **8**: 190.

Hutcheson, S. W., J. Bretz, T. Sussan, S. Jin and K. Pak (2001). "Enhancer-binding proteins HrpR and HrpS interact to regulate hrp-encoded type III protein secretion in Pseudomonas syringae strains." J Bacteriol **183**(19): 5589-5598.

Iliffe-Lee, E. R. and G. McClarty (1999). "Glucose metabolism in Chlamydia trachomatis: the 'energy parasite' hypothesis revisited." Mol Microbiol **33**(1): 177-187.

Iliffe-Lee, E. R. and G. McClarty (2000). "Regulation of carbon metabolism in Chlamydia trachomatis." Mol Microbiol **38**(1): 20-30.

Ishimoto, K. S. and S. Lory (1989). "Formation of pilin in Pseudomonas aeruginosa requires the alternative sigma factor (RpoN) of RNA polymerase." Proc Natl Acad Sci U S A **86**(6): 1954-1957.

Ito, K. and Y. Akiyama (2005). "Cellular functions, mechanism of action, and regulation of FtsH protease." Annu Rev Microbiol **59**: 211-231.

Jack, R., M. De Zamaroczy and M. Merrick (1999). "The signal transduction protein GlnK is required for NifL-dependent nitrogen control of nif gene expression in Klebsiella pneumoniae." J Bacteriol **181**(4): 1156-1162.

Jacobi, S., R. Schade and K. Heuner (2004). "Characterization of the alternative sigma factor sigma54 and the transcriptional regulator FleQ of Legionella pneumophila, which are both involved in the regulation cascade of flagellar gene expression." J Bacteriol **186**(9): 2540-2547.

Jacobson, M. P., R. A. Friesner, Z. Xiang and B. Honig (2002). "On the role of the crystal environment in determining protein side-chain conformations." J Mol Biol **320**(3): 597-608.

Jacobson, M. P., D. L. Pincus, C. S. Rapp, T. J. Day, B. Honig, D. E. Shaw and R. A. Friesner (2004). "A hierarchical approach to all-atom protein loop prediction." Proteins **55**(2): 351-367.

Jagannathan, A., C. Constantinidou and C. W. Penn (2001). "Roles of rpoN, fliA, and flgR in expression of flagella in Campylobacter jejuni." J Bacteriol **183**(9): 2937-2942.

Janausch, I. G., E. Zientz, Q. H. Tran, A. Kroger and G. Unden (2002). "C4-dicarboxylate carriers and sensors in bacteria." Biochim Biophys Acta **1553**(1-2): 39-56.

Jason-Moller, L., M. Murphy and J. Bruno (2006). "Overview of Biacore systems and their applications." Curr Protoc Protein Sci **Chapter 19**: Unit 19 13.

Jewett, T. J., E. R. Fischer, D. J. Mead and T. Hackstadt (2006). "Chlamydial TARP is a bacterial nucleator of actin." Proc Natl Acad Sci U S A **103**(42): 15599-15604.

Jiang, P. and A. J. Ninfa (1999). "Regulation of autophosphorylation of Escherichia coli nitrogen regulator II by the PII signal transduction protein." J Bacteriol **181**(6): 1906-1911.

Jiang, P. and A. J. Ninfa (2009). "Sensation and signaling of alpha-ketoglutarate and adenylylate energy charge by the Escherichia coli PII signal transduction protein require cooperation of the three ligand-binding sites within the PII trimer." Biochemistry **48**(48): 11522-11531.

Kabsch, W. S., C. (1983). "Dictionary of protein secondary structure: pattern recognition of hydrogen-bonded and geometrical features." Biopolymers **22**(12): 2577-2637.

Kang, C. M., M. S. Brody, S. Akbar, X. Yang and C. W. Price (1996). "Homologous pairs of regulatory proteins control activity of Bacillus subtilis transcription factor sigma(b) in response to environmental stress." J Bacteriol **178**(13): 3846-3853.

Kang, C. M., K. Vijay and C. W. Price (1998). "Serine kinase activity of a Bacillus subtilis switch protein is required to transduce environmental stress signals but not to activate its target PP2C phosphatase." Mol Microbiol **30**(1): 189-196.

Karimova, G., J. Pidoux, A. Ullmann and D. Ladant (1998). "A bacterial two-hybrid system based on a reconstituted signal transduction pathway." Proc Natl Acad Sci U S A **95**(10): 5752-5756.

Keener, J. and S. Kustu (1988). "Protein kinase and phosphoprotein phosphatase activities of nitrogen regulatory proteins NTRB and NTRC of enteric bacteria: roles of the conserved amino-terminal domain of NTRC." Proc Natl Acad Sci U S A **85**(14): 4976-4980.

Knittler, M. R. and K. Sachse (2015). "Chlamydia psittaci: update on an underestimated zoonotic agent." Pathog Dis **73**(1): 1-15.

Koehler, J. E., R. R. Burgess, N. E. Thompson and R. S. Stephens (1990). "Chlamydia trachomatis RNA polymerase major sigma subunit. Sequence and structural comparison of conserved and unique regions with Escherichia coli sigma 70 and Bacillus subtilis sigma 43." J Biol Chem **265**(22): 13206-13214.

Kohler, T., S. Harayama, J. L. Ramos and K. N. Timmis (1989). "Involvement of Pseudomonas putida RpoN sigma factor in regulation of various metabolic functions." J Bacteriol **171**(8): 4326-4333.

Kokes, M., J. D. Dunn, J. A. Granek, B. D. Nguyen, J. R. Barker, R. H. Valdivia and R. J. Bastidas (2015). "Integrating Chemical Mutagenesis and Whole-Genome Sequencing as a Platform for Forward and Reverse Genetic Analysis of Chlamydia." Cell Host & Microbe **17**(5): 716-725.

Koo, I. C. and R. S. Stephens (2003). "A developmentally regulated two-component signal transduction system in Chlamydia." J Biol Chem **278**(19): 17314-17319.

Koo, I. C., D. Walthers, P. S. Hefty, L. J. Kenney and R. S. Stephens (2006). "ChxR is a transcriptional activator in Chlamydia." Proc Natl Acad Sci U S A **103**(3): 750-755.

Kozak, N. A., S. Mattoo, A. K. Foreman-Wykert, J. P. Whitelegge and J. F. Miller (2005). "Interactions between partner switcher orthologs BtrW and BtrV regulate type III secretion in Bordetella." J Bacteriol **187**(16): 5665-5676.

Krissinel, E. (2012). "Enhanced fold recognition using efficient short fragment clustering." J Mol Biochem **1**(2): 76-85.

Kustu, S., E. Santero, J. Keener, D. Popham and D. Weiss (1989). "Expression of sigma 54 (ntrA)-dependent genes is probably united by a common mechanism." Microbiol Rev **53**(3): 367-376.

LaBrie, S. D., Z. E. Dimond, K. S. Harrison, S. Baid, J. Wickstrum, R. J. Suchland and P. S. Hefty (2019). "Transposon Mutagenesis in Chlamydia trachomatis Identifies CT339 as a ComEC Homolog Important for DNA Uptake and Lateral Gene Transfer." mBio **10**(4).

Langer, G., S. X. Cohen, V. S. Lamzin and A. Perrakis (2008). "Automated macromolecular model building for X-ray crystallography using ARP/wARP version 7." Nat Protoc **3**(7): 1171-1179.

Lau, C. Y. and A. K. Qureshi (2002). "Azithromycin versus doxycycline for genital chlamydial infections: a meta-analysis of randomized clinical trials." Sex Transm Dis **29**(9): 497-502.

Lee, J. K., G. A. Enciso, D. Boassa, C. N. Chander, T. H. Lou, S. S. Pairawan, M. C. Guo, F. Y. M. Wan, M. H. Ellisman, C. Sutterlin and M. Tan (2018). "Replication-dependent size reduction precedes differentiation in Chlamydia trachomatis." Nat Commun **9**(1): 45.

Leonhartsberger, S., A. Huber, F. Lottspeich and A. Bock (2001). "The hydH/G Genes from Escherichia coli code for a zinc and lead responsive two-component regulatory system." J Mol Biol **307**(1): 93-105.

Liang, P., M. Rosas-Lemus, D. Patel, X. Fang, K. Tuz and O. Juarez (2018). "Dynamic energy dependency of Chlamydia trachomatis on host cell metabolism during intracellular growth: Role of sodium-based energetics in chlamydial ATP generation." J Biol Chem **293**(2): 510-522.

Liechti, G. W., E. Kuru, E. Hall, A. Kalinda, Y. V. Brun, M. VanNieuwenhze and A. T. Maurelli (2014). "A new metabolic cell-wall labelling method reveals peptidoglycan in Chlamydia trachomatis." Nature **506**(7489): 507-510.

Liu, J., J. Yang, J. Wen, Y. Yang, X. Wei, X. Zhang and Y. P. Wang (2014). "Mutational analysis of dimeric linkers in peri- and cytoplasmic domains of histidine kinase DctB reveals their functional roles in signal transduction." Open Biol **4**(6): 140023.

Liu, X., M. Afrane, D. E. Clemmer, G. Zhong and D. E. Nelson (2010). "Identification of Chlamydia trachomatis outer membrane complex proteins by differential proteomics." J Bacteriol **192**(11): 2852-2860.

Liu, Y., C. Chen, S. Gong, S. Hou, M. Qi, Q. Liu, J. Baseman and G. Zhong (2014). "Transformation of Chlamydia muridarum reveals a role for Pgp5 in suppression of plasmid-dependent gene expression." J Bacteriol **196**(5): 989-998.

Liu, Y. C., M. A. Machuca, S. A. Beckham, M. J. Gunzburg and A. Roujeinikova (2015). "Structural basis for amino-acid recognition and transmembrane signalling by tandem Per-Arnt-Sim (tandem PAS) chemoreceptor sensory domains." Acta Crystallogr D Biol Crystallogr **71**(Pt 10): 2127-2136.

Longbottom, D. and L. J. Coulter (2003). "Animal chlamydioses and zoonotic implications." J Comp Pathol **128**(4): 217-244.

Madan Babu, M., S. A. Teichmann and L. Aravind (2006). "Evolutionary dynamics of prokaryotic transcriptional regulatory networks." J Mol Biol **358**(2): 614-633.

Magasanik, B. (1982). "Genetic control of nitrogen assimilation in bacteria." Annu Rev Genet **16**: 135-168.

Mariotti, S. P., D. Pascolini and J. Rose-Nussbaumer (2009). "Trachoma: global magnitude of a preventable cause of blindness." Br J Ophthalmol **93**(5): 563-568.

Marsh, J. W., M. S. Humphrys and G. S. A. Myers (2017). "A Laboratory Methodology for Dual RNA-Sequencing of Bacteria and their Host Cells In Vitro." Front Microbiol **8**: 1830.

Martin-Verstraete, I., J. Stulke, A. Klier and G. Rapoport (1995). "Two different mechanisms mediate catabolite repression of the Bacillus subtilis levanase operon." J Bacteriol **177**(23): 6919-6927.

Mascher, T., N. G. Margulis, T. Wang, R. W. Ye and J. D. Helmann (2003). "Cell wall stress responses in Bacillus subtilis: the regulatory network of the bacitracin stimulon." Mol Microbiol **50**(5): 1591-1604.

Mathews, S. A. and P. Timms (2000). "Identification and mapping of sigma-54 promoters in Chlamydia trachomatis." J Bacteriol **182**(21): 6239-6242.

Mathews, S. A., K. M. Volp and P. Timms (1999). "Development of a quantitative gene expression assay for Chlamydia trachomatis identified temporal expression of sigma factors." FEBS Lett **458**(3): 354-358.

Matthews, B. W. (1968). "Solvent content of protein crystals." J Mol Biol **33**(2): 491-497.

Mattoo, S., M. H. Yuk, L. L. Huang and J. F. Miller (2004). "Regulation of type III secretion in Bordetella." Mol Microbiol **52**(4): 1201-1214.

McClarty, G., H. D. Caldwell and D. E. Nelson (2007). "Chlamydial interferon gamma immune evasion influences infection tropism." Curr Opin Microbiol **10**(1): 47-51.

McCoy, A. J., R. W. Grosse-Kunstleve, P. D. Adams, M. D. Winn, L. C. Storoni and R. J. Read (2007). "Phaser crystallographic software." J Appl Crystallogr **40**(Pt 4): 658-674.

McCoy, A. J., R. C. Sandlin and A. T. Maurelli (2003). "In vitro and in vivo functional activity of Chlamydia MurA, a UDP-N-acetylglucosamine enolpyruvyl transferase involved in peptidoglycan synthesis and fosfomycin resistance." J Bacteriol **185**(4): 1218-1228.

McGann, M. (2011). "FRED pose prediction and virtual screening accuracy." J Chem Inf Model **51**(3): 578-596.

Mehlitz, A., E. Eylert, C. Huber, B. Lindner, N. Vollmuth, K. Karunakaran, W. Goebel, W. Eisenreich and T. Rudel (2017). "Metabolic adaptation of Chlamydia trachomatis to mammalian host cells." Mol Microbiol **103**(6): 1004-1019.

Merrick, M. J. (1993). "In a class of its own--the RNA polymerase sigma factor sigma 54 (sigma N)." Mol Microbiol **10**(5): 903-909.

Michiels, J., M. Moris, B. Dombrecht, C. Verreth and J. Vanderleyden (1998). "Differential regulation of Rhizobium etli rpoN2 gene expression during symbiosis and free-living growth." J Bacteriol **180**(14): 3620-3628.

Miller, J. (1972). Experiments in molecular genetics. Cold Spring Harbor, NY, Cold Spring Harbor Laboratory Press.

Mooney, R. A., S. A. Darst and R. Landick (2005). "Sigma and RNA polymerase: an on-again, off-again relationship?" Mol Cell **20**(3): 335-345.

Moore, E. R. and S. P. Ouellette (2014). "Reconceptualizing the chlamydial inclusion as a pathogen-specified parasitic organelle: an expanded role for Inc proteins." Front Cell Infect Microbiol **4**: 157.

Morett, E. and M. Buck (1989). "In vivo studies on the interaction of RNA polymerase-sigma 54 with the Klebsiella pneumoniae and Rhizobium meliloti nifH promoters. The role of NifA in the formation of an open promoter complex." J Mol Biol **210**(1): 65-77.

Morris, A. R. and K. L. Visick (2013). "The response regulator SypE controls biofilm formation and colonization through phosphorylation of the syp-encoded regulator SypA in Vibrio fischeri." Mol Microbiol **87**(3): 509-525.

Moulder, J. W. (1991). "Interaction of chlamydiae and host cells in vitro." Microbiol Rev **55**(1): 143-190.

Murakami, K. S. and S. A. Darst (2003). "Bacterial RNA polymerases: the wholo story." Curr Opin Struct Biol **13**(1): 31-39.

Nan, B., X. Liu, Y. Zhou, J. Liu, L. Zhang, J. Wen, X. Zhang, X. D. Su and Y. P. Wang (2010). "From signal perception to signal transduction: ligand-induced dimeric switch of DctB sensory domain in solution." Mol Microbiol **75**(6): 1484-1494.

Neuwald, A. F., L. Aravind, J. L. Spouge and E. V. Koonin (1999). "AAA+: A class of chaperone-like ATPases associated with the assembly, operation, and disassembly of protein complexes." Genome Res **9**(1): 27-43.

Newhall, W. J. and R. B. Jones (1983). "Disulfide-linked oligomers of the major outer membrane protein of chlamydiae." J Bacteriol **154**(2): 998-1001.

Nguyen, B. D. and R. H. Valdivia (2012). "Virulence determinants in the obligate intracellular pathogen Chlamydia trachomatis revealed by forward genetic approaches." Proceedings of the National Academy of Sciences of the United States of America **109**(4): 1263-1268.

Nguyen, M. N., K. P. Tan and M. S. Madhusudhan (2011). "CLICK--topology-independent comparison of biomolecular 3D structures." Nucleic Acids Res **39**(Web Server issue): W24-28.

Nicholson, T. L., L. Olinger, K. Chong, G. Schoolnik and R. S. Stephens (2003). "Global stage-specific gene regulation during the developmental cycle of Chlamydia trachomatis." J Bacteriol **185**(10): 3179-3189.

Niehus, E., E. Cheng and M. Tan (2008). "DNA supercoiling-dependent gene regulation in Chlamydia." J Bacteriol **190**(19): 6419-6427.

Niehus, E., H. Gressmann, F. Ye, R. Schlapbach, M. Dehio, C. Dehio, A. Stack, T. F. Meyer, S. Suerbaum and C. Josenhans (2004). "Genome-wide analysis of transcriptional

hierarchy and feedback regulation in the flagellar system of Helicobacter pylori." Mol Microbiol **52**(4): 947-961.

Niesen, F. H., H. Berglund and M. Vedadi (2007). "The use of differential scanning fluorimetry to detect ligand interactions that promote protein stability." Nat Protoc **2**(9): 2212-2221.

Ninfa, A. J. and B. Magasanik (1986). "Covalent modification of the glnG product, NRI, by the glnL product, NRII, regulates the transcription of the glnALG operon in Escherichia coli." Proc Natl Acad Sci U S A **83**(16): 5909-5913.

Nishiyama, S., Y. Takahashi, K. Yamamoto, D. Suzuki, Y. Itoh, K. Sumita, Y. Uchida, M. Homma, K. Imada and I. Kawagishi (2016). "Identification of a Vibrio cholerae chemoreceptor that senses taurine and amino acids as attractants." Sci Rep **6**: 20866.

O'Hearn, S. D., A. J. Kusalik and J. F. Angel (2003). "MolCom: a method to compare protein molecules based on 3-D structural and chemical similarity." Protein Eng **16**(3): 169-178.

Orillard, E. and M. Tan (2016). "Functional analysis of three topoisomerases that regulate DNA supercoiling levels in Chlamydia." Mol Microbiol **99**(3): 484-496.

Ouellette, S. P., T. P. Hatch, Y. M. AbdelRahman, L. A. Rose, R. J. Belland and G. I. Byrne (2006). "Global transcriptional upregulation in the absence of increased translation in Chlamydia during IFNgamma-mediated host cell tryptophan starvation." Mol Microbiol **62**(5): 1387-1401.

Packiam, M., B. Weinrick, W. R. Jacobs, Jr. and A. T. Maurelli (2015). "Structural characterization of muropeptides from Chlamydia trachomatis peptidoglycan by mass spectrometry resolves "chlamydial anomaly"." Proc Natl Acad Sci U S A **112**(37): 11660-11665.

Paget, M. S. (2015). "Bacterial Sigma Factors and Anti-Sigma Factors: Structure, Function and Distribution." Biomolecules **5**(3): 1245-1265.

Painter, J. and E. A. Merritt (2006). "Optimal description of a protein structure in terms of multiple groups undergoing TLS motion." Acta Crystallogr D Biol Crystallogr **62**(Pt 4): 439-450.

Panzetta, M. E., R. H. Valdivia and H. A. Saka (2018). "Chlamydia Persistence: A Survival Strategy to Evade Antimicrobial Effects in-vitro and in-vivo." Front Microbiol **9**: 3101.

Pearson, J. P., E. C. Pesci and B. H. Iglewski (1997). "Roles of Pseudomonas aeruginosa las and rhl quorum-sensing systems in control of elastase and rhamnolipid biosynthesis genes." J Bacteriol **179**(18): 5756-5767.

Pilhofer, M., K. Aistleitner, J. Biboy, J. Gray, E. Kuru, E. Hall, Y. V. Brun, M. S. VanNieuwenhze, W. Vollmer, M. Horn and G. J. Jensen (2013). "Discovery of chlamydial peptidoglycan reveals bacteria with murein sacculi but without FtsZ." Nat Commun **4**: 2856.

Porritt, R. A. and T. R. Crother (2016). "Chlamydia pneumoniae Infection and Inflammatory Diseases." For Immunopathol Dis Therap **7**(3-4): 237-254.

Quinn, T. C., S. E. Goodell, E. Mkrtichian, M. D. Schuffler, S. P. Wang, W. E. Stamm and K. K. Holmes (1981). "Chlamydia trachomatis proctitis." N Engl J Med **305**(4): 195-200.

Rahman, H., R. M. King, L. K. Shewell, E. A. Semchenko, L. E. Hartley-Tassell, J. C. Wilson, C. J. Day and V. Korolik (2014). "Characterisation of a multi-ligand binding chemoreceptor CcmL (Tlp3) of Campylobacter jejuni." PLoS Pathog **10**(1): e1003822.

Rao, X., P. Deighan, Z. Hua, X. Hu, J. Wang, M. Luo, J. Wang, Y. Liang, G. Zhong, A. Hochschild and L. Shen (2009). "A regulator from Chlamydia trachomatis modulates the activity of RNA polymerase through direct interaction with the beta subunit and the primary sigma subunit." Genes Dev **23**(15): 1818-1829.

Resnikoff, S., D. Pascolini, D. Etya'ale, I. Kocur, R. Pararajasegaram, G. P. Pokharel and S. P. Mariotti (2004). "Global data on visual impairment in the year 2002." Bull World Health Organ **82**(11): 844-851.

Rico-Jimenez, M., F. Munoz-Martinez, C. Garcia-Fontana, M. Fernandez, B. Morel, A. Ortega, J. L. Ramos and T. Krell (2013). "Paralogous chemoreceptors mediate chemotaxis towards protein amino acids and the non-protein amino acid gamma-aminobutyrate (GABA)." Mol Microbiol **88**(6): 1230-1243.

Robichon, D., E. Gouin, M. Debarbouille, P. Cossart, Y. Cenatiempo and Y. Hechard (1997). "The rpoN (sigma54) gene from Listeria monocytogenes is involved in resistance to mesentericin Y105, an antibacterial peptide from Leuconostoc mesenteroides." J Bacteriol **179**(23): 7591-7594.

Rosario, C. J., B. R. Hanson and M. Tan (2014). "The transcriptional repressor EUO regulates both subsets of Chlamydia late genes." Mol Microbiol **94**(4): 888-897.

Rosario, C. J., K. R. Soules, P. S. Hefty and M. Tan (2020). *Chlamydia* Gene Regulation Chlamydia Biology: From Genome to Disease. M. Tan, J. H. Hegemann and C. Sutterlin. Norfolk, UK, Caister Acedemic Press**:** 219-240.

Rosario, C. J. and M. Tan (2012). "The early gene product EUO is a transcriptional repressor that selectively regulates promoters of Chlamydia late genes." Mol Microbiol **84**(6): 1097-1107.

Rosario, C. J. and M. Tan (2016). "Regulation of Chlamydia Gene Expression by Tandem Promoters with Different Temporal Patterns." J Bacteriol **198**(2): 363-369.

Samuels, D. J., J. G. Frye, S. Porwollik, M. McClelland, J. Mrazek, T. R. Hoover and A. C. Karls (2013). "Use of a promiscuous, constitutively-active bacterial enhancer-binding protein to define the sigma(5)(4) (RpoN) regulon of Salmonella Typhimurium LT2." BMC Genomics **14**: 602.

Schaumburg, C. S. and M. Tan (2006). "Arginine-dependent gene regulation via the ArgR repressor is species specific in chlamydia." J Bacteriol **188**(3): 919-927.

Schoborg, R. V. (2011). "Chlamydia persistence -- a tool to dissect chlamydia--host interactions." Microbes Infect **13**(7): 649-662.

Schultz, J., F. Milpetz, P. Bork and C. P. Ponting (1998). "SMART, a simple modular architecture research tool: identification of signaling domains." Proc Natl Acad Sci U S A **95**(11): 5857-5864.

Schumacher, J., N. Joly, M. Rappas, X. Zhang and M. Buck (2006). "Structures and organisation of AAA+ enhancer binding proteins in transcriptional activation." J Struct Biol **156**(1): 190-199.

Shaw, E. I., C. A. Dooley, E. R. Fischer, M. A. Scidmore, K. A. Fields and T. Hackstadt (2000). "Three temporal classes of gene expression during the Chlamydia trachomatis developmental cycle." Mol Microbiol **37**(4): 913-925.

Shen, B. A. and R. Landick (2019). "Transcription of Bacterial Chromatin." J Mol Biol **431**(20): 4040-4066.

Shi, Y. (2009). "Serine/threonine phosphatases: mechanism through structure." Cell **139**(3): 468-484.

Snider, J., G. Thibault and W. A. Houry (2008). "The AAA+ superfamily of functionally diverse proteins." Genome Biol **9**(4): 216.

Song, L., J. H. Carlson, W. M. Whitmire, L. Kari, K. Virtaneva, D. E. Sturdevant, H. Watkins, B. Zhou, G. L. Sturdevant, S. F. Porcella, G. McClarty and H. D. Caldwell (2013). "Chlamydia trachomatis plasmid-encoded Pgp4 is a transcriptional regulator of virulence-associated genes." Infect Immun **81**(3): 636-644.

Soules, K. R., A. Dmitriev, S. D. LaBrie, Z. E. Dimond, B. H. May, D. K. Johnson, Y. Zhang, K. P. Battaile, S. Lovell and P. S. Hefty (2019). "Structural and ligand binding analyses of the periplasmic sensor domain of RsbU in Chlamydia trachomatis supports role in TCA cycle regulation." Mol Microbiol.

Spaeth, K. E., Y. S. Chen and R. H. Valdivia (2009). "The Chlamydia type III secretion system C-ring engages a chaperone-effector protein complex." PLoS Pathog **5**(9): e1000579.

Stephens, R. S., S. Kalman, C. Lammel, J. Fan, R. Marathe, L. Aravind, W. Mitchell, L. Olinger, R. L. Tatusov, Q. Zhao, E. V. Koonin and R. W. Davis (1998). "Genome sequence of an obligate intracellular pathogen of humans: Chlamydia trachomatis." Science **282**(5389): 754-759.

Storz, G. (2002). "An expanding universe of noncoding RNAs." Science **296**(5571): 1260-1263.

Tan, M. (2006). Regulation of gene expression. *Chlamydia*: Genomics and Pathogenesis. P. M. Bavoil and P. B. Wyrick. Wymondham, U.K., Horizon Bioscience**:** 103-131.

Tan, M. (2012). Temporal gene regulation during the chlamydial developmental cycle. Intracellular Pathogens I: *Chlamydiales*. M. Tan and P. M. Bavoil. Washington, D.C. , ASM Press**:** 149-169.

Tattersall, J., G. V. Rao, J. Runac, T. Hackstadt, S. S. Grieshaber and N. A. Grieshaber (2012). "Translation inhibition of the developmental cycle protein HctA by the small RNA IhtA is conserved across Chlamydia." PLoS One **7**(10): e47439.

Thompson, C. C., C. Griffiths, S. S. Nicod, N. M. Lowden, S. Wigneshweraraj, D. J. Fisher and M. O. McClure (2015). "The Rsb Phosphoregulatory Network Controls Availability of the Primary Sigma Factor in Chlamydia trachomatis and Influences the Kinetics of Growth and Development." PLoS Pathog **11**(8): e1005125.

Tjaden, J., H. H. Winkler, C. Schwoppe, M. Van Der Laan, T. Mohlmann and H. E. Neuhaus (1999). "Two nucleotide transport proteins in Chlamydia trachomatis, one for net

nucleoside triphosphate uptake and the other for transport of energy." J Bacteriol **181**(4): 1196-1202.

Tuz, K., K. G. Mezic, T. Xu, B. Barquera and O. Juarez (2015). "The Kinetic Reaction Mechanism of the Vibrio cholerae Sodium-dependent NADH Dehydrogenase." J Biol Chem **290**(33): 20009-20021.

Valdivia, R. H. (2008). "Chlamydia effector proteins and new insights into chlamydial cellular microbiology." Curr Opin Microbiol **11**(1): 53-59.

Voelker, U., A. Dufour and W. G. Haldenwang (1995). "The Bacillus subtilis rsbU gene product is necessary for RsbX-dependent regulation of sigma B." J Bacteriol **177**(1): 114-122.

Voelker, U., A. Voelker, B. Maul, M. Hecker, A. Dufour and W. G. Haldenwang (1995). "Separate mechanisms activate sigma B of Bacillus subtilis in response to environmental and metabolic stresses." J Bacteriol **177**(13): 3771-3780.

Vonrhein, C., C. Flensburg, P. Keller, A. Sharff, O. Smart, W. Paciorek, T. Womack and G. Bricogne (2011). "Data processing and analysis with the autoPROC toolbox." Acta Crystallogr D Biol Crystallogr **67**(Pt 4): 293-302.

Weber, A., E. Menzlaff, B. Arbinger, M. Gutensohn, C. Eckerskorn and U. I. Flugge (1995). "The 2-oxoglutarate/malate translocator of chloroplast envelope membranes: molecular cloning of a transporter containing a 12-helix motif and expression of the functional protein in yeast cells." Biochemistry **34**(8): 2621-2627.

Weber, M. M., J. L. Lam, C. A. Dooley, N. F. Noriea, B. T. Hansen, F. H. Hoyt, A. B. Carmody, G. L. Sturdevant and T. Hackstadt (2017). "Absence of Specific Chlamydia trachomatis Inclusion Membrane Proteins Triggers Premature Inclusion Membrane Lysis and Host Cell Death." Cell Rep **19**(7): 1406-1417.

Wickstrum, J., L. R. Sammons, K. N. Restivo and P. S. Hefty (2013). "Conditional gene expression in Chlamydia trachomatis using the tet system." PLoS One **8**(10): e76743.

Wigneshweraraj, S., D. Bose, P. C. Burrows, N. Joly, J. Schumacher, M. Rappas, T. Pape, X. Zhang, P. Stockley, K. Severinov and M. Buck (2008). "Modus operandi of the bacterial RNA polymerase containing the sigma54 promoter-specificity factor." Mol Microbiol **68**(3): 538-546.

Wilson, A. C. and M. Tan (2002). "Functional analysis of the heat shock regulator HrcA of Chlamydia trachomatis." J Bacteriol **184**(23): 6566-6571.

Wilson, A. C. and M. Tan (2004). "Stress response gene regulation in Chlamydia is dependent on HrcA-CIRCE interactions." J Bacteriol **186**(11): 3384-3391.

Winkler, H. H. and H. E. Neuhaus (1999). "Non-mitochondrial ATP transport." Trends Biochem Sci **24**(2): 64-68.

Winn, M. D., C. C. Ballard, K. D. Cowtan, E. J. Dodson, P. Emsley, P. R. Evans, R. M. Keegan, E. B. Krissinel, A. G. Leslie, A. McCoy, S. J. McNicholas, G. N. Murshudov, N. S. Pannu, E. A. Potterton, H. R. Powell, R. J. Read, A. Vagin and K. S. Wilson (2011). "Overview of the CCP4 suite and current developments." Acta Crystallogr D Biol Crystallogr **67**(Pt 4): 235-242.

Winn, M. D., M. N. Isupov and G. N. Murshudov (2001). "Use of TLS parameters to model anisotropic displacements in macromolecular refinement." Acta Crystallogr D Biol Crystallogr **57**(Pt 1): 122-133.

Wise, A. A. and C. W. Price (1995). "Four additional genes in the sigB operon of Bacillus subtilis that control activity of the general stress factor sigma B in response to environmental signals." J Bacteriol **177**(1): 123-133.

Wishart, D. S., Y. D. Feunang, A. Marcu, A. C. Guo, K. Liang, R. Vazquez-Fresno, T. Sajed, D. Johnson, C. Li, N. Karu, Z. Sayeeda, E. Lo, N. Assempour, M. Berjanskii, S. Singhal, D. Arndt, Y. Liang, H. Badran, J. Grant, A. Serra-Cayuela, Y. Liu, R. Mandal, V. Neveu, A. Pon, C. Knox, M. Wilson, C. Manach and A. Scalbert (2018). "HMDB 4.0: the human metabolome database for 2018." Nucleic Acids Res **46**(D1): D608-D617.

Wishart, D. S., C. Knox, A. C. Guo, R. Eisner, N. Young, B. Gautam, D. D. Hau, N. Psychogios, E. Dong, S. Bouatra, R. Mandal, I. Sinelnikov, J. Xia, L. Jia, J. A. Cruz, E. Lim, C. A. Sobsey, S. Shrivastava, P. Huang, P. Liu, L. Fang, J. Peng, R. Fradette, D. Cheng, D. Tzur, M. Clements, A. Lewis, A. De Souza, A. Zuniga, M. Dawe, Y. Xiong, D. Clive, R. Greiner, A. Nazyrova, R. Shaykhutdinov, L. Li, H. J. Vogel and I. Forsythe (2009). "HMDB: a knowledgebase for the human metabolome." Nucleic Acids Res **37**(Database issue): D603-610.

Wishart, D. S., D. Tzur, C. Knox, R. Eisner, A. C. Guo, N. Young, D. Cheng, K. Jewell, D. Arndt, S. Sawhney, C. Fung, L. Nikolai, M. Lewis, M. A. Coutouly, I. Forsythe, P. Tang, S. Shrivastava, K. Jeroncic, P. Stothard, G. Amegbey, D. Block, D. D. Hau, J. Wagner, J. Miniaci, M. Clements, M. Gebremedhin, N. Guo, Y. Zhang, G. E. Duggan, G. D. Macinnis, A. M. Weljie, R. Dowlatabadi, F. Bamforth, D. Clive, R. Greiner, L. Li, T. Marrie, B. D. Sykes, H. J. Vogel and L. Querengesser (2007). "HMDB: the Human Metabolome Database." Nucleic Acids Res **35**(Database issue): D521-526.

Wu, R., M. Gu, R. Wilton, G. Babnigg, Y. Kim, P. R. Pokkuluri, H. Szurmant, A. Joachimiak and M. Schiffer (2013). "Insight into the sporulation phosphorelay: crystal structure of the sensor domain of Bacillus subtilis histidine kinase, KinD." Protein Sci **22**(5): 564-576.

Xu, H., B. Gu, B. T. Nixon and T. R. Hoover (2004). "Purification and characterization of the AAA+ domain of Sinorhizobium meliloti DctD, a sigma54-dependent transcriptional activator." J Bacteriol **186**(11): 3499-3507.

Xu, J. and Y. Zhang (2010). "How significant is a protein structure similarity with TM-score = 0.5?" Bioinformatics **26**(7): 889-895.

Yamamoto, K., H. Watanabe and A. Ishihama (2014). "Expression levels of transcription factors in Escherichia coli: growth phase- and growth condition-dependent variation of 90 regulators from six families." Microbiology **160**(Pt 9): 1903-1913.

Yang, C., L. Kari, G. L. Sturdevant, L. Song, M. J. Patton, C. E. Couch, J. M. Ilgenfritz, T. R. Southern, W. M. Whitmire, M. Briones, C. Bonner, C. Grant, P. Hu, G. McClarty and H. D. Caldwell (2017). "Chlamydia trachomatis ChxR is a transcriptional regulator of virulence factors that function in in vivo host-pathogen interactions." Pathog Dis **75**(3).

Yang, J., R. Yan, A. Roy, D. Xu, J. Poisson and Y. Zhang (2015). "The I-TASSER Suite: protein structure and function prediction." Nat Methods **12**(1): 7-8.

Yang, X., C. M. Kang, M. S. Brody and C. W. Price (1996). "Opposing pairs of serine protein kinases and phosphatases transmit signals of environmental stress to activate a bacterial transcription factor." Genes Dev **10**(18): 2265-2275.

Yu, H. H., E. G. Di Russo, M. A. Rounds and M. Tan (2006). "Mutational analysis of the promoter recognized by Chlamydia and Escherichia coli sigma(28) RNA polymerase." J Bacteriol **188**(15): 5524-5531.

Yu, H. H., D. Kibler and M. Tan (2006). "In silico prediction and functional validation of sigma28-regulated genes in Chlamydia and Escherichia coli." J Bacteriol **188**(23): 8206-8212.

Yu, H. H. and M. Tan (2003). "Sigma28 RNA polymerase regulates hctB, a late developmental gene in Chlamydia." Mol Microbiol **50**(2): 577-584.

Yu, Y. H., Y. Lu, Y. Q. He, S. Huang and J. L. Tang (2015). "Rapid and efficient genome-wide characterization of Xanthomonas TAL effector genes." Sci Rep **5**: 13162.

Zhang, L., A. L. Douglas and T. P. Hatch (1998). "Characterization of a Chlamydia psittaci DNA binding protein (EUO) synthesized during the early and middle phases of the developmental cycle." Infect Immun **66**(3): 1167-1173.

Zhang, L., M. M. Howe and T. P. Hatch (2000). "Characterization of in vitro DNA binding sites of the EUO protein of Chlamydia psittaci." Infect Immun **68**(3): 1337-1349.

Zhang, S. and W. G. Haldenwang (2005). "Contributions of ATP, GTP, and redox state to nutritional stress activation of the Bacillus subtilis sigmaB transcription factor." J Bacteriol **187**(22): 7554-7560.

Zhang, W., J. Yang, B. He, S. E. Walker, H. Zhang, B. Govindarajoo, J. Virtanen, Z. Xue, H. B. Shen and Y. Zhang (2016). "Integration of QUARK and I-TASSER for Ab Initio Protein Structure Prediction in CASP11." Proteins **84 Suppl 1**: 76-86.

Zhang, Y., E. L. Pohlmann and G. P. Roberts (2005). "GlnD is essential for NifA activation, NtrB/NtrC-regulated gene expression, and posttranslational regulation of nitrogenase activity in the photosynthetic, nitrogen-fixing bacterium Rhodospirillum rubrum." J Bacteriol **187**(4): 1254-1265.

Zhang, Y. and J. Skolnick (2004). "Scoring function for automated assessment of protein structure template quality." Proteins **57**(4): 702-710.

Zhang, Y. and J. Skolnick (2005). "TM-align: a protein structure alignment algorithm based on the TM-score." Nucleic Acids Res **33**(7): 2302-2309.

Zhang, Z. and W. A. Hendrickson (2010). "Structural characterization of the predominant family of histidine kinase sensor domains." J Mol Biol **400**(3): 335-353.

Zhong, G. (2017). "Chlamydial Plasmid-Dependent Pathogenicity." Trends Microbiol **25**(2): 141-152.

Zhou, Y. F., B. Nan, J. Nan, Q. Ma, S. Panjikar, Y. H. Liang, Y. Wang and X. D. Su (2008). "C4-dicarboxylates sensing mechanism revealed by the crystal structures of DctB sensor domain." J Mol Biol **383**(1): 49-61.

Zhulin, I. B., A. N. Nikolskaya and M. Y. Galperin (2003). "Common extracellular sensory domains in transmembrane receptors for diverse signal transduction pathways in bacteria and archaea." J Bacteriol **185**(1): 285-294.